Universiteit
Leiden
The Netherlands

The use of activity based protein profiling to study proteasome biology

Paniagua Soriano, Guillem

Citation
Paniagua Soriano, G. (2016, February 11). *The use of activity based protein profiling to study proteasome biology*. Retrieved from https://hdl.handle.net/1887/37766

Version:	Corrected Publisher's Version
License:	Licence agreement concerning inclusion of doctoral thesis in the Institutional Repository of the University of Leiden
Downloaded from:	https://hdl.handle.net/1887/37766

Note: To cite this publication please use the final published version (if applicable).

Cover Page

Universiteit Leiden

The handle http://hdl.handle.net/1887/37766 holds various files of this Leiden University dissertation.

Author: Paniagua Soriano, Guillem
Title: The use of activity based protein profiling to study proteasome biology
Issue Date: 2016-02-11

The Use of Activity-Based Protein Profiling to Study Proteasome Biology

PROEFSCHRIFT

ter verkrijging van

de graad van Doctor aan de Universiteit van Leiden,

op gezag van Rector Magnificus prof. Mr. C.J.J.M. Stolker,

volgens besluit van het College voor Promoties

te verdedigen op donderdag 11 February 2016

klokke 10:00 uur

door

Guillem Paniagua Soriano

geboren te Valencia in 1984

Prommotiecommissie

Promotor: Prof. Dr. H. S. Overkleeft

Co-promotor: Dr. B. I. Florea

Overige leden: Prof. Dr. J. Brouwer

Prof. Dr. C. Driessen

Prof. Dr. H. Ovaa

Dr. S. van Kasteren

Dr. C. Berkers

Table of Contents

Chapter 1:

General Introduction 7

Chapter 2:

Towards Understanding Induction of Oxidative Stress and Apoptosis by Proteasome Inhibitors 15

Chapter 3:

An Overview of Direct and Two-Step Activity-Based Proteasome Profiling Strategies 43

Chapter 4:

Comparative Activity-Based Proteasome Profiling in Zebrafish and Mice 55

Chapter 5:

Proteasome Inhibitor-Adapted Myeloma Cells Show Proteomic Alterations that Suggest Complex Changes in Metabolic Pathways 65

Chapter 6:

Summary and Future Prospects 81

Resumen 87

Curriculum Vitae 89

List of Publications 91

a mi familia

Chapter 1: General Introduction

The ubiquitin-proteasome system

Protein degradation is essential for cellular homeostasis and thus for cell survival. Having a regulated protein degradation machinery is crucial to protect functional proteins from degradation, to control proteins half-life or to degrade misfolded or damaged proteins which can be harmful to the cells. The ubiquitin-proteasome system (UPS) is the main degradation pathway in eukaryotes [1, 2]. The UPS marks the proteins for degradation with a poly-ubiquitin chain by means of three different enzyme families which work in cascade [3] to first identify the substrate and then attach to it a poly-ubiquitin chain (figure 1). Ubiquitin itself is a small protein (76 amino acids) that is mostly used as a post-translational modification (PTM) as effected in a cascade of reactions executed by three different types of enzyme families known as E1, E2 and E3 (figure 1). In this process, an isopeptidic linkage is produced starting from lysine side chain amines and the C-terminal carboxylate of ubiquitin. Ubiquitination of proteins can regulate the substrate cellular localization, control its degradation and plays a role in protein-protein interactions. All these cellular processes are regulated by a variety of ubiquitin modifications. Protein substrates can be modified with a single ubiquitin molecule or with a poly-ubiquitin chain. Ubiquitin has seven different lysine residues through which they can be linked to each other to build a poly-ubiquitin chain. These chains can be linear, branched or mixed with other ubiquitin-like molecules. The best-characterized poly-ubiquitin chains are so far the lysine 63- and lysine 48-linked chains while for the other types little is known. Lysine 48 (K48)-linked poly-ubiquitinated proteins are directed towards the proteasome where they are processed into small oligopeptide fragments. The majority of these peptides are further recycled into single amino acids by different peptidases, but a small fraction (estimated to be about 1%) of the peptides generated by the proteasome and partially processed by downstream aminopeptidases are presented on MHC-class I molecules for presentation to the immune system. CD8-positive cytotoxic T cells have developed to recognize peptide-loaded MHC class I molecules and to discriminate between self-peptides and foreign peptides. In this fashion, the UBP plays an important role in immunity and assists in reporting on, for instance, viral infections.

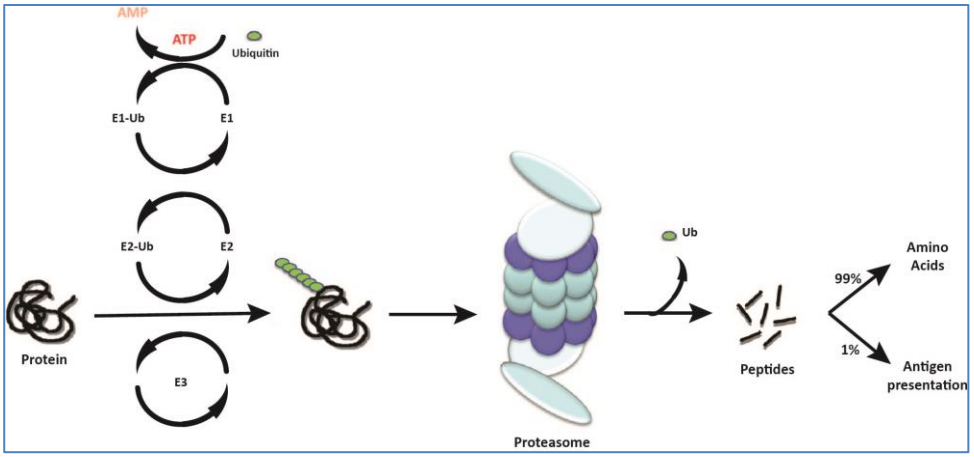

Figure 1. *Schematic representation of the UPS. Ubiquitin is transferred from an E1 ubiquitin transferase to an E2 transferase. This E2-Ub complex binds and transfers the ubiquitin to a protein substrate, which is bound to an E3 enzyme. This last step is repeated (not necessarily by the same pair of enzymes) to build a poly-ubiquitin chain on the substrate, which targets the protein for proteasome degradation. Proteasomes degrade proteins into smaller peptide fragments while the ubiquitin moieties are released and recycled. The generated peptides are further degraded into single amino acids by aminopeptidases. About 1% of the peptides are loaded onto MHC-class I molecules for antigen presentation on the cellular membrane.*

The proteasome is a large protein complex of around 2.5 MDa. It consists of a barrel-shaped core particle, termed 20S, and a small variety of regulatory particles (RP) of which the most common is the 19S RP [4]. The 19S RP binds to one and potentially both sides of the 20S, and triggers an opening to the inside where the catalytic sites are situated. The ubiquitinated substrates are recognized by the 19S RP, which unfold and translocate them into the 20S inner chamber for degradation. The protein will be cleaved into small peptides, which vary between 3 and 15 amino acids in length. The 19S subunit Rpn11 shows deubiquitylating (DUB) activity, which cleaves the bond between the substrate and the poly-ubiquitin chain; this chain will be recycled into single ubiquitin molecules by other DUBs [5]. The 20S proteasome consist of 14 pairs of alpha and beta subunits, which are stacked in rings, being the two alpha rings (each of 7 subunits) on the outer site of the barrel with the two beta rings on the inside. In prokaryotes all seven beta subunits have a catalytic activity which does not differ between subunits, but in eukaryotes only three of the seven beta subunits remain catalytically active, namely β1, β2 and β5. These subunits show differences in their substrate specificity, with β1 cutting preferably the C-terminal of acidic amino acids, β2 after basic ones and β5 rather after bulky or uncharged amino acids [4]. In organisms that have evolved an immune system, the UPS has increased its capability of generating different peptides from a single protein by expressing

immunoproteasomes 20S particles, where the active subunits of the constitutively expressed proteasome (constitutive proteasome, active subunits termed β1c, β2c and β5c) have been replaced by their immunoproteasomes counterparts, β1i, β2i and β5i. These subunits have slightly different cleavage pattern compared to their constitutive counterparts, which has increased the rate of generating peptides suitable for antigen presentation [6, 7]. Having 6 different subunits has expanded the possible pool of proteasomes, since all subunit combinations can be expected, giving rise to hybrids proteasomes in which both immunoproteasome and constitutive proteasome subunits are assembled into the same 20S particle.

Proteasome inhibitors and multiple myeloma

It was thought that disruption of the proteasome was not an option in drug development due to its major role in cellular protein homeostasis. But the discovery of epoxomicin, a broad-spectrum proteasome inhibitor (PI) synthetized by bacteria to fight against fungi infections, which caused cellular apoptosis and the posterior evidence that the UPS regulates cell cycle progression and NFkB signaling, boosted the idea of the UPS blockade as a suitable antineoplastic strategy [8, 9]. Since then major efforts have been made to contribute to this hypothesis, and today two proteasome inhibitors (bortezomib and carfilzomib) have been approved by the FDA for the treatment of mantle cell lymphoma and specifically multiple myeloma (MM) [10, 11]. Currently PIs are being tested in clinical trials alone or in combination with other drugs against a variety of human diseases including breast cancer, arteriosclerosis and Alzheimer's disease.

In the case of MM patients, PIs have evolved from last resort therapy to being the principal treatment. Its phenotype may explain why especially this specific type of cancer is sensitive against proteasome inhibition. MM is a hematopoietic cancer affecting mainly plasma cells, which are fully differentiated B-cells responsible for antibody production. MM plasma cells have a high protein synthesis rate due to the large amount of a single class of antibodies generated for secretion. This high synthesis rate is coupled to a strict quality control check, where misfolded proteins need to be quickly degraded to avoid accumulation or aggregation of misfolded or damaged proteins, which can be detrimental to the cell survival. The proteasome is one of the main players in this quality control system. This difference in protein synthesis rate opens a therapeutic window for the treatment of MM with proteasome inhibitors. The success in extending patients lifespan is clear but PIs are not a cure, and patients always relapse after a certain amount of years. An acquired resistance against proteasome inhibitors is the main drawback in finding an

effective cure. The mechanisms behind the development of adaption are not completely understood [4, 12, 13]. Some studies with PI resistant cell lines suggest that point mutations in the pocket of the β5 subunit, which is the main target of bortezomib and carfilzomib, impede the proper binding of the inhibitors within the active site pocket destabilizing the interaction [14]. Although these cell lines mimic the resistance found in patients, no mutations in the β5 subunit have been found in patients with relapse or refractory myeloma [15, 16]. This suggests that different mechanisms may drive the acquisition of resistance. Most of the secreted proteins, such as immunoglobulin, are synthetized in the endoplasmic reticulum (ER). Misfolded or damaged proteins located in the ER are degraded through the ER associated degradation (ERAD) pathway in which the proteasome is the main protease in charge of their degradation [17]. If the ERAD pathway capacity to deplete the ER-stress produced by the accumulation of misfolded proteins is exceeded, the UPR will be triggered, which through different synergistic mechanisms will alleviate the ER-stress (figure 2 and Chapter 2 of this thesis) [18]. These mechanisms are characterized by an increase in the cellular oxidative folding machinery, an enhancement of the proteasome activity together with autophagy activation and a lower protein synthesis rate. If the UPR activation is not enough to compensate ER-stress, the cell will become apoptotic and die [19]. It is the current view that this is the actual way of action of PI for inducing cell death and also the reason why cancerous plasma cells are especially sensitive against this treatment since they are overproducing immunoglobulin for secretion and it is already provoking a basal ER-stress [20]. Recent studies suggest that a modulation of the ER and its associated unfolded protein response (UPR) could be the reason for the adaptation against PIs [20-22].

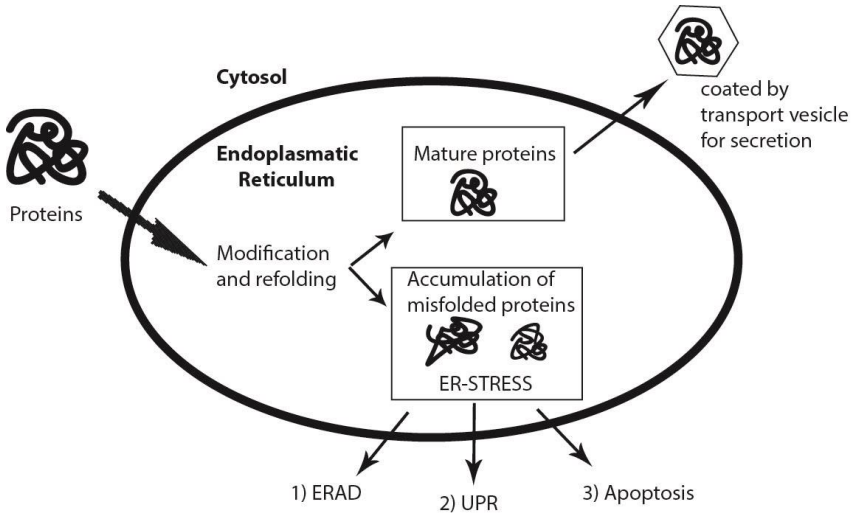

Figure 2. *Schematic representation of ER-stress. Proteins need to be properly folded and in some cases modified prior secretion. This process takes place mainly in the ER. ERAD (1) tags misfolded proteins with poly-ubiquitin chains for proteasomal degradation. If these misfolded or damaged proteins start to accumulate in the ER lumen, the unfolded protein response (UPR) will be triggered (2). The UPR will increase the ERAD capacity and the folding machinery of the ER and at the same time will slow down general protein synthesis in the cell. If UPR activation is not enough for alleviating the stress caused by accumulation of misfolded proteins, cells will enter apoptosis and die (3).*

Activity-based protein profiling (ABPP)

Enzymes are dynamic proteins or protein complexes acting as catalysts in biological reactions. They can be very selective, having a small subset of substrates, or much broader, where they can react with a large variety of substrates. Enzyme activity needs to be tightly regulated, so that only the necessary reactions depending on the cellular needs take place. This can be done with activators, inhibitors, regulatory particles, in some cases by posttranslational modifications (PTMs) or even by keeping the enzyme in a specific cellular compartment where it can only access substrates, which are in the same compartment.

Measuring enzyme activity has always been of great interest for researchers both for fundamental reasons, to expand the knowledge of enzymatic reactions or signaling pathways, and for applied biomedical reasons. Some diseases are directly related to an altered enzyme activity and therefore modulating the activity of some enzymes can be used as treatment against diseases, as is demonstrated in the case of MM by the inhibition of the proteasome. Proteasome activity has been measured mostly by means of

quenched fluorogenic substrates, which become fluorescent after being processed by the proteasome. These substrates allow distinguishing between the three different active sites of the proteasome, β1, β2 and β5, but do not permit the differentiation between the constitutive proteasome and immunoproteasome subunits. In the last 15 years a new method for measuring enzyme activities has been developed, termed activity based protein profiling (ABPP) [23-25]. This technique makes use of tagged inhibitors, called activity-based probes (ABPs), which create a covalent and irreversible bond with the catalytic active site of the enzyme allowing its direct measurement. By means of fluorescent-tagged ABPs the separation and quantification of the 6 different proteasome activities was achieved [26, 27]. ABPP was also used to demonstrate the activity of a new proteasome active subunit, the β5t, which is exclusively expressed in the thymus [28].

ABPs can be used to identify and quantify enzyme activities on gel when bearing a fluorescent tag or for enzyme affinity purification if tagged with an affinity handle such as a biotin moiety. ABPs consist of three parts, an electrophilic trap or warhead, a linker or enzyme targeting moiety and a tag. The warhead is the chemical entity, mostly a nucleophile, which reacts with the active site of the target enzyme creating a covalent bond between the ABP and the enzyme. The linker or backbone is used for enzyme targeting thus making the ABP specific against a single or a broader range or enzymes. This backbone in most cases mimics the enzyme substrate structure or the one of natural compounds found to bind the target enzyme. In some cases the presence of a tag can interfere with the selectivity or potency of the probe and when using it on living cells also to its cellular localization. To avoid these possible caveats the tag can be replaced by a bio-orthogonal handle, generating two-step ABPs [29, 30]. Bio-orthogonal tags are small chemical moieties which are chemically inert under physiological conditions and are able to perform a reaction with another chemical entity under these conditions without interfering with the surrounding [31]. Azide or alkyne groups are the most popular bioorthogonal tags due to their small size, comprising just few atoms, and their highly selective reactions. All these different features are what make ABPP a broadly used technique in the study of a large variety of enzymes. It has been shown to be a robust and reliable concept, which allows quantification of the enzymatic activity or the enrichment of the target enzyme.

Aim and outline of this thesis

The work described in the first part of this thesis (Chapters 3 and 4) is focused on expanding the knowledge about proteasome activity-based probes by in depth

characterization. The use of ABPP and mass spectrometry (MS) in the elucidation of the resistance mechanisms which confer resistance towards proteasome inhibitors in multiple myeloma samples is presented in Chapter 5.

Chapter 2 comprises a literature overview, which covers in more detail the link between the proteasome, proteasome inhibitors and multiple myeloma. The possible adaptation mechanisms will also be briefly discussed with a focus on the UPR and the redox machinery of the cell.

First part of **Chapter 3** presents an overview of two-step proteasome ABPP strategies reported in literature performing different bio-orthogonal reactions. The second part of this chapter describes the characterization of a broad-spectrum ABP and the determination of the unlabeled proteasome fraction after probe exposure.

Chapter 4 describes a screen of 7 different ABPs in mouse and zebrafish tissue extracts.

Chapter 5 provides a study on the mechanisms of adaptation towards proteasome inhibitors in multiple myeloma samples by a combination of ABPP and MS-based proteomics.

Chapter 6 is a summary of the whole thesis and the future prospects for the different chapters.

References

1. Baumeister, W., *et al.*, *The proteasome: paradigm of a self-compartmentalizing protease.* Cell, 1998. **92**(3): p. 367-380.
2. Hershko, A. and A. Ciechanover, *The ubiquitin system.* Annu. Rev. Biochem., 1998. **67**: p. 425-479.
3. Finley, D., *Recognition and processing of ubiquitin-protein conjugates by the proteasome.* Annu. Rev. Biochem., 2009. **78**: p. 477-513.
4. Tanaka, K., T. Mizushima, and Y. Saeki, *The proteasome: molecular machinery and pathophysiological roles.* Biol. Chem., 2012. **393**(4): p. 217-234.
5. Besche, H.C., A. Peth, and A.L. Goldberg, *Getting to first base in proteasome assembly.* Cell, 2009. **138**(1): p. 25-28.
6. Kloetzel, P.M., *The proteasome and MHC class I antigen processing.* Biochim. Biophys. Acta, 2004. **1695**(1-3): p. 225-233.
7. Groettrup, M., C.J. Kirk, and M. Basler, *Proteasomes in immune cells: more than peptide producers?* Nat. Rev. Immunol., 2010. **10**(1): p. 73-78.
8. Meng, L., *et al.*, *Epoxomicin, a potent and selective proteasome inhibitor, exhibits in vivo antiinflammatory activity.* Proc. Natl. Acad. Sci. U. S .A., 1999. **96**(18): p. 10403-10408.
9. Adams, J., *et al.*, *Proteasome inhibitors: a novel class of potent and effective antitumor agents.* Cancer Res., 1999. **59**(11): p. 2615-2622.
10. Goldberg, A.L., *Development of proteasome inhibitors as research tools and cancer drugs.* J. Cell. Biol., 2012. **199**(4): p. 583-588.

11. Kisselev, A.F., W.A. van der Linden, and H.S. Overkleeft, *Proteasome inhibitors: an expanding army attacking a unique target.* Chem. Biol., 2012. **19**(1): p. 99-115.
12. Kale, A.J. and B.S. Moore, *Molecular mechanisms of acquired proteasome inhibitor resistance.* J. Med. Chem., 2012. **55**(23): p. 10317-10327.
13. McBride, A. and P.Y. Ryan, *Proteasome inhibitors in the treatment of multiple myeloma.* Exp. Rev. Anticancer Ther., 2013. **13**(3): p. 339-358.
14. Ri, M., *et al.*, *Bortezomib-resistant myeloma cell lines: a role for mutated PSMB5 in preventing the accumulation of unfolded proteins and fatal ER stress.* Leukemia, 2010. **24**(8): p. 1506-1512.
15. Lichter, D.I., *et al.*, *Sequence analysis of beta-subunit genes of the 20S proteasome in patients with relapsed multiple myeloma treated with bortezomib or dexamethasone.* Blood, 2012. **120**(23): p. 4513-4516.
16. Politou, M., *et al.*, *No evidence of mutations of the PSMB5 (beta-5 subunit of proteasome) in a case of myeloma with clinical resistance to Bortezomib.* Leuk. Res., 2006. **30**(2): p. 240-241.
17. Ron, D. and P. Walter, *Signal integration in the endoplasmic reticulum unfolded protein response.* Nat Rev. Mol. Cell Biol., 2007. **8**(7): p. 519-529.
18. Walter, P. and D. Ron, *The unfolded protein response: from stress pathway to homeostatic regulation.* Science, 2011. **334**(6059): p. 1081-1086.
19. Tabas, I. and D. Ron, *Integrating the mechanisms of apoptosis induced by endoplasmic reticulum stress.* Nat. Cell Biol., 2011. **13**(3): p. 184-190.
20. Gu, J.L., *et al.*, *Differentiation induction enhances bortezomib efficacy and overcomes drug resistance in multiple myeloma.* Biochem. Biophys. Res. Commun., 2012. **420**(3): p. 644-650.
21. Oyadomari, S., *et al.*, *Cotranslocational degradation protects the stressed endoplasmic reticulum from protein overload.* Cell, 2006. **126**(4): p. 727-739.
22. Niewerth, D., *et al.*, *Molecular basis of resistance to proteasome inhibitors in hematological malignancies.* Drug Resist. Updat., 2015. **18**: p. 18-35.
23. Willems, L.I., H.S. Overkleeft, and S.I. van Kasteren, *Current developments in activity-based protein profiling.* Bioconjug. Chem., 2014. **25**(7): p. 1181-1191.
24. Cravatt, B.F., A.T. Wright, and J.W. Kozarich, *Activity-based protein profiling: from enzyme chemistry to proteomic chemistry.* Annu. Rev. Biochem., 2008. **77**: p. 383-414.
25. Evans, M.J. and B.F. Cravatt, *Mechanism-based profiling of enzyme families.* Chem. Rev., 2006. **106**(8): p. 3279-3301.
26. Gu, C., *et al.*, *Proteasome activity profiling: a simple, robust and versatile method revealing subunit-selective inhibitors and cytoplasmic, defense-induced proteasome activities.* Plant J., 2010. **62**(1): p. 160-170.
27. Verdoes, M., *et al.*, *A panel of subunit-selective activity-based proteasome probes.* Org. Biomol. Chem., 2010. **8**(12): p. 2719-2727.
28. Florea, B.I., *et al.*, *Activity-based profiling reveals reactivity of the murine thymoproteasome-specific subunit beta5t.* Chem. Biol., 2010. **17**(8): p. 795-801.
29. van der Linden, W.A., *et al.*, *Two-step bioorthogonal activity-based proteasome profiling using copper-free click reagents: a comparative study.* Bioorg. Med. Chem., 2012. **20**(2): p. 662-666.
30. Willems, L.I., *et al.*, *Bioorthogonal chemistry: applications in activity-based protein profiling.* Acc. Chem. Res., 2011. **44**(9): p. 718-729.
31. Shieh, P. and C.R. Bertozzi, *Design strategies for bioorthogonal smart probes.* Org. Biomol. Chem., 2014. **12**(46): p. 9307-9320.

Chapter 2: Towards Understanding Induction of Oxidative Stress and Apoptosis by Proteasome Inhibitors*

Introduction

The ubiquitin-proteasome system (UPS) is the major cytosolic and nuclear protein turnover machinery [1, 2]. Ubiquitylated proteins are recognized and processed to produce small- and medium size oligopeptides that are further processed by aminopeptidases to deliver amino acids for reuse in protein synthesis. The UPS ensures controlled protein turnover by the time-dependent targeting and degradation of its substrates and in this fashion determines the half-life of each cytosolic and nuclear protein. The UPS also partakes in the degradation of misfolded and dislocated proteins from the ER and therefore plays a major role in the cellular response to ER stress, and is responsible for the removal of proteins damaged by oxidative stress [3, 4]. Part of the peptide pool produced by proteasomes and further trimmed by downstream aminopeptidases are transported to the luminal side of the endoplasmic reticulum, where they are loaded onto major histocompatibility complex class I (MHCI) molecules for presentation at the outer cell surface to the immune system [5-8]. $CD4^+$ cytotoxic T-cells discriminate between self peptides and foreign peptides presented in this fashion and by processing virally encoded proteins for MHCI mediated antigen presentation proteasomes contribute to the detection and eradication of virally infected cells.

Proteasomes are expressed almost ubiquitously throughout the kingdoms of life (Eubacteria generally do not contain proteasomes except some actinomycetes and mycobacteria). Although proteasomes have evolved over time, the overall layout of the inner proteolytic assemblies, called 20S core particles (CP), has remained remarkably conserved. 20S proteasomes are C2-symmetric barrel-like structures that consist of four rings of seven protein subunits each, arranged in an αββα fashion with two outer α rings and two inner β rings. In 1995, the crystal structure of the archaeal 20S proteasome was solved [9]. In prokaryotes the α-subunits are identical and the same holds true for the β-subunits. In 1997 the crystal structure of the yeast 20S proteasome was solved [10] and in 2002 the structure for mammalian 20S was determined [11]. In eukaryotes both α-subunits and β-subunits have diverged such that, though the overall C2-symmetrical geometry is maintained, the seven α-subunits in each α ring are unique, as is the case for the seven β-subunits. In prokaryotes each β-subunit is catalytically active. In yeast and all

* Antioxid. Redox Signal., 2014 Dec; **21**(17): p. 2419-2443

other eukaryotes however, each β ring contains only three β-subunits with enzymatic activity (β1, β2 and β5). Thus eukaryotes lack enzymatic activity of β3, β4, β6 and β7 but this loss is offset by a diverged substrate specificity of the remaining subunits. Of these, β1 is also known as 'caspase-like' because it recognises and processes substrates having acidic residues at position 1 (P1 – the amino acid occupying in the proteasome active site the position containing the scissile amide bond). The β2-subunit cuts preferentially C-terminal of basic amino acids and is therefore also referred to as 'trypsin-like', whereas β5 prefers hydrophobic residues and is referred to as 'chymotrypsin-like'.

Proteasome subunits are only catalytically active when part of a 20S core particle. The assembly of 20S particles have been subject to intensive studies leading to detailed insight into the various consecutive steps by which these superstructures are formed [12, 13]. The proteasome-assembling chaperones (PAC) 1-4 form heterodimers that direct the α ring assembly. Once seven α-subunits are assembled into one ring, the β-subunits are incorporated. UMP1 is essential for correct assembly of the β-subunits. Their precursor peptides (β-propeptides) are essential for proper β ring formation. The β7-subunit is the last subunit incorporated into the ring, forming one half of a 20S proteasome. Assembly of a core 20S particle from two halves is guided by the C-terminal tail of the β7-subunits, which acts as a chaperone. Finally, CP maturation is accomplished by intramolecular clevage of the propeptide of the inactive subunits to generate the active site [12-14]. Experimental data suggests that the N-terminus of the α-subunits in the α-rings form a gate that closes the pore of the catalytic chamber, restricting the access of substrates. As a consequence, the 20S core particle alone shows a basal catalytic activity, which is enhanced when bound to regulatory particles (RP) [14].

In vertebrates, specific tissues express the interferon-gamma-inducible immunoproteasomes. In these particles the catalytic β subunits of the constitutive proteasome are replaced by β1i, β2i and β5i respectively [15, 16], The immunoproteasome 20S core particle are assembled *de novo* and cannot derive from subunit exchange starting from constitutive proteasome 20S particles, as proposed earlier [17, 18]. Immunoproteasomes have a slightly different substrate preference compared to constitutive proteasomes and this difference in cleavage correlates with MHC Class I peptide bonding specificity, which is a very important feature in immunology [6]. Recently the crystal structure of the mouse immunoproteasome at 2.9 Å resolution was solved this structure revealed some differences between the immunoproteasome and constitutive proteasome active sites, thus underscoring that the substrate specificity is slightly different [19].

In 2007, Murata *et al.* discovered a new protein with an overall sequence highly similar to β5 and β5i, suggesting that this protein may belong to the same protein family although of a larger size [20]. This protein, named β5t, is expressed specifically in thymic cortical epithelial cells, where it substitutes β5i, in immunoproteasomes [21]. This resulting 20S core particle has been dubbed the thymoproteasome and ensuing studies suggested a specific role for thymoproteasomes in positive T-cell selection. In 2010, our group showed by means of activity-based protein profiling that β5t is catalytically active. The inhibitor profile resulting from a competitive activity-based protein profiling assay performed on thymoproteasomes moreover suggests that the β5t active site pocket is more hydrophilic than β5 and β5i [22]. This altered inhibitor preference may reflect an altered substrate preference as well, which in turn may help explaining the role of β5t in positive T cell selection.

Next to the three distinct 20S proteasome core particles (constitutive proteasome, immunoproteasome and thymoproteasome), a number of hybrid or 'intermediate' 20S particles have been discovered in the past decade [23-28]. These particles may contain mixtures of constitutive proteasome and immunoproteasome active sites. Although to date only intermediate proteasomes have been identified that contain one (β5i) or two (β1i and β5i) of the three inducible catalytic subunits of the immunoproteasome, it may well be that more, and more complex intermediate proteasomes exist, adding to the complexity of the 20S core particle (20S-CP) family and its contribution to protein turnover and antigen presentation.

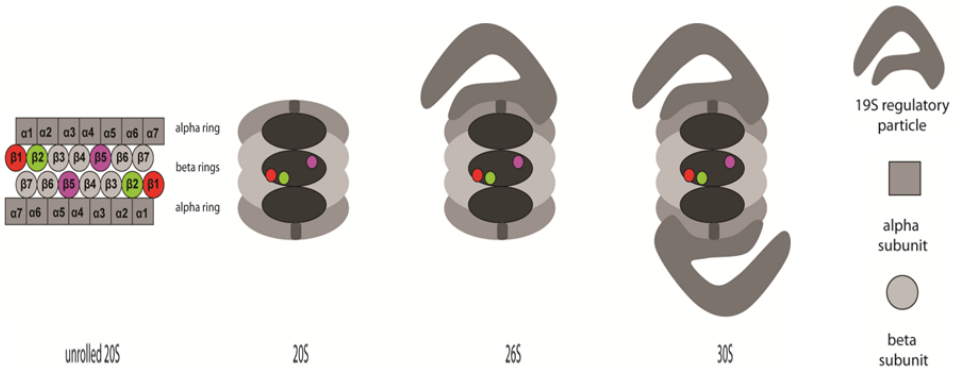

Figure 1. *Schematic representation of the eukaryotic constitutive proteasome. Cross section of the 20S core particle containing the β1, β2 and β5 active subunits that confer the caspase-like, tryptic-like and chymotryptic-like activity. Attachment of one 19S regulatory particle to the 20S core yields the 26S proteasome and two 19S caps with one 20S yields the 30S proteasome particle. In immune*

competent tissues the active subunits can be replaced by their immunologic counter parts β1i, β2i and β5i forming the immunoproteasome. Replacement of β5i by the thymus specific β5t makes the thymoproteasome.

20S core particles are capable of degrading peptides and small, or unfolded proteins but their physiological role is limited. To become fully functional, 20S particles associate with one or two of a number of regulatory caps [29]. Of these, the 19S cap is the most studied and the most important complex to associate with constitutive proteasome 20S core particles. 19S caps bind to the α-rings of a mature 20S thus giving rise to 26S proteasomes (one 19S cap associated) or 30S proteasomes (one 19S cap at both ends of the 20S barrel, Figure 1). 19S caps regulate 20S mediated protein turnover in an ATP-dependent fashion by identifying and binding polyubiquitinated proteins, unfolding the substrates, and translocating these into the 20S catalytic chamber. 19S caps are assembled from 19 subunits, which can be divided in two subcomplexes: the lid and the base. The base is composed of 10 different proteins, 4 non ATPases and 6 AAA+ ATPases that form a hetero-hexameric ring, which in presence of ATP, binds the α-rings of the 20S facilitating the opening of the gate [30]. The base promotes the unfolding of the substrate, opens the pore to permit the entrance of the targeted substrates into the 20S inner chamber and translocates these. Of the 4 non-ATPases proteins, two are ubiquitin receptors and the other two can bind to the ubiquitin shuttle proteins Rad23, Ddi1 and Dsk2 [30]. The lid is situated on top of the base and contains 9 non-ATPases proteins. Its main function is to recognize and bind polyubiquitinated substrates and deubiquitylate these. The lid subunit Rpn 11 is the only deubiquitinating enzyme (DUB) incorporated into the 26S proteasome. Two additional DUBs, Usp14 and Uch37, are described as proteasome-associated proteins, however their precise binding position to the 26S is unknown [31].

Apart from the 19S caps, other proteasome activators have been found such as the PA28 protein family and PA200. These regulatory particles activate the proteasome in an ATP-independent manner in contrast to the 19S cap. The PA28 complex, also known as 11S, has 3 isoforms in higher eukaryotes, called PA28α, β and γ. PA28α and PA28β form a heteroheptamer, while the PA28γ, which is mainly found in the nucleus forms a homoheptamer [32]. Both complexes bind to the α rings and promote gate opening. Some studies have been reported that reveal the involvement of 11S activators in the production of peptides for antigen presentation through MHC class I complexes. However some cells and tissues which are not involved in the immune system, do express the 11S regulatory particles. 11S particles may also be part of hybrid proteasomes, with a 19S cap on one end and an 11S activator on the other [32]. The monomeric activator PA200 (Blm10 in yeast) can partially open the gate of the 20S-CP, thus helping substrate entry in the proteolytic chamber. Although the 20S-CP is expressed in all eukaryotes, plants and

yeasts only contain PA200/Blm10 and do not have any of the PA28 isoforms. The function of the PA200 is poorly understood, but some studies point towards its involvement in the degradation of specific substrates [14].

Proteasome inhibitors

Many different proteasome inhibitors (PIs) have been described over the past decades. PIs are derived both from natural sources and through organic synthesis. Both covalent reversible, covalent irreversible and non-covalent inhibitors are known. PIs have been reviewed extensively before [33-35], thus we will here focus mainly on site-selective inhibitors, for which we provide both a qualitative (different types of inhibitors) and a quantitative (potency and subunit selectivity) analysis. Figure 2 shows five classes of covalent inhibitors and their inhibition mechanisms. The first class is represented by the peptide aldehydes, with **MG-132** as its most widely used member. Aldehydes form covalent, reversible bonds within proteasome active sites, and inactivate catalytic activities by hemiacetal formation with the N-terminal threonine of the proteasome subunits. A major drawback of aldehydes is their cross reactivity towards cysteine and serine proteases [35]. A well-known class of electrophilic traps is the family of epoxyketones. Inhibitors containing the epoxyketone moiety are highly selective for the proteasome, and no off targets have been found to date [36]. The structure of **epoxomicin** co-crystallized in yeast proteasomes reveals the molecular basis for this specificity. A morpholine ring is formed between the active site threonine and the epoxyketone, in which both the γ-hydroxyl and the free amine of the N-terminal threonine participate [37]. Another class of PIs are the boronic acids, with **Bortezomib** as the most renowned example [38]. Bortezomib (Velcade, PS-341) has been approved for the treatment of multiple myeloma (MM) patients [39]. Boronates form tetrahedral adducts with active site threonines, which are stabilized by hydrogen bonding [40]. Vinyl sulfones were initially used as cysteine protease inhibitors, but were also found to be potent PI's [41, 42]. Vinyl sulfones are more readily synthesised than epoxyketones and have been used in many peptide inhibitors and activity based probes. Vinyl sulfones form a covalent adduct by conjugate addition of the hydroxyl-group of the active site threonine [43]. The last class of PIs discussed here are β-lactones, which form a covalent and relatively stable adduct to the proteasome by the attack of the catalytic threonine to the lactone, thereby forming a ester bond. In case of **Marizomib** (salinosporamide A, NPI-0052), the nucleophilic displacement of the chloride by the hydroxyl results in the formation of a tetrahydrofuran ring, which further stabilizes the adduct [44].

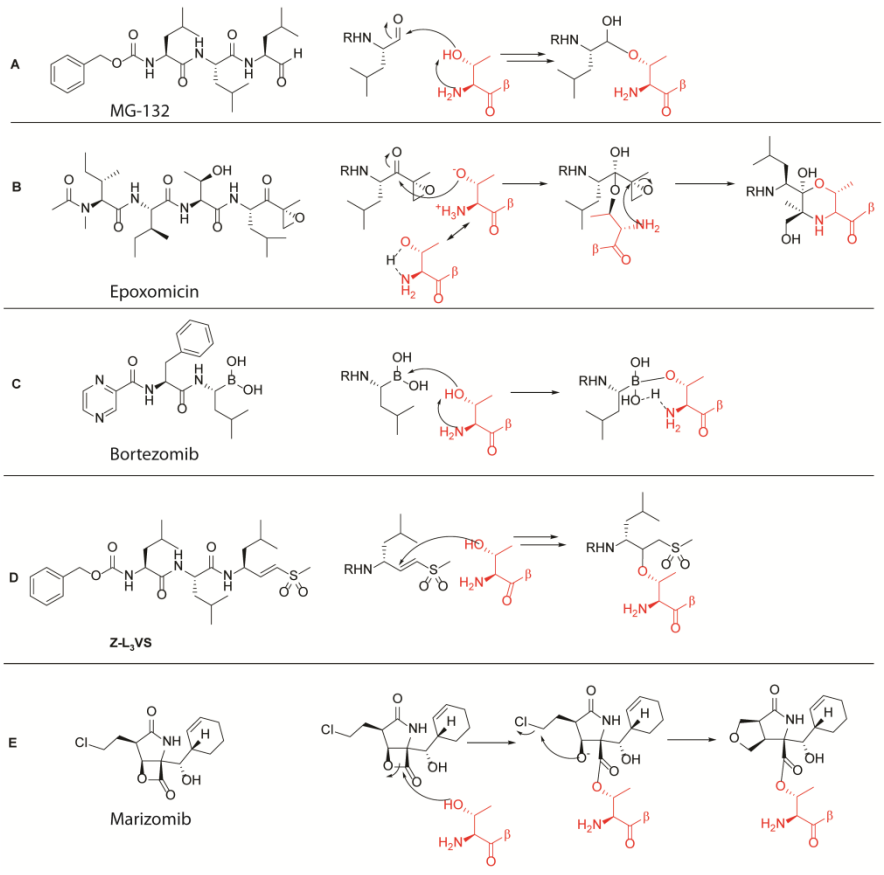

Figure 2. *Chemical structures of covalently binding proteasome inhibitors and the reaction mechanism of the electrophilic trap with the N-terminal active site threonine of the proteasome. MG132 is an example of an aldehyde warhead, Epoxomicin contains an epoxyketone, Bortezomib bears a boronic acid, ZL3VS holds a vinylsulfone and Marizomib is an example of β-lactone warhead.*

Proteasome inhibitors as drugs and clinical candidates

Figure 3 shows the molecular structure of several PIs currently used in the clinic or that are studied as clinical candidates. Bortezomib was the first PI approved by the FDA for the treatment of multiple myeloma (MM) and refractory mantle cell lymphoma (MCL). Based on the great success of Bortezomib [45], other proteasome inhibitors have entered clinical trials, and **Carfilzomib** was recently approved for the treatment of MM. Unfortunately,

patients treated with Bortezomib often develop resistance against the drug. The mechanisms behind Bortezomib resistance are poorly understood, but recent studies in cell lines indicated three main pathways by which cells can acquire resistance to PIs: 1) by upregulation of proteasome subunits, 2) by mutations in the β5 subunit or 3) by upregulation of efflux pumps [46], although other mechanisms such as PI-resistant NF-kB activity, upregulation of chaperones such as Hsp27, Gp78 and Hsp90, overexpression of anti-apoptotic proteins like Bcl2 and XIAP or activation of autophagy can confer resistance to Bortezomib [47].

Two other boronates are currently under clinical investigation. These are **Delanzomib** (CEP-18770) and **Ixazomib citrate** (MLN-9708). Delanzomib was developed as an orally available analogue of Bortezomib (administered intravenously [48]). Delanzomib showed promising results in toxicity studies and is currently under Phase I-II clinical investigations [49]. MLN-9708, another orally bioavailable boronate currently in Phase III trials (http://clinicaltrials.gov, Newly Diagnosed Multiple Myeloma NCT01850524; Relapsed and/or Refractory Multiple Myeloma NCT01564537; Relapsed or Refractory Systemic Light Chain (AL) Amyloidosis NCT01659658), has improved properties compared to Bortezomib, such as slower off rate, large volume of distribution, improved pharmacodynamics and pharmacokinetics and antitumor activity. Importantly, MLN-9708 also shows activity in solid tumors [50]. Peptide epoxyketones have entered clinical trials as well and Carfilzomib was recently approved for the treatment of MM. Carfilzomib causes higher inhibition of chymotrypsin-like activity (88%) at maximal tolerated dose than Bortezomib (70%) and also higher partial response rates than Bortezomib [51]. In addition, side effects are reduced upon treatment with Carfilzomib compared to Bortezomib, which may be due to a lower number of off targets thanks to the proteasome-specific electrophilic trap represented by the epoxyketone [52, 53]. Extensive medicinal chemistry studies led to the development of the orally bioavailable epoxyketone **ONX-0912**, which is currently in Phase I clinical studies for the treatment of MM [54]. Finally, the β-lactone, Marizomib, is under clinical investigation for the treatment of MM, leukemia, lymphomas and solid tumors. Marizomib is the most potent of all PIs under clinical investigations and inhibits not only β5 but also β1 and β2 [55].

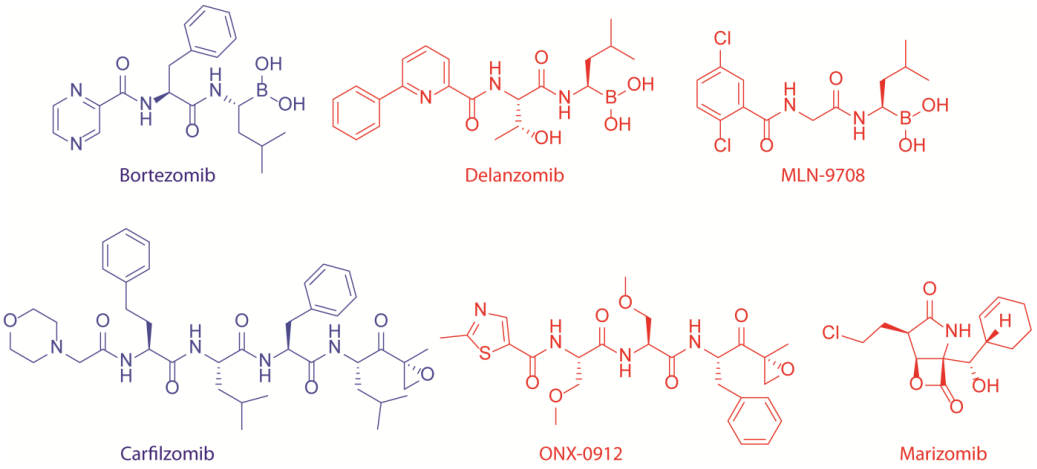

Figure 3. *Chemical structures of drugs (blue) or drug candidates (red) based on proteasome inhibitors.*

Current research aims at novel therapeutic applications of inhibitors/modulators of the ubiquitin proteasome system in cancer and other diseases which emphasizes the increasing importance of these compounds for the clinic. In this issue some of these topics will be discussed such as the design of small-molecule noncompetitive regulators that target proteasome function by allostery and dynamics [56], the design of small-molecule noncompetitive neddylation regulators for targeted anti-cancer therapy with less anticipated cytotoxicity compared to PIs [57], how impairment of the UPS is implicated in the pathogenesis of a wide variety of neurodegenerative disorders [58], the impact of proteasome inhibition and the potential prognostic value of proteasome activities in heart diseases [59] and in atherosclerosis [60] and why the proteasome is a promising therapeutic target to combat malignant tumour growth in the lung [61].

Activity based probes

In the past decades, various activity based probes (ABPs) for the proteasome β-subunits have been developed. Generally, ABPs consist out of three parts: 1. The electrophilic trap ('warhead'), which covalently modifies the active site threonine of the β-subunit; 2. A recognition element, providing recognition by β-subunits; and 3. A reporter group, such as a radiolabel, biotin or fluorophore. The first activity-based proteasome probe reported is **[^{3}H]-lactacystin** [62, 63], which was used to establish binding of lactacystin to all

proteasome β-subunits in a 2D-gel electrophoresis experiment. The natural product epoxomicin, which was found to exhibit antitumor effects, was found to target the proteasome by using **biotin-epoxomicin** as a probe, followed by detection of luminescence upon treatment with avidin-horseradish peroxidase [64, 65]. **^{125}I-NIP-L$_3$VS** was used to prove that vinyl sulfones not only target cysteine proteases, but also covalently bind to proteasome β-subunits [41]. All β-subunit were visualized by NLVS in a 2D-gel electrophoresis experiment using autoradiography detection of ^{125}I. More recently, ^{125}I-NIP-L$_3$VS was used to screen for inhibitors of the proteasome by incubation of cellular extracts with a potential inhibitor, followed by labelling of residual proteasome activity by ^{125}I-NIP-L$_3$VS. Next, the samples were resolved on SDS-PAGE and inhibition of a proteasome β-subunit is reflected by a decrease in intensity of the corresponding band [66].

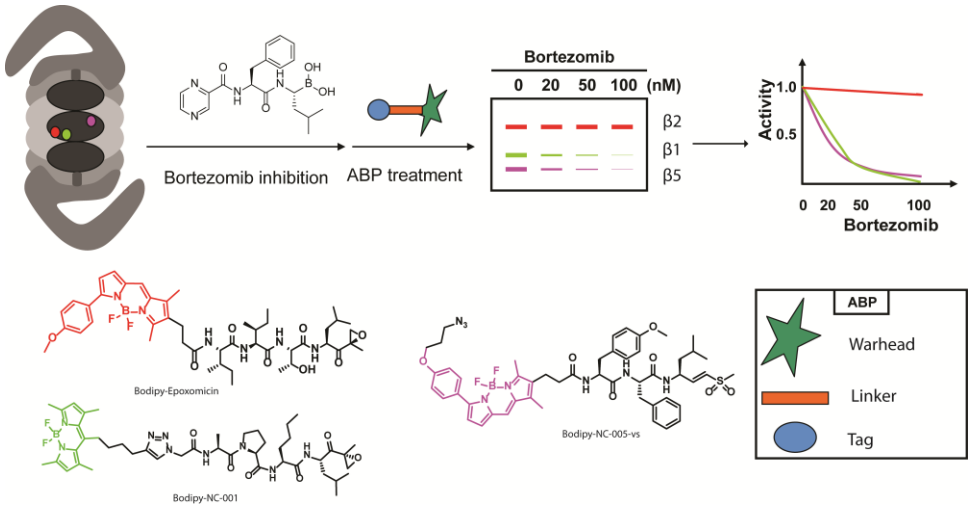

Figure 4. *Schematic workflow of a competitive activity-based proteasome profiling (ABPP) experiment. After exposure to Bortezomib the residual proteasome activity was determined with two subunit specific ABPs for β1 (BODIPY-NC-001) and β5 (BODIPY-NC-005-vs), while the pan-reactive ABP (BODIPY-epoxomicin) will label residual β2 subunit activity. Proteins were resolved by SDS-PAGE and band intensity can be quantified after scanning the gel. In this example a relatively insensitive cell line was tested hence the high Bortezomib concentrations used.*

In the last years, various fluorescent ABPs for the proteasome subunits have been developed. The first such probe developed is the weakly fluorescent **dansyl-Ahx$_3$-L$_3$-VS** [67], which was followed by the BODIPY TMR containing **MV151** [68] and **Bodipy-FL-Ahx$_3$-L$_3$-VS** [69]. Using pan-reactive fluorescent probes MV151 and **BODIPY-epoxomicin** [70], all

subunits of both the constitutive and immunoproteasome can be visualized by fluorescent scanning, directly after resolving cellular extracts that have been incubated with the probes on SDS-PAGE. Figure 4 shows a schematic overview of the work-flow used for activity-based proteasome profiling. Visualization of proteasome activity by fluorescent ABP is straight forward, time efficient and provides higher resolution compared to either biotinylated or radiolabelled probes. MV151 and BODIPY-epoxomicin can be used both in living cells and in cell extracts [68, 70]. Next to ABPs that target all subunits, β-subunit specific ABPs have been developed. Based on NC-001, **BODIPY-NC-001** shows highly specific labelling of both β1c and β1i, without labelling of the other subunits. The same applies to **BODIPY-NC-005-vs**, which is based on NC-005-mvs, which only labels β5c and β5i subunits [70]. However, generating a fluorescent ABP for β2 proved to be more difficult: attachment of a BODIPY fluorophore to **LU112** yielded a compound that also labels β5 [71]. Therefore a two steps labelling using **N_3-NC-002** has to be used to specifically label β2 subunits [72]. **UK101-B660** and **UK101-Fluor**, both based on the β1i selective inhibitor UK101, are used to selectively label β1i, both in cell extracts and in living cells [73]. Interestingly, the fluorophore is not attached to the N-terminus of the inhibitor, but to the P2 substituent, since the S2 pocket is rather large and solvent exposed, allowing for the introduction of bulky substituents. In general the proteasome ABPs can be used to quantify relative proteasome activity, to perform competitive activity based protein profiling (ABPP) to test the inhibition profile of potentially new inhibitors and as imaging probes according to the scheme in figure 4 [74].

Molecular mechanisms of proteasome inhibitors-induced apoptosis

Review of clinical, preclinical and biochemical literature on the use of PIs in organisms, tissues and cells shows several corroborative observations: PIs induce cell cycle arrest and caspase mediated apoptosis that somehow affects oncogenically transformed cells more than healthy tissues [75]. This suggests that proteasome inhibition impacts stronger on fast proliferating tissues [76] and that PIs are remarkably “clean” in their mode of action by specifically targeting only the active subunits of the proteasome [36, 77]. Having said so, a plethora of exceptions to this dogma have become known. For instance, PIs do show adverse effects in the clinic, indicating that healthy tissues are affected, the anti-neoplastic effects are limited to the treatment of several fast proliferative myeloma types of cancers but is less effective against quiescent cells or solid tumours and transformed cells evolve resistance to PI treatments [78]. Work in cell cultures showed that prerequisite of PIs for apoptosis induction is that they should deactivate at least two out of the three active proteasome subunits with potencies that eliminate >50% of the

subunits activity [79, 80]. It has been observed that multiple myeloma cells showing increased proteasome stress (balance between poly- and free ubiquitin) with the proteasome workload exceeding the proteasome capacity to process substrates are more sensitive to PI induced apoptosis [81]. Next to this, tremendous scientific efforts have been undertaken in the past decade to unravel the molecular mechanisms of PI-induced apoptosis. It is remarkable that proteasomes – major factors in protein homeostasis in every cell type – are in fact valid therapeutic targets and a detailed understanding in the mode of action of clinical proteasome drugs in effecting apoptosis may give invaluable information for designing future drugs. What makes understanding the mechanisms of apoptosis induction by PIs even more complicated is that the knowledge of the cell biological basis evolved alongside the development of more specific PIs leading to several controversies in the literature. On top of this, the above mentioned cellular effects of PIs may induce both cell protective and cell death pathways simultaneously, stressing the need to understand the kinetics and the cross-talk between the different effects.

Besides its role of guarding the cellular amino acid homeostasis by degrading damaged or misfolded proteins, the UPS is instrumental for defining the repertoire of peptides used for antigen presentation of every cell and is vital for regulating signal transduction molecules that decide between cell survival and cell death both in the cytoplasm and the nucleus [36, 82]. Proteasome inhibition has been reported to have numerous effects on cells [82, 83], including the following: 1) Cell cycle arrest by activation of G2/M checkpoints, 2) Perturbation of cyto-protective and pro-death signaling transduction pathways, 3) ER stress and Ca^{2+} release, 4) Oxidative stress by Reactive Oxygen Species (ROS) production, 5) Depolarization of mitochondrial potential, and as a consequence of these effects, apoptosis. Also in patients, cell death is caused by non-cell autonomous mechanisms such as inhibition of IL6 secretion, inhibition of VEGF secretion and angiogenesis [77, 78].

In the mid 90's, the discovery that the UPS regulates cell cycle progression [84] and NFkB signalling [85] combined with early observations that PIs induce apoptosis [76], sparked the idea that the proteasome might be a suitable anti-neoplastic target that should be targeted with specific inhibitors [86]. Cell cycle progression is driven by oscillations in the activity of cyclin-dependent kinase (CDK) complexes with cyclins. CDK is activated by cyclins (short-lived regulatory proteins that undergo fast degradation at exit from cell cycle) and inhibited by p21 (WAF1/CIP1) or p27 (KIP1) proteins at the G2/M and G1/S transitions, respectively [84]. Cell cycle dependent phosphatases (CDC25A-C) antagonize the CDK complex kinase activity to ensure strict control of the cell cycle and fidelity of proliferation. Levels of all proteins engaged in this pathway is tightly controlled by the UPS and intervention via PIs disrupts the cell cycle accompanied by observations of p53

stabilization, decrease in NFkB level and accumulation of CDK complex activators and inhibitors, in different cell types both in cell culture as in animal models [36, 86-88]. It is not clear why cells arrest at the G2/M and not at the G1/S checkpoint but this might be explained by cell cycle dependent life-time of the p27 protein [89] or by the inability of the UPS to degrade cohesion complexes that hold together sister chromatids prior to mitosis [90]. It is also not clear how cells induce apoptosis under prolonged G2/M arrest. Investigations focused on the elevated levels of the tumour suppressor protein p53 as signalling molecule in this. The p53 protein is a short-lived sensor of DNA damage and oncogene activation, and in non-stressed p53 levels are maintained at low concentration via ubiquitination by the specific E3 ligase MDM2 [91]. Stress and DNA damage sensing kinase pathways (MAPK and ATM) mediated p53 phosphorylation [92] prevents its degradation and activates the transcription factor function of p53 that drives the expression of pro-apoptotic genes like Bax [93]. Early investigations showed a controversial role for the tumour suppressor gene p53 upon PI exposure where apoptosis was p53 dependent [94], p53 independent [95, 96] or showed mixed effects [87] indicating that forced accumulation of p53 might not be an universal pathway for PI induced apoptosis.

The nuclear factor-kB (NFkB) family is an ubiquitously expressed group of transcription factors essential for leukocyte differentiation that drive a strong pro-survival program encompassing the synthesis of growth factors such as interleukin-6 (IL-6), cell adhesion molecules (E-selectin), detoxifiers (COX2 cyclooxygenase-2, NOS nitric oxide synthase) and anti-apoptotic factors (Bcl-2) in response to noxious stimuli including (oxidative) stress, bacterial/viral antigens, inflammation and UV radiation [36]. NFkB is sequestered in the cytoplasm by its inhibitory binding partner (IkB), which after receptor activation is phosphorylated, poly-ubiquitinated and degraded via the UPS allowing the free NFkB to translocates to the nucleus and activate transcription [85, 97]. Reports from the Anderson lab [87, 98, 99] revealed the elevated NFkB activity in hematopoietic cancers, which justifies the rationale of using PIs to inhibit this pathway for malignant cell survival. Of particular interest is their analysis of the gene expression profile in a MM cell line exposed to Bortezomib at concentrations that induce cell cycle arrest and apoptosis [98]. Data showed the expected down regulation of survival pathways and anti-apoptotic proteins as well as up-regulation of cell death signals via the canonical mitochondrial release of cytochrome C and caspase 9 activation but also via the Jun kinase and death receptor/caspase 8 dependent apoptotic pathway. Expression of the 26S proteasome complex genes was found elevated and surprisingly protein folding chaperones like heat shock protein 70 went up indicating activation of a stress response. It was reported

previously that NFkB inhibition might not be enough to induce cell death in MM cells [100], a finding supported by studies on carcinoma cells [101] and myeloma cells [102].

In 2003, three studies, with partially overlapping observations, of PI induced apoptosis appeared. The combined results suggest that a) disruption of the unfolded protein response leads to apoptosis [103], b) generation of reactive oxygen species (ROS) and mitochondrial dysfunction triggers apoptosis [104] and c) induction of the pro-apoptotic Jun kinase pathway together with ROS kills leukemic cells [105]. Accumulation of polyubiquitinated and improperly folded proteins is an undisputed result of proteasome activity inhibition that imposes an unfolded protein burden on the ER [102, 106]. The ER is the cell organelle that serves functions in lipid metabolism, regulated Ca^{2+} storage and chiefly, the assembly, folding and post-translational modification of newly synthesized proteins [107]. Misfolded proteins are retained in the ER and retrotranslocated into the cytosol for proteasome based degradation, a process called ER-associated degradation (ERAD) [8]. PIs can block ERAD, leading to protein accumulation in the ER, which activates the cytoprotective phase of the Unfolded Protein Response (UPR), but also cause cytosolic accumulation of misfolded proteins in the nucleus and cytosol and the heat-shock response in the cytosol. The UPR consists of three branches activated by distinct sensors: the rapidly induced PERK (double-stranded RNA-activated protein kinase (PKR)-like ER kinase), the evolutionarily conserved IRE-1 (inositol requiring enzyme 1) and the ATF6 (activating transcription factor 6), recently reviewed by Hetz [108]. The three sensors are transmembrane proteins that contain a luminal ER domain that interacts and senses unfolded proteins and a cytosolic part that conveys the signal to the nucleus in order to modulate gene expression programs. The initial signals from the UPR as conveyed by PERK result in a general slowdown in protein synthesis for immediate alleviation of the ER protein burden. IRE-1 in turn induces the synthesis of lipids, ERAD proteins and chaperones to increase the ER protein processing capacity and ATF6 induces the synthesis of ER-resident protein folding chaperones such as BiP (member of the heat shock protein HSP70 family [109]. Interestingly, the UPR seems to be activated in two waves: a first acute signalling through PERK, IRE-1 and an autophagy signal aimed mainly at repressing protein synthesis, followed by a second wave of IRE-1, ATF6 and PERK signalling to accommodate and equip the ER for facing up to a stress situation [108]. However, in the case of sustained ERAD block and protein burden, the IRE-1 and AFT6 signals decline while the PERK signalling persists and eventually leads to apoptosis induction via the eIF2α/ATF4/CHOP pathway [110].

The question how a basically cytoprotective pathway like the UPR, can also drive a cell's commitment to apoptosis has just recently been elucidated [111] and it might be physiologically relevant for host defence against the intracellular organisms

Mycobacterium tuberculosis [112]. PERK-mediated phosphorylation of the ubiquitous translation initiating factor eIF2α leads to its inactivation and thereby to global inhibition of mRNA translation but specifically induces ATF4 (activating transcription factor 4) translation [113]. ATF4 drives the expression of another transcription factor, CHOP (C/EBP-homologous protein), which has pro-apoptotic effects by repressing transcription of the anti-apoptotic Bcl-2 protein, induction of TRAIL-R2 death receptors that activate caspase 8 mediated apoptosis, cytotoxic Jun kinase activation and elevation in ROS by upregulating the ERO1α (ER oxidase 1α) that promotes disulfide bond formation in newly translated proteins. [110] The recent mechanism proposed by the Kaufman lab [111] states that immediately after an insult eIF2α phosphorylation slows down translation and subsequent induction of ATF4/CHOP and their downstream gene targets function to restore protein synthesis. In case protein synthesis increases before proteostasis equilibrium is achieved, ERO1α activity continues to increase the ROS levels driving the cell in a pro-apoptotic state that will lead to cell death.

Dissection of the timing of activation, the sequence of events and the magnitude of the signal induced by the three UPR branches discussed above has been performed both in cell lines [114] and in tissues of UPR gene defective mice [113] using ER specific inhibitors of protein folding and trafficking like thapsigargin (Tg) and tunicamycin (Tm). Although ER stress induction by PIs is undisputed in the literature, the nature of a PI effect on the three UPR branches is less clear. At one end of the spectrum Bortezomib induced apoptosis by disrupting the IRE1 signalling in myeloma cells [103] or by inhibiting PERK and eIF2α phosphorylation but activating the ER resident caspase 4 mediated apoptosis in pancreatic cells [115]. These observations can be explained from the mechanism detailed above: although IRE1 signalling seemed disrupted [103], the paper showed a clear accumulation of CHOP that can drive apoptosis. In pancreatic cells CHOP and eIF2α activities were found [115] which according to the Kauffmann model [111] of ER-stress-induced transcription regulation increase protein synthesis leading to apoptosis. At the other side of the spectrum, PIs were found to induce apoptosis via the PERK/ATF4/CHOP terminal UPR in multiple myeloma [102] and head and neck squamous cell carcinoma cells [101]. Interestingly, PI induced UPR via PERK can also activate the expression of cytoprotective elements like the anti-apoptotic Mcl-1 protein [116] and the Nrf2 (nuclear factor-erythroid 2–related factor 2) transcription factor. Moreover, accumulating evidence points towards the existence of an ER-mediated apoptotic cascade proceeding via the ER-resident caspase 4 activation [117-119] besides the two canonical apoptosis pathways regulated by death receptors via caspase 8 and mitochondrial damage in conjunction with capsase 9.

A second mechanism of PI induced apoptosis that has been the subject of intense scrutiny comes from the observation that PIs cause intracellular ROS levels to steadily rise inducing

an oxidative state that pushes the cell towards cell death. Anti-oxidants like vitamin C, *N*-acetylcysteine and gluthathione are able to quench the ROS molecules and prevent apoptotic death [120] except in one study that found that vitamin C can complex to Bortezomib preventing it from inhibiting the proteasome [121]. Although studies with PIs equipped with structurally unrelated warheads to Bortezomib [122, 123] show cytoprotective effects upon antioxidant treatment, the results of antioxidant studies should be interpreted carefully.

Cells robustly maintain their reduction/oxidation (redox) homeostasis in a reducing state to prevent oxidative damage or degradation of vital bio-molecules [124]. This "reductive field" regulates levels of ROS molecules providing them a physiological function as signalling molecules for differentiation, cell cycle progression, growth arrest and apoptosis. ROS molecules such as the superoxide anion ($O_2^{\bullet -}$) hydroxyl radical ($OH^{\bullet}$), hydrogen peroxide (H_2O_2) and several other organic radicals are either side products of electron transport chains in the mitochondrial respiration cycle, of enzymatic metabolism (for instance, p450 cytochrome) or function as signalling molecules produced by the NADPH oxidases (NOX) family [125]. From the atoms necessary for life, sulphur is easily oxidized and sulphur containing amino acids like methionine and cysteine are prone to react with ROS. Cysteine is the main nucleophile in the active site of most phosphatises [126], ubiquitin chain E1,E2,E3 ubiquitin ligases and their antagonists deubiquitinating enzymes [127] which are essential enzymes for the post-translational control of vital pathways in the cell. Evidence accumulates that ROS can exert both physiological and pathological effects by oxidizing active cysteines and that a plethora of regulatory proteins (NFkB, p53, pyruvate kinase, ATM, amongst others) have evolved ROS sensing propensities by strategically incorporating cysteine residues that upon reacting with ROS influence the activity of the protein [128].

ROS are continuously produced by leakage of electrons in the mitochondrial respiratory chain, in the ER by the activity of the ERO1α flavoenzyme needed for disulfide bond formation of newly translated proteins, in phagosomes for host defense against microorganisms and by NOXs at the cytosol side of the plasma membrane upon recruitment by major signalling receptors to participate via ROS production to the amplification of their signalling cascades in growth and proliferation (e.g. neuronal growth factor, NGF), immune response (e.g. toll like receptors, TLR) and apoptosis (e.g. tumor necrosis factor α ,TNFα) [129]. Although the first evaluations that PI induced ROS is necessary for apoptosis were performed in solid-tumour model systems [101, 104], the PI effects in hematopoietic malignancies like mantle cell lymphoma [96], leukemia cells [123] and MM [130, 131] showed to be more robust. Mitochondria, and ER-stress induced ROS [101], were indicated as source of ROS generation because all studies found a decrease of

the mitochondrial membrane potential ($\Delta\psi_m$) that is indicative of mitochondrial damage leading to leakage of ROS in the cytoplasm. Mitochondria received most attention because they are both a ROS producer and a convergence point for ROS induced apoptosis which upon damage release cytochrome C that together with Apaf-1 and pro-caspase 9 form the canonical apoptosome system that activates executioner caspases to induce cell death [120]. Treatment with anti-oxidants reduced the ROS levels and the apoptotic events, indicating that ROS play an essential role in PI induced apoptosis. However, the use of organelle specific ROS reporters would be advisable for the future for more precise determination of the ROS source.

Interestingly, differences in apoptosis induction pathways were found between different PIs with Bortezomib mainly functioning through the mitochondria/caspase 9 pathway [101, 104, 130] and NPI-0052 mainly through the FADD (Fas associated death domain)/caspase 8 pathway [123, 130]. Bortezomib has been shown to repress the cyto-protective Bcl-2 protein [130] leading to release of the pro-apoptotic Bax protein which together with Bak injures the mitochondria [132]. Activation of the FADD is more difficult to explain but it might proceed via JNK signalling or terminal UPR response to ER stress [110]. It should be mentioned that the proapoptotic Bak and Bax proteins also reside in the ER and are suggested to regulate Ca^{2+} storage and apoptotic events [133]. Release of Ca^{2+} in the cytoplasm can trigger apoptosis by activating the Ca^{2+} dependent CaMKII that signals to downstream apoptotic pathways [134]. Alternative mechanisms of Bortezomib induced apoptosis are the stabilization of the pro-apoptotic protein NOXA in medulloblastoma independently of p53 activity [135] or p53 dependent in mantle cell lymphoma [96]. Both were ROS dependent and function because NOXA binds to and displaces the anti-apoptotic Mcl-1 from a complex with Bak [136], which upon release binds to Bax promoting mitochondrial injury. As an exception, PI induced but ROS independent apoptosis was found in colon cancer models to proceed by p53 stabilization, driving the expression of pro-apoptotic PUMA (p53 up-regulated modulator of apoptosis) that in turn promoted Bax activated apoptosis [83]. Evidence is accumulating that the ER plays a central role in PI mediated apoptosis by release of Ca^{2+} in the cytoplasm, UPR signalling and via an ER resident caspase 4 pathway [117-119] that gets activated upon ER stress. Recent work shows that caspase 4 is recruited to the ER by transmembrane protein 214 (TMEM214), which was essential for ER stress-induced pro-caspase-4 activation and apoptosis [119]. Taken together, a logic interpretation is that ROS report upon the stress state and integrity of an organelle like the ER or the mitochondrium and in some cases, excessive ROS production might be a symptom of their injury.

The onset of apoptosis by PIs has been linked to activation of intracellular stress sensing kinase cascades like the MAPK (mitogen-activated protein kinase) pathways, which

physiologically govern cell proliferation, stress response and survival [137]. Of the three MAPK modules, the Jun-N-terminal kinase (JNK) and p38 MAPK branches are associated with induction of apoptosis while the extracellular signal-regulating kinase (ERK) is cytoprotective [138]. PIs appear to induce apoptosis in MM cells in part by suppressing ERK and activating JNK [105, 137, 139], which was accompanied with increased ROS production. It remains unclear whether ROS production led to JNK activation and ERK repression or merely a symptom of damaged mitochondria after action of Bax-Bak membrane destabilizing complexes. Interestingly, caspase 8 activation was found to take place [105, 137] indicating that the extracellular death receptor pathway was activated. Studies of ER stress and JNK activation showed that the IRE1 branch of UPR binds to TRAF2 (TNF receptor associated factor 2) an adaptor protein of the TNFα receptor and via a kinase signalling cascade can activate JNK [140]. Recent studies, reviewed by David Ron [110], show that both IRE1 and the PERK branches of the UPR can activate the pro-apoptotic JNK pathway or directly interact with mitochondrial membrane permeabilizing factors which link the ER stress effects of PIs with the four known pathways of apoptosis induction via the extrinsic caspase 8, the mitochondrial caspase 9, the ER resident caspase 4 and the Ca^{2+} dependent CaMKII. Lately, Bortezomib has been used in clinical experiments with organ transplantation as an agent to deplete healthy plasma cells that produce donor-specific anti-human leukocyte antigen antibodies (DSAs), responsible for graft rejection (reviewed by the Woodle group [141]). Although the mechanism of cell death is not known, this work suggests that some of the mechanisms discussed above are also at play in healthy tissues.

Resistance to proteasome inhibitors

PIs ability to overcome the resistance to classic anticancer therapies brought about a wave of initial enthusiasm [87]. However, PI resistant tumour clones appeared that employ various mechanisms of protection including upregulating proteasome synthesis (80), drug efflux pumps such as Pgp [142], and PI metabolizing enzymes [78]. Interestingly, PI induced UPR via PERK can also activate the expression of cytoprotective elements such as the anti-apoptotic Mcl-1 protein [116] and the Nrf2 (nuclear factor-erythroid 2–related factor 2) transcription factor. Nrf2 phosphorylation liberates it from its inhibitor Kelch-like ECH-associated protein 1 (KEAP1), driving the expression of some 200 genes involved in oxidative stress/redox signalling [143] which can ensue resistance to PI treatment.

Constitutive activation of Nrf2 is emerging as a prominent molecular feature in many tumour types [144] and Nrf2 phosphorylation likely restores the redox balance in

oxidatively stressed tumours and clears electrophilic xenobiotics. Elevated Nrf2 levels in acute myeloma leukaemia [145] correlated with reduced ROS levels and sensitivity for Bortezomib treatment and it has been shown that Nrf2 and Nrf1 [146, 147] also upregulate the expression of proteasome genes that increases the capacity to remove damaged proteins and scavenge PIs [148]. Other mechanism of PI resistance in human myelomonocytic THP1 cells were an Ala49Thr mutation in the highly conserved binding pocket of the β5 subunit accompanied by overexpression of the PSMB5 gene [149]. Another study of induced Bortezomib adaptation in leukaemia and myeloma cells showed increased expression of functional β5, β2 and β1 subunits, 11S activator caps, alongside reduced protein biosynthesis and transcription of chaperones [150].

Aggresome formation [115], upregulation of chaperones HSP27 and HSP70 [115] and autophagy are also pathways that convey resistance to PIs. Autophagy meditates the breakdown of insoluble protein aggregates and aggresomes in the cytosol through encasing it in a double-layered membrane that are lately fused with the lysosome for degradation into its constitutive components [151]. Autophagy can take over the processing of proteasome substrates, mitigating cellular stress and ultimately apoptosis and cell death. The link between autophagy and the proteasome is still uncertain but evidence is pointing towards ER-stress mediated autophagy [152, 153]. However, the role of autophagy in PI induced apoptosis is controversial as some studies suggest that autophagy is a mechanism of resistance to PIs [152, 153] while others suggest that autophagy might enhance PI lethality perhaps depending on the cell type and the cell state being either normal or oncogenicaly transformed [154-156]. An intriguing study in yeast proteasomes showed that S-glutathiolation, a post-translational modification, controls the 20S gate opening. The 20S CP itself might be under redox control as the activity of S-glutathiolation on two discrete cysteine residues of the α5 subunits that control 20S gate opening proved to open the gate, increasing the protein processing power of the proteasome [157].

It should be noted that the mechanistic knowledge discussed here comes from studies in different cell culture models, primary cell cultures and animals. Immortal cell cultures often have disturbed genetic patterns that might not reflect the defects encountered during oncogenesis *in vivo,* so they might react differently to PI stress. The un-physiologically high glucose concentrations in cell culture media might be taken into account as well; it affects the cell metabolism and may influence the PI response. There are clear differences in PI response between tissues, as hematopoietic cells show fast activation of terminal UPR, intensified ROS production, mitochondrial damage and onset of apoptosis. In contrary, adherent growing neuronal, epithelial or fibroblast cell models or the ones closer to normal tissues like MEFs (mouse embryonic fibroblasts) show a

higher tolerance to PI requiring higher PI dosing, more delayed apoptotic responses, less ROS induction and apoptosis onset via other pathways than the mitochondrial. This might be in part explained by the composition of the proteasome in the cell, either constitutive or immune proteasome which is often overlooked in studies but it is not unimportant because PIs have different affinities for constitutive and immune proteasome. Physiological details like the total proteasome concentration in the cell, the presence of efflux pumps and perhaps the shape of the cell might matter. In a spherical cell mitochondria might be closer to the ER thus ROS species emanating from the stressed ER [109] might reach other organelles faster by diffusion and affect a larger area than in the case of a polarized and elongated cell where the signalling gradient might be more diffuse giving the cell more time to take counteractive actions by activating defence mechanisms like anti-oxidant or anti-apoptotic factors production. It has been postulated that secretory cells like B-cell that produce large quantities of antibodies or β-cells from pancreatic islets endowed with the production of insulin poses an intrinsically stressed ER that activates a terminal UPR earlier than other cell types [78]. Poor oxygen transport into solid tumours might render the cells hypoxic, which activates the HIF1α (hypoxia induced factor) that in turn can activate Nrf2 to drive ROS quenching genes [128] making these cells less vulnerable to PI induced ROS.

In conclusion, this review illustrates that many genes and cellular events are involved in PI-induced apoptosis. Global systems biology approaches may be used to identify the gene partners, their regulation, post-translational modification and kinetics in order to establish which pathway is chiefly responsible for induction of apoptosis. A cell's decision to commit to apoptosis might be a convergence of signals from several pathways underscoring the need for system wide analysis. Moreover, ROS and Ca^{2+} levels should also be determined because these factors have important regulatory and signalling function. First of all, the concentration, constitution and activity of the proteasome in a given cell population should be determined [74]. Second, global mass spectrometry driven proteomics studies can be used to determine the protein concentrations of as much as possible proteins in order to see which pathways are up or down regulated. Third, analysis of the transcriptome is necessary to determine the response at the level of gene transcription. Fourth, these measurements should be performed at several time points after PI treatment to determine the kinetics of different pathway responses. With the advent of superior MS methods and machines, determination of PTM status of proteins has become increasingly feasible as in the case of kinases [158] and phosphatases [126] activities. An interesting method to probe the reactivity of cysteine side chains has been recently launched [159] which might be instrumental for determination of the oxidation state of proteins, an important PTM to be scored when dealing with ROS induced phenomena.

This technique uses a smart adaptation of the general alkylation principle of cysteines by iodoacetamide combined with global activity based profiling, to determine the hyper reactive cysteines in the proteome suggested to play a role in the catalytic site of enzymes or function as ROS sensors (see Figure 5). Combination of these techniques might provide us with a clearer picture of the course of events during PI induced apoptosis and will surely afford novel start points for therapy.

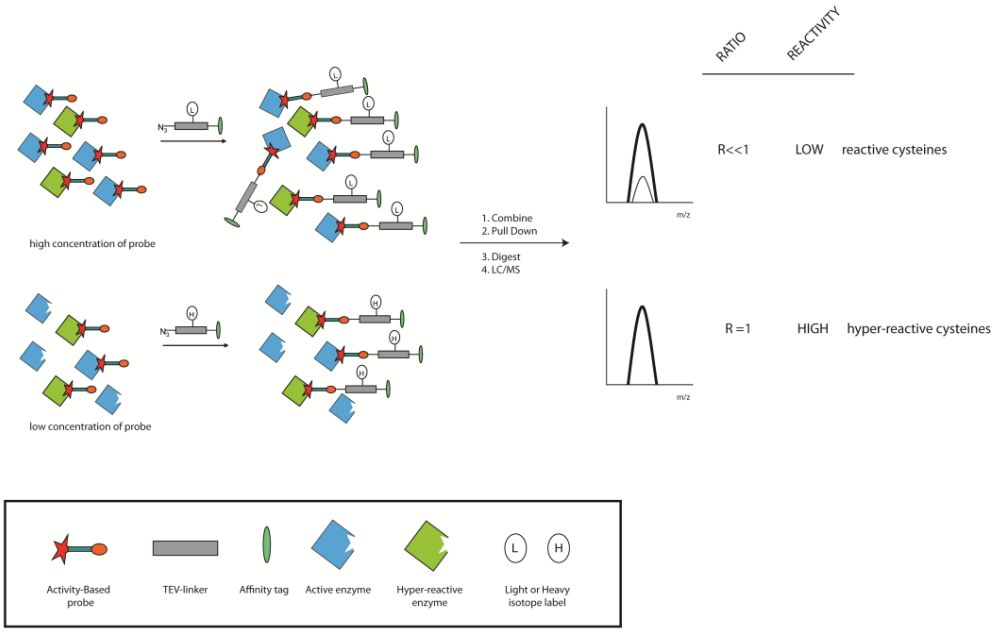

***Figure 5**. Basic scheme of two-step ABPP coupled with isotope labeling which allows quantification of the cysteine reactivity status.*

The global picture emerges that under physiological conditions, the cell is kept in a reductive state in order to prevent oxidative damage of essential bio-molecules like DNA, RNA, proteins and lipids. Blocking the proteasome in the nucleus, cytoplasm and in the ERAD leads to arrest of NFkB signalling, increased p53 levels, cell cycle arrest, ER stress inducing some form of UPR signalling, possible ER-resident caspase 4 activation and elevated production of ROS. Release of Ca^{2+} from the ER, depletion of glutathione pools and signalling via the JNK pathway injure the mitochondria impairing the oxidative phosphorylation energy pathway which further increases ROS production pushing the cell in an oxidative phase. If protein synthesis continues, ROS production will further damage the mitochondria induce cytochrome C release and activation of caspase 9 that, in

conjunction with caspase 8 activation via upregulation of death receptor signalling, mediate the onset of cell death by apoptosis (Figure 6).

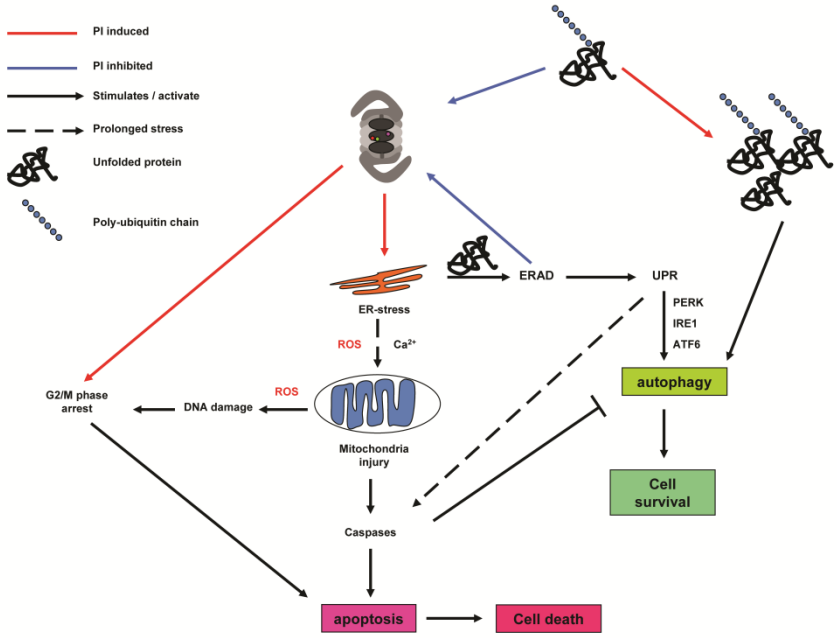

Figure 6. *Global picture of our view of the cell behavior after PI exposure. Under physiological conditions, proteins assigned for degradation are cleared by the ubiquitin proteasome system. Acute proteasome inhibition leads to adverse effects on cells: cell cycle arrest in the G2/M phase checkpoint, ER stress, activation of the UPR system and accumulation of polyubiquitinated proteins that in some cases are cleared via autophagy. Sustained proteasome inhibition leads to release of ROS, mitochondrial injury, DNA damage, activation of cell death pathways and onset of apoptosis.*

References

1. Baumeister, W., *et al.*, *The proteasome: paradigm of a self-compartmentalizing protease.* Cell, 1998. **92**(3): p. 367-380.
2. Hershko, A. and A. Ciechanover, *The ubiquitin system.* Annu. Rev. Biochem., 1998. **67**: p. 425-479.
3. Hershko, A., *The ubiquitin pathway for protein degradation.* Trends Biochem. Sci., 1991. **16**(7): p. 265-268.
4. Grune, T., T. Reinheckel, and K.J. Davies, *Degradation of oxidized proteins in mammalian cells.* FASEB, 1997. **11**(7): p. 526-534.
5. Groettrup, M., C.J. Kirk, and M. Basler, *Proteasomes in immune cells: more than peptide producers?* Nat. Rev. Immun., 2010. **10**(1): p. 73-78.
6. Kloetzel, P.M., *Antigen processing by the proteasome.* Nat. Rev. Mol. Cell Bio., 2001. **2**(3): p. 179-187.

7. Kloetzel, P.M. and F. Ossendorp, *Proteasome and peptidase function in MHC-class-I-mediated antigen presentation.* Cur. Op. Immu., 2004. **16**(1): p. 76-81.
8. Smith, M.H., H.L. Ploegh, and J.S. Weissman, *Road to Ruin: Targeting Proteins for Degradation in the Endoplasmic Reticulum.* Science, 2011. **334**(6059): p. 1086-1090.
9. Lowe, J., *et al.*, *Crystal structure of the 20S proteasome from the archaeon T. acidophilum at 3.4 A resolution.* Science, 1995. **268**(5210): p. 533-539.
10. Groll, M., *et al.*, *Structure of 20S proteasome from yeast at 2.4 A resolution.* Nature, 1997. **386**(6624): p. 463-471.
11. Unno, M., *et al.*, *Structure determination of the constitutive 20S proteasome from bovine liver at 2.75 A resolution.* J. Biochem., 2002. **131**(2): p. 171-173.
12. Gallastegui, N. and M. Groll, *The 26S proteasome: assembly and function of a destructive machine.* Trends Biochem. Sci., 2010. **35**(11): p. 634-642.
13. Tomko, R.J., Jr. and M. Hochstrasser, *Order of the proteasomal ATPases and eukaryotic proteasome assembly.* Cell Biochem. and Bioph., 2011. **60**(1-2): p. 13-20.
14. Tanaka, K., T. Mizushima, and Y. Saeki, *The proteasome: molecular machinery and pathophysiological roles.* Biol. Chem., 2012. **393**(4): p. 217-234.
15. Tanaka, K., *Role of proteasomes modified by interferon-gamma in antigen processing.* J. Leuko. Biol., 1994. **56**(5): p. 571-575.
16. Akiyama, K., *et al.*, *cDNA cloning and interferon gamma down-regulation of proteasomal subunits X and Y.* Science, 1994. **265**(5176): p. 1231-1234.
17. Griffin, T.A., *et al.*, *Immunoproteasome assembly: cooperative incorporation of interferon gamma (IFN-gamma)-inducible subunits.* J. Exp. Med., 1998. **187**(1): p. 97-104.
18. Groettrup, M., *et al.*, *The subunits MECL-1 and LMP2 are mutually required for incorporation into the 20S proteasome.* PNAS, 1997. **94**(17): p. 8970-8975.
19. Huber, Eva M., *et al.*, *Immuno- and Constitutive Proteasome Crystal Structures Reveal Differences in Substrate and Inhibitor Specificity.* Cell, 2012. **148**(4): p. 727-738.
20. Murata, S., *et al.*, *Regulation of CD8+ T cell development by thymus-specific proteasomes.* Science, 2007. **316**(5829): p. 1349-1353.
21. Tomaru, U., *et al.*, *Exclusive expression of proteasome subunit {beta}5t in the human thymic cortex.* Blood, 2009. **113**(21): p. 5186-5191.
22. Florea, B.I., *et al.*, *Activity-based profiling reveals reactivity of the murine thymoproteasome-specific subunit beta5t.* Chem. & Biol., 2010. **17**(8): p. 795-801.
23. Drews, O., *et al.*, *Mammalian proteasome subpopulations with distinct molecular compositions and proteolytic activities.* MCP, 2007. **6**(11): p. 2021-2031.
24. Guillaume, B., *et al.*, *Two abundant proteasome subtypes that uniquely process some antigens presented by HLA class I molecules.* PNAS, 2010. **107**(43): p. 18599-18604.
25. Klare, N., *et al.*, *Intermediate-type 20 S proteasomes in HeLa cells: "asymmetric" subunit composition, diversity and adaptation.* J. Mol. Biol., 2007. **373**(1): p. 1-10.
26. Vigneron, N. and B.J. Van den Eynde, *Proteasome subtypes and the processing of tumor antigens: increasing antigenic diversity.* Curr. Op. Immu., 2012. **24**(1): p. 84-91.
27. De, M., *et al.*, *Beta 2 subunit propeptides influence cooperative proteasome assembly.* J. Biol. Chem., 2003. **278**(8): p. 6153-6159.
28. Gomes, A.V., *et al.*, *Contrasting proteome biology and functional heterogeneity of the 20 S proteasome complexes in mammalian tissues.* Molecular & cellular proteomics : MCP, 2009. **8**(2): p. 302-315.
29. Glickman, M.H., *et al.*, *A subcomplex of the proteasome regulatory particle required for ubiquitin-conjugate degradation and related to the COP9-signalosome and eIF3.* Cell, 1998. **94**(5): p. 615-623.
30. Lander, G.C., *et al.*, *Complete subunit architecture of the proteasome regulatory particle.* Nature, 2012. **482**(7384): p. 186-191.
31. Liu, C.W. and A.D. Jacobson, *Functions of the 19S complex in proteasomal degradation.* Trends Biochem. Sci., 2013. **38**(2): p. 103-110.
32. Stadtmueller, B.M. and C.P. Hill, *Proteasome activators.* Mol. Cell, 2011. **41**(1): p. 8-19.
33. Beck, P., C. Dubiella, and M. Groll, *Covalent and non-covalent reversible proteasome inhibition.* Biol. Chem., 2012. **393**(10): p. 1101-1120.

34. Kisselev, Alexei F., W.A. van der Linden, and Herman S. Overkleeft, *Proteasome Inhibitors: An Expanding Army Attacking a Unique Target.* Chem. & Bio., 2012. **19**(1): p. 99-115.
35. Rentsch, A., *et al.*, *Synthesis and Pharmacology of Proteasome Inhibitors.* Ang. Chem. Int. Ed., 2013. **52**(21): p. 5450-5488.
36. Adams, J., *The proteasome: a suitable antineoplastic target.* Nat Rev Cancer, 2004. **4**(5): p. 349-360.
37. Groll, M., *et al.*, *Crystal Structure of Epoxomicin:20S Proteasome Reveals a Molecular Basis for Selectivity of α′,β′-Epoxyketone Proteasome Inhibitors.* JACS, 2000. **122**(6): p. 1237-1238.
38. Adams, J., *et al.*, *Potent and selective inhibitors of the proteasome: Dipeptidyl boronic acids.* Bioorg. & Med. Chem. Let., 1998. **8**(4): p. 333-338.
39. San Miguel, J.F., H. van de Velde, and P.G. Richardson, *Bortezomib plus Melphalan and Prednisone for Multiple Myeloma Reply.* New Eng. J. Med., 2008. **359**(24): p. 2613-2614.
40. Groll, M., *et al.*, *Crystal Structure of the Boronic Acid-Based Proteasome Inhibitor Bortezomib in Complex with the Yeast 20S Proteasome.* Structure, 2006. **14**(3): p. 451-456.
41. Bogyo, M., *et al.*, *Covalent modification of the active site threonine of proteasomal β subunits and the Escherichia coli homolog HslV by a new class of inhibitors.* PNAS, 1997. **94**(13): p. 6629-6634.
42. Nazif, T. and M. Bogyo, *Global analysis of proteasomal substrate specificity using positional-scanning libraries of covalent inhibitors.* PNAS, 2001. **98**(6): p. 2967-2972.
43. Groll, M., *et al.*, *Probing Structural Determinants Distal to the Site of Hydrolysis that Control Substrate Specificity of the 20S Proteasome.* Chem. & Biol., 2002. **9**(5): p. 655-662.
44. Groll, M., R. Huber, and B.C.M. Potts, *Crystal Structures of Salinosporamide A (NPI-0052) and B (NPI-0047) in Complex with the 20S Proteasome Reveal Important Consequences of β-Lactone Ring Opening and a Mechanism for Irreversible Binding.* JACS, 2006. **128**(15): p. 5136-5141.
45. Goldberg, A.L., *Development of proteasome inhibitors as research tools and cancer drugs.* J. Cell Biol., 2012. **199**(4): p. 583-588.
46. Kale, A.J. and B.S. Moore, *Molecular mechanisms of acquired proteasome inhibitor resistance.* J. Med. Chem., 2012. **55**(23): p. 10317-10327.
47. Chauhan, D., *et al.*, *The bortezomib/proteasome inhibitor PS-341 and triterpenoid CDDO-Im induce synergistic anti-multiple myeloma (MM) activity and overcome bortezomib resistance.* Blood, 2004. **103**(8): p. 3158-3166.
48. Dorsey, B.D., *et al.*, *Discovery of a Potent, Selective, and Orally Active Proteasome Inhibitor for the Treatment of Cancer.* J. Med. Chem., 2008. **51**(4): p. 1068-1072.
49. Piva, R., *et al.*, *CEP-18770: A novel, orally active proteasome inhibitor with a tumor-selective pharmacologic profile competitive with bortezomib.* Blood, 2008. **111**(5): p. 2765-2775.
50. Kupperman, E., *et al.*, *Evaluation of the Proteasome Inhibitor MLN9708 in Preclinical Models of Human Cancer.* Cancer Res., 2010. **70**(5): p. 1970-1980.
51. O'Connor, O.A., *et al.*, *A Phase 1 Dose Escalation Study of the Safety and Pharmacokinetics of the Novel Proteasome Inhibitor Carfilzomib (PR-171) in Patients with Hematologic Malignancies.* Clinical Cancer Res., 2009. **15**(22): p. 7085-7091.
52. Arastu-Kapur, S., *et al.*, *Nonproteasomal Targets of the Proteasome Inhibitors Bortezomib and Carfilzomib: a Link to Clinical Adverse Events.* Clinical Cancer Research, 2011. **17**(9): p. 2734-2743.
53. Molineaux, S.M., *Molecular Pathways: Targeting Proteasomal Protein Degradation in Cancer.* Clin. Cancer Res., 2012. **18**(1): p. 15-20.
54. Zhou, H.-J., *et al.*, *Design and Synthesis of an Orally Bioavailable and Selective Peptide Epoxyketone Proteasome Inhibitor (PR-047).* J. Med. Chem., 2009. **52**(9): p. 3028-3038.
55. C. Potts, B., *et al.*, *Marizomib, a Proteasome Inhibitor for All Seasons: Preclinical Profile and a Framework for Clinical Trials.* Curr. Cancer Drug Targ., 2011. **11**(3): p. 254-284.
56. Gaczynska, M. and P.A. Osmulski, *Harnessing proteasome dynamics and allostery in drug design.* Antioxid. Redox Signal., 2013.
57. Zhao, Y., *et al.*, *Targeting neddylation pathways to inactivate Cullin-RING ligases for anti-cancer therapy.* Antioxid. Redox Signal., 2013.
58. McKinnon, C. and S.J. Tabrizi, *The Ubiquitin-Proteasome System in Neurodegeneration.* Antioxid. Redox Signal., 2013.
59. Drews, O. and H. Taegtmeyer, *Regulation of the Ubiquitin-Proteasome System in Heart Disease: The Basis for New Therapeutic Strategies.* Antioxid. Redox Signal., 2013.

60. Wilck, N. and A. Ludwig, *Targeting the Ubiquitin-Proteasome System in Atherosclerosis: Status quo, challenges and perspectives.* Antioxid. Redox Signal., 2013.
61. Meiners, S., *et al.*, *Regulation of the Proteasome: Evaluating the Lung Proteasome as a New Therapeutic Target.* Antioxid. Redox Signal., 2013.
62. Craiu, A., *et al.*, *Lactacystin and clasto-Lactacystin β-Lactone Modify Multiple Proteasome β-Subunits and Inhibit Intracellular Protein Degradation and Major Histocompatibility Complex Class I Antigen Presentation.* J. Biol. Chem., 1997. **272**(20): p. 13437-13445.
63. Fenteany, G., *et al.*, *Inhibition of proteasome activities and subunit-specific amino-terminal threonine modification by lactacystin.* Science, 1995. **268**(5211): p. 726-731.
64. Sin, N., *et al.*, *Total synthesis of the-potent proteasome inhibitor epoxomicin: a useful tool for understanding proteasome biology.* Bioorg. & Med. Chem. Lett., 1999. **9**(15): p. 2283-2288.
65. Meng, L., *et al.*, *Epoxomicin, a potent and selective proteasome inhibitor, exhibits in vivo antiinflammatory activity.* PNAS, 1999. **96**(18): p. 10403-10408.
66. Bogyo, M., *Screening for selective small molecule inhibitors of the proteasome using activity-based probes.* Ubi. Prot. Degra., Pt B, 2005. **399**: p. 609-+.
67. Berkers, C.R., *et al.*, *Activity probe for in vivo profiling of the specificity of proteasome inhibitor bortezomib.* Nat. Methods, 2005. **2**(5): p. 357-362.
68. Verdoes, M., *et al.*, *A Fluorescent Broad-Spectrum Proteasome Inhibitor for Labeling Proteasomes In Vitro and In Vivo.* Chem. & Biol., 2006. **13**(11): p. 1217-1226.
69. Verdoes, M., *et al.*, *Chemical proteomics profiling of proteasome activity.* Methods Mol. Biol., 2006. **328**: p. 51-69.
70. Verdoes, M., *et al.*, *A panel of subunit-selective activity-based proteasome probes.* Org. & Biomol. Chem., 2010. **8**(12): p. 2719-2727.
71. Geurink, P.P., *et al.*, *Incorporation of Non-natural Amino Acids Improves Cell Permeability and Potency of Specific Inhibitors of Proteasome Trypsin-like Sites.* J. Med. Chem., 2013.
72. Mirabella, Anne C., *et al.*, *Specific Cell-Permeable Inhibitor of Proteasome Trypsin-like Sites Selectively Sensitizes Myeloma Cells to Bortezomib and Carfilzomib.* Chem. & Biol., 2011. **18**(5): p. 608-618.
73. Carmony, K.C., *et al.*, *A bright approach to the immunoproteasome: Development of LMP2/β1i-specific imaging probes.* Bioorg. & Med. Chem., 2012. **20**(2): p. 607-613.
74. Li, N., *et al.*, *Relative quantification of proteasome activity by activity-based protein profiling and LC-MS/MS.* Nat. Protoc., 2013. **8**(6): p. 1155-1168.
75. An, B., *et al.*, *Novel dipeptidyl proteasome inhibitors overcome Bcl-2 protective function and selectively accumulate the cyclin-dependent kinase inhibitor p27 and induce apoptosis in transformed, but not normal, human fibroblasts.* Cell Death Differ., 1998. **5**(12): p. 1062-1075.
76. Drexler, H.C., *Activation of the cell death program by inhibition of proteasome function.* PNAS, 1997. **94**(3): p. 855-860.
77. Adams, J. and R. Stein, *Novel inhibitors of the proteasome and their therapeutic use in inflammation.* Annu.Rep. Med. Chem., 1996. **31**: p. 279-288.
78. Orlowski, R.Z. and D.J. Kuhn, *Proteasome inhibitors in cancer therapy: lessons from the first decade.* Clin. Cancer Res., 2008. **14**(6): p. 1649-1657.
79. Kisselev, A.F., A. Callard, and A.L. Goldberg, *Importance of the different proteolytic sites of the proteasome and the efficacy of inhibitors varies with the protein substrate.* J. Biol. Chem., 2006. **281**(13): p. 8582-8590.
80. Miller, C.P., *et al.*, *Specific and prolonged proteasome inhibition dictates apoptosis induction by marizomib and its analogs.* Chemico-Biol. Interac., 2011. **194**(1): p. 58-68.
81. Bianchi, G., *et al.*, *The proteasome load versus capacity balance determines apoptotic sensitivity of multiple myeloma cells to proteasome inhibition.* Blood, 2009. **113**(13): p. 3040-3049.
82. Nencioni, A., *et al.*, *Proteasome inhibitors: antitumor effects and beyond.* Leukemia, 2007. **21**(1): p. 30-36.
83. Ding, W.X., *et al.*, *A coordinated action of Bax, PUMA, and p53 promotes MG132-induced mitochondria activation and apoptosis in colon cancer cells.* Mol. Cancer Ther., 2007. **6**(3): p. 1062-1069.
84. King, R.W., *et al.*, *How proteolysis drives the cell cycle.* Science, 1996. **274**(5293): p. 1652-1659.
85. Palombella, V.J., *et al.*, *The Ubiquitin-Proteasome Pathway Is Required for Processing the Nf-Kappa-B1 Precursor Protein and the Activation of Nf-Kappa-B.* Cell, 1994. **78**(5): p. 773-785.

86. Adams, J., *et al.*, *Proteasome inhibitors: A novel class of potent and effective antitumor agents.* Cancer Res., 1999. **59**(11): p. 2615-2622.
87. Hideshima, T., *et al.*, *The proteasome inhibitor PS-341 inhibits growth, induces apoptosis, and overcomes drug resistance in human multiple myeloma cells.* Cancer Res., 2001. **61**(7): p. 3071-3076.
88. Ling, Y.H., *et al.*, *Mechanisms of proteasome inhibitor PS-341-induced G(2)-M-phase arrest and apoptosis in human non-small cell lung cancer cell lines.* Clin. Cancer Res., 2003. **9**(3): p. 1145-1154.
89. Pagano, M., *et al.*, *Role of the Ubiquitin-Proteasome Pathway in Regulating Abundance of the Cyclin-Dependent Kinase Inhibitor P27.* Science, 1995. **269**(5224): p. 682-685.
90. Rao, H., *et al.*, *Degradation of a cohesin subunit by the N-end rule pathway is essential for chromosome stability.* Nature, 2001. **410**(6831): p. 955-959.
91. Haupt, Y., *et al.*, *Mdm2 promotes the rapid degradation of p53.* Nature, 1997. **387**(6630): p. 296-299.
92. Wu, G.S., *The functional interactions between the p53 and MAPK signaling pathways.* Cancer Biol. & Ther., 2004. **3**(2): p. 156-161.
93. Miyashita, T. and J.C. Reed, *Tumor-Suppressor P53 Is a Direct Transcriptional Activator of the Human Bax Gene.* Cell, 1995. **80**(2): p. 293-299.
94. Lopes, U.G., *et al.*, *p53-dependent induction of apoptosis by proteasome inhibitors.* J Biol. Chem., 1997. **272**(20): p. 12893-12896.
95. Herrmann, J.L., *et al.*, *Prostate carcinoma cell death resulting from inhibition of proteasome activity is independent of functional Bcl-2 and p53.* Oncogene, 1998. **17**(22): p. 2889-2899.
96. Perez-Galan, P., *et al.*, *The proteasome inhibitor bortezomib induces apoptosis in mantle-cell lymphoma through generation of ROS and Noxa activation independent of p53 status.* Blood, 2006. **107**(1): p. 257-264.
97. Ghosh, S. and M. Karin, *Missing pieces in the NF-kappa B puzzle.* Cell, 2002. **109**: p. S81-S96.
98. Mitsiades, N., *et al.*, *Molecular sequelae of proteasome inhibition in human multiple myeloma cells.* PNAS, 2002. **99**(22): p. 14374-14379.
99. Mitsiades, N., *et al.*, *The proteasome inhibitor PS-341 potentiates sensitivity of multiple myeloma cells to conventional chemotherapeutic agents: therapeutic applications.* Blood, 2003. **101**(6): p. 2377-2380.
100. Hideshima, T., *et al.*, *NF-kappa B as a therapeutic target in multiple myeloma.* J. Biol.l Chem., 2002. **277**(19): p. 16639-16647.
101. Fribley, A., Q.H. Zeng, and C.Y. Wang, *Proteasome inhibitor PS-341 induces a apoptosis through induction of endoplasmic reticulum stress-reactive oxygen species in head and neck squamous cell carcinoma cells.* Mol. Cell. Biol., 2004. **24**(22): p. 9695-9704.
102. Obeng, E.A., *et al.*, *Proteasome inhibitors induce a terminal unfolded protein response in multiple myeloma cells.* Blood, 2006. **107**(12): p. 4907-4916.
103. Lee, A.H., *et al.*, *Proteasome inhibitors disrupt the unfolded protein response in myeloma cells.* PNAS, 2003. **100**(17): p. 9946-9951.
104. Ling, Y.H., *et al.*, *Reactive oxygen species generation and mitochondrial dysfunction in the apoptotic response to bortezomib, a novel proteasome inhibitor, in human H460 non-small cell lung cancer cells.* J. Biol. Chem., 2003. **278**(36): p. 33714-33723.
105. Yu, C.R., *et al.*, *The proteasome inhibitor bortezomib interacts synergistically with histone deacetylase inhibitors to induce apoptosis in Bcr/Abl(+) cells sensitive and resistant to STI571.* Blood, 2003. **102**(10): p. 3765-3774.
106. Werner, E.D., J.L. Brodsky, and A.A. McCracken, *Proteasome-dependent endoplasmic reticulum-associated protein degradation: an unconventional route to a familiar fate.* PNAS, 1996. **93**(24): p. 13797-13801.
107. Ellgaard, L. and A. Helenius, *Quality control in the endoplasmic reticulum.* Nature Rev. Mol. Cell Biol., 2003. **4**(3): p. 181-191.
108. Hetz, C., *The unfolded protein response: controlling cell fate decisions under ER stress and beyond.* Nature Rev. Mol. Cell Biol., 2012. **13**(2): p. 89-102.
109. Walter, P. and D. Ron, *The unfolded protein response: from stress pathway to homeostatic regulation.* Science, 2011. **334**(6059): p. 1081-1086.
110. Tabas, I. and D. Ron, *Integrating the mechanisms of apoptosis induced by endoplasmic reticulum stress.* Nature Cell Biol., 2011. **13**(3): p. 184-190.

111. Han, J., *et al.*, *ER-stress-induced transcriptional regulation increases protein synthesis leading to cell death.* Nature Cell Biol., 2013. **15**(5): p. 481-+.
112. Seimon, T.A., *et al.*, *Induction of ER stress in macrophages of tuberculosis granulomas.* PLoS One, 2010. **5**(9): p. e12772.
113. Harding, H.P., *et al.*, *Regulated translation initiation controls stress-induced gene expression in mammalian cells.* Mol. Cell, 2000. **6**(5): p. 1099-1108.
114. Lin, J.H., *et al.*, *IRE1 signaling affects cell fate during the unfolded protein response.* Science, 2007. **318**(5852): p. 944-949.
115. Nawrocki, S.T., *et al.*, *Bortezomib inhibits PKR-like endoplasmic reticulum (ER) kinase and induces apoptosis via ER stress in human pancreatic cancer cells.* Cancer Res., 2005. **65**(24): p. 11510-11519.
116. Hu, J.S., *et al.*, *Activation of ATF4 mediates unwanted Mcl-1 accumulation by proteasome inhibition.* Blood, 2012. **119**(3): p. 826-837.
117. Binet, F., S. Chiasson, and D. Girard, *Evidence that endoplasmic reticulum (ER) stress and caspase-4 activation occur in human neutrophils.* Biochem. Biophys. Res. Commu., 2010. **391**(1): p. 18-23.
118. Yamamuro, A., *et al.*, *Caspase-4 Directly Activates Caspase-9 in Endoplasmic Reticulum Stress-Induced Apoptosis in SH-SY5Y Cells.* J. Pharm.l Sci., 2011. **115**(2): p. 239-243.
119. Li, C., *et al.*, *Transmembrane Protein 214 (TMEM214) Mediates Endoplasmic Reticulum Stress-induced Caspase 4 Enzyme Activation and Apoptosis.* J. Biol. Chem., 2013. **288**(24): p. 17908-17917.
120. Chandra, J., *Oxidative Stress by Targeted Agents Promotes Cytotoxicity in Hematologic Malignancies.* Antioxid. Redox Signal., 2009. **11**(5): p. 1123-1137.
121. Zou, W., *et al.*, *Vitamin C inactivates the proteasome inhibitor PS-341 in human cancer cells.* Clin. Cancer Res., 2006. **12**(1): p. 273-280.
122. Papa, L., E. Gomes, and P. Rockwell, *Reactive oxygen species induced by proteasome inhibition in neuronal cells mediate mitochondrial dysfunction and a caspase-independent cell death.* Apoptosis, 2007. **12**(8): p. 1389-1405.
123. Miller, C.P., *et al.*, *NPI-0052, a novel proteasome inhibitor, induces caspase-8 and ROS-dependent apoptosis alone and in combination with HDAC inhibitors in leukemia cells.* Blood, 2007. **110**(1): p. 267-277.
124. Goel, A., D.R. Spitz, and G.J. Weiner, *Manipulation of cellular redox parameters for improving therapeutic responses in B-cell lymphoma and multiple myeloma.* J. Cell. Biochem., 2012. **113**(2): p. 419-425.
125. Brieger, K., *et al.*, *Reactive oxygen species: from health to disease.* Swiss Medical Weekly, 2012. **142**.
126. Karisch, R., *et al.*, *Global Proteomic Assessment of the Classical Protein-Tyrosine Phosphatome and "Redoxome".* Cell, 2011. **146**(5): p. 826-840.
127. Bedford, L., *et al.*, *Ubiquitin-like protein conjugation and the ubiquitin-proteasome system as drug targets.* Nat. Rev. Drug Discov., 2011. **10**(1): p. 29-46.
128. Nathan, C. and A. Cunningham-Bussel, *Beyond oxidative stress: an immunologist's guide to reactive oxygen species.* Nat. Rev. Immu., 2013. **13**(5): p. 349-361.
129. Bae, Y.S., *et al.*, *Regulation of reactive oxygen species generation in cell signaling.* Mol. Cells, 2011. **32**(6): p. 491-509.
130. Chauhan, D., *et al.*, *A novel orally active proteasome inhibitor induces apoptosis in multiple myeloma cells with mechanisms distinct from Bortezomib.* Cancer Cell, 2005. **8**(5): p. 407-419.
131. Nerini-Molteni, S., *et al.*, *Redox homeostasis modulates the sensitivity of myeloma cells to bortezomib Redox homeostasis modulates the sensitivity of myeloma cells to bortezomib.* Brit. J. Haem., 2008. **141**(4): p. 494-503.
132. Soriano, M.E. and L. Scorrano, *The interplay between BCL-2 family proteins and mitochondrial morphology in the regulation of apoptosis.* Adv. Exp. Med. Biol., 2010. **687**: p. 97-114.
133. Scorrano, L., *et al.*, *BAX and BAK regulation of endoplasmic reticulum Ca2+: A control point for apoptosis.* Science, 2003. **300**(5616): p. 135-139.
134. Timmins, J.M., *et al.*, *Calcium/calmodulin-dependent protein kinase II links ER stress with Fas and mitochondrial apoptosis pathways.* J. Clin. Inv., 2009. **119**(10): p. 2925-2941.
135. Ohshima-Hosoyama, S., *et al.*, *Bortezomib stabilizes NOXA and triggers ROS-associated apoptosis in medulloblastoma.* J. Neuro-Onc., 2011. **105**(3): p. 475-483.
136. Willis, S.N., *et al.*, *Proapoptotic Bak is sequestered by Mcl-1 and Bcl-x(L), but not Bcl-2, until displaced by BH3-only proteins.* Genes & Dev., 2005. **19**(11): p. 1294-1305.

137. Yu, C.R., *et al.*, *The hierarchical relationship between MAPK signaling and ROS generation in human leukemia cells undergoing apoptosis in response to the proteasome inhibitor Bortezomib.* Exp. Cell Res., 2004. **295**(2): p. 555-566.
138. Ichijo, H., *et al.*, *Induction of apoptosis by ASK1, a mammalian MAPKKK that activates SAPK/JNK and p38 signaling pathways.* Science, 1997. **275**(5296): p. 90-94.
139. Hideshima, T., *et al.*, *Molecular mechanisms mediating antimyeloma activity of proteasome inhibitor PS-341.* Blood, 2003. **101**(4): p. 1530-1534.
140. Urano, F., *et al.*, *Coupling of stress in the ER to activation of JNK protein kinases by transmembrane protein kinase IRE1.* Science, 2000. **287**(5453): p. 664-666.
141. Walsh, R.C., *et al.*, *Proteasome inhibitor-based therapy for antibody-mediated rejection.* Kid. Int., 2012. **81**(11): p. 1067-1074.
142. Rumpold, H., *et al.*, *Knockdown of PgP resensitizes leukemic cells to proteasome inhibitors.* Biochem. Biophys. Res. Com., 2007. **361**(2): p. 549-554.
143. Cullinan, S.B., *et al.*, *Nrf2 is a direct PERK substrate and effector of PERK-dependent cell survival.* Mol. Cell. Biol., 2003. **23**(20): p. 7198-7209.
144. Hast, B.E., *et al.*, *Proteomic Analysis of Ubiquitin Ligase KEAP1 Reveals Associated Proteins That Inhibit NRF2 Ubiquitination.* Cancer Res., 2013. **73**(7): p. 2199-2210.
145. Rushworth, S.A., K.M. Bowles, and D.J. MacEwan, *High Basal Nuclear Levels of Nrf2 in Acute Myeloid Leukemia Reduces Sensitivity to Proteasome Inhibitors.* Cancer Res., 2011. **71**(5): p. 1999-2009.
146. Radhakrishnan, S.K., *et al.*, *Transcription Factor Nrf1 Mediates the Proteasome Recovery Pathway after Proteasome Inhibition in Mammalian Cells.* Mol. Cell, 2010. **38**(1): p. 17-28.
147. Steffen, J., *et al.*, *Proteasomal Degradation Is Transcriptionally Controlled by TCF11 via an ERAD-Dependent Feedback Loop.* Mol. Cell, 2010. **40**(1): p. 147-158.
148. Sykiotis, G.P. and D. Bohmann, *Stress-Activated Cap'n'collar Transcription Factors in Aging and Human Disease.* Sci. Signal., 2010. **3**(112).
149. Oerlemans, R., *et al.*, *Molecular basis of bortezomib resistance: proteasome subunit beta 5 (PSMB5) gene mutation and overexpression of PSMB5 protein.* Blood, 2008. **112**(6): p. 2489-2499.
150. Ruckrich, T., *et al.*, *Characterization of the ubiquitin-proteasome system in bortezomib-adapted cells.* Leukemia, 2009. **23**(6): p. 1098-1105.
151. Rapino, F., M. Jung, and S. Fulda, *BAG3 induction is required to mitigate proteotoxicity via selective autophagy following inhibition of constitutive protein degradation pathways.* Oncogene, 2013.
152. Aronson, L.I. and F.E. Davies, *DangER: protein ovERload. Targeting protein degradation to treat myeloma.* Haematologica, 2012. **97**(8): p. 1119-30.
153. Rosati, A., *et al.*, *BAG3: a multifaceted protein that regulates major cell pathways.* Cell death & Disease, 2011. **2**: p. e141.
154. Ding, W.X., *et al.*, *Oncogenic transformation confers a selective susceptibility to the combined suppression of the proteasome and autophagy.* Mol. Cancer Ther., 2009. **8**(7): p. 2036-2045.
155. Hoang, B., *et al.*, *Effect of autophagy on multiple myeloma cell viability.* Mol. Cancer Ther., 2009. **8**(7): p. 1974-1984.
156. Myeku, N. and M.E. Figueiredo-Pereira, *Dynamics of the Degradation of Ubiquitinated Proteins by Proteasomes and Autophagy ASSOCIATION WITH SEQUESTOSOME 1/p62.* J. Biol. Chem., 2011. **286**(25): p. 22426-22440.
157. Silva, G.M., *et al.*, *Redox control of 20S proteasome gating.* Antioxid. Redox Signal., 2012. **16**(11): p. 1183-1194.
158. Ge, F., *et al.*, *Quantitative phosphoproteomics of proteasome inhibition in multiple myeloma cells.* PLoS One, 2010. **5**(9).
159. Weerapana, E., *et al.*, *Quantitative reactivity profiling predicts functional cysteines in proteomes.* Nature, 2010. **468**(7325): p. 790-U79.

Chapter 3: An Overview of Direct and Two-Step Activity-Based Proteasome Profiling Strategies

Introduction

Activity-based protein profiling (ABPP) is a chemical proteomics technique used for identification and quantitative comparison of enzymatic activities. ABPP is widely applied to study a broad range of enzyme families *in vitro, in situ* in cell cultures and sometimes also *in vivo* in animal models [1]. ABPP has some advantages compared to other proteomics techniques. Experiments are robust, fast and simple. In case of cell permeable activity-based probes (ABPs), imaging of living cells or in animal models makes its applications broader by allowing localization and dynamic studies of the target enzymes [2, 3].

However, ABPP has also some limitations. The covalent bond between the probe and the target enzyme does not allow the recovering of enzymatic activity in a sample treated with ABP. The ABPP platform makes absolute quantification challenging and only relative quantification is possible by comparing the test samples to control ones. Another possible disadvantage of one step ABPP is that the reporter tag is normally a large moiety, which might affect the probe properties, like cell-permeability, selectivity, affinity or bioavailability. To overcome these problems a new strategy has become increasingly popular in the last years, termed two-step ABPP. In this approach the ABP reporter tag has been replaced by a ligation handle, which will be coupled with the reporter group after the attachment of the probe to its target enzyme. This tactic allows researchers to decide in every condition which reporter group to use depending on the desired method of analysis [4]. The reaction between the ABP ligation handle and the reporter group needs to be fast and selective, with ideally no side reactions.

Bioorthogonal chemistry is suitable for two-step ABPP since it allows the performance of selective chemical modifications in complex biological samples it [5]. The term bioorthogonal stands for a chemoselective reaction that ideally can take place in the aqueous environment of a biological system without any side reaction. Nowadays many bioorthogonal reactions are reported in literature, which differ in tag size, selectivity and biocompatibility as well as in reaction rates, making the choice an important decision [6]. Ideally the tag would be a small biocompatible chemical moiety that is able to perform a selective reaction with a non-bioavailable reagent, which should also be biocompatible. The ideal tag should also have a relative small size minimizing its interference with the

target environment. Alkynes and azide groups have emerged as favorites due their dimensions, just comprising few atoms. The most used bioorthogonal reactions used in proteasome two-step ABPP include the Staudinger-Bertozzi ligation in which an azide-containing ABP is reacted with a phosphine reagent equipped tag, the copper(I)-catalyzed click reaction between an azide and an alkyne, the copper-free strain-promoted azide-alkyne cycloaddition and the inverse-electron-demand Diels-Alder reaction of tetrazine with strained alkenes [7-10]. Each of these bioorthogonal reactions has its intrinsic advantages and disadvantages. The Staudinger-Bertozzi ligation is selective but the use of the large phosphine moiety may give problems especially in native conditions where the ABP is found inside an enzyme pocket. The copper(I)-catalyzed click reaction is a versatile ligation but the need for copper salts does not recommend its application in living cells due to its high toxicity. The copper-free cycloaddition is a fast and efficient ligation method but due to the relatively high reactivity of the tags, often gives off-target reactions. The inverse-electron-demand Diels-Alder reaction is very selective under native conditions probably being the most versatile reaction. The first part of this chapter shows a literature overview of the methodology used in two-step ABPP of the proteasome. The labeling of the different proteasome active sites using the Staudinger-Bertozzi ligation, copper-free cycloaddition and a tandem ligation strategy is described. The second part of this chapter is a case study of the residual activity of the proteasome after ABP labeling in human and mouse cell extracts.

Two-step ABPP overview

In the first report on two-step proteasome ABPP published in 2003, the proteasome subunits could be successfully labeled by means of the Staudinger-Bertozzi ligation [11]. A broad spectrum azide-containing ABP was incubated either in living cells or cell lysates and posteriorly subjected to Staudinger ligation under denaturing conditions. The ability of the probe to cross the cellular membrane *in situ,* efficiently bind and thus inhibit the proteasome is proven by the accumulation of a green fluorescent protein (GFP) fused to an ubiquitin chain, which targets it for degradation via the proteasome. This study shows that the incorporation of an azide group in an ABP has no influence in its selectivity towards proteasome both *in situ* and *in vitro.*

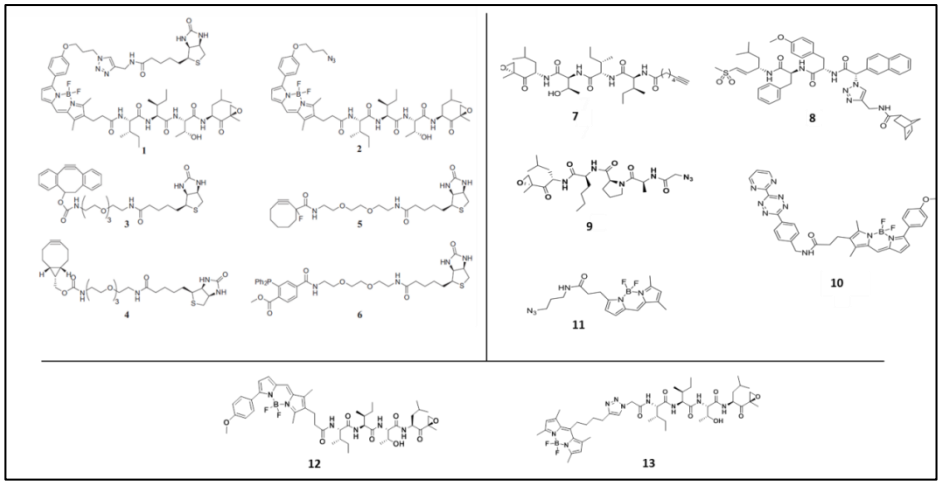

***Figure 1**. ABPs and ligation handles used in the different here presented studies. **1**: biotin-BODIPY-epoxomicin; **2**: azido-BODIPY-epoxomicin; biotin-cyclooctyne derivatives **3:** Dibenzocyclooctynol (DIBO); **4**: Bicyvlenonyne (BCN); **5**: Monofluorinated cyclooctyne (MFCO); **6**: biotin-phosphine; **7**: pan-reactive alkyne-epoxomicin; **8**: β5/β5i selective norbonene-equipped vinyl sulfone; **9**: β1/β1i selective azide-equipped epoxyketone; **10**: Tetrazine-Bodipy-TMR; **11**: Azido-Bodipy; **12**: MVB003 (BODIPY-TMR epoxomicin); **13**: LWA300 (BODIPY-FL epoxomicin).*

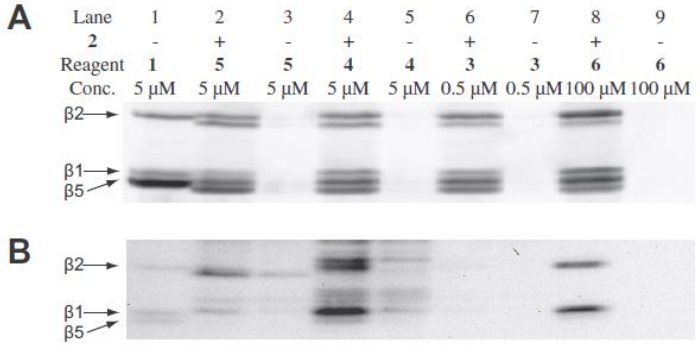

***Figure 2**. [12] A) Fluorescent readout and B) streptavidin blot of labeled cell lysates. HeLa cells were exposed to **2** for 2 hours, excess reagents was removed prior incubation with two-step reagents **3**-**6** for 4 hours. Cells were lysed and resolved by SDS-PAGE.*

In a later study the copper-free click ligation with three different cyclooctynes (figure 1, compounds **3**, **4** and **5**) was tested for two-step proteasome ABPP and compared to the Staudinger-Bertozzi ligation with compound **6** [12]. The use of the azide-bearing fluorescent ABP **2** allows observation the probe in two different ways, by biotin read-out after biorthogonal ligations and by a shift of the modified proteasome subunits in the

fluorescent image due to the incorporated biorthogonal reagents size (figure 2, lane 1 compared to the rest). Comparing both biorthogonal reactions performance, the Staudinger-Bertozzi ligation turned out to be more specific, although longer reaction times are needed, than the copper-free click cycloadditions due to the high background found and the low signal intensity of the different cyclooctynes (figure 2B). The results obtained for the different ligations *in situ* demonstrate the applicability of these ligation techniques in the labeling of proteasomes in living cells.

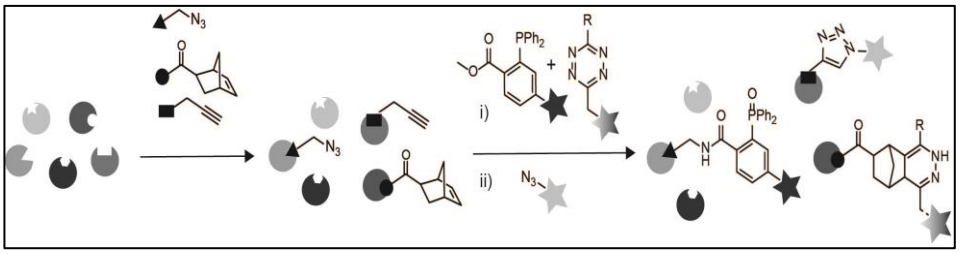

Figure 3. *Schematic workflow of the triple ligation strategy involving a copper(I)-catalyzed click ligation, Staudinger-Bertozzi ligation and tetrazine ligation.*

The use of subunit selective proteasome probes in a two-step proteasome ABPP setup was used to test orthogonality between the different ligation reactions and to develop a strategy, which selectively labels each subunit with a different readout-tag [13]. In figure 3 a schematic workflow of the triple ligation strategy used by Willems and coworkers is shown. The chemical tools used in this strategy are shown in figure 1. The three active proteasome subunits were labeled with a different tag via one of the different ligation reactions. The β5-subunit selective norbornene-tagged ABP **8** together with the β1-selective azide-functionalized ABP **9** were incubated with HEK293T lysate. After exposure to ABP **8** and **9**, panreactive ABP **7** was added, which due to the fact that the β5 and β1 sites were already blocked, could only label the free β2-subunits. This addition sequence allows to selective tag the β5-subunits with a norbornene, the β1-subunits with an azide and the β2-subunits with an alkyne. Next, the cell extracts were incubated with tetrazine **10** and phosphine **6** for 1h. Reagent excess was removed before performing the copper(I)-catalyzed click ligation for an extra hour with azide **11**. The washing step before the click reactions is required to remove both the excess of tetrazine and phosphine, which might react with the cooper catalyst and the azide ABP, respectively. By using two different fluorophores and a biotin tag, the proteasome subunits labeled by the different ligation techniques can be visualized. As it can be seen in figure 4, the triple ligation strategy successfully labels the different proteasome subunits in a selective manner. The results obtained by the separate bioorthogonal reactions (last 3 lanes in fig. 4) are comparable to those of the simultaneous triple ligation, showing the value of the triple ligation strategy.

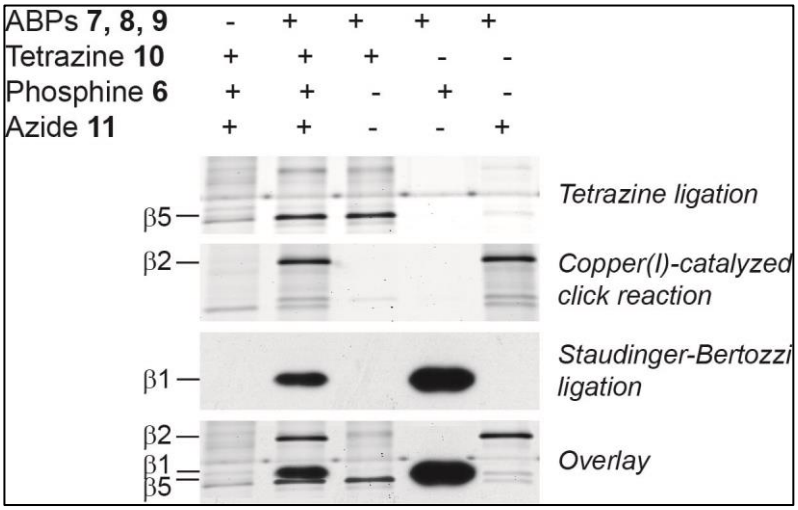

Figure 4*. [13] Anti-biotin blots and in-gel fluorescent imaging to visualize the proteasome labeling patterns in each single reaction and for the simultaneous triple ligation.*

Determination of the unlabeled free proteasome fraction

The second part of this chapter describes the evaluation in human and mouse cell lines of residual proteasome activity after exposure to pan-reactive ABP **12**. Next the optimal labeling conditions for probe **12** in the mouse B-lymphocyte cell line B3/25 were determined. Incubation of B3/25 lysate with varying concentrations of ABP **12** for one hour (figure 5B) shows that above 0.5 µM the plateau phase is observed and that an increase in probe concentration does not result in a rise of signal but in a higher background. Figure 5A shows that although after one hour of incubation the maximum labeling is not reached, an extra exposure of 30 minutes results in only a small increase in signal percentage (around 10%). But again, in this case the signal to background ratio is compromised, indicating that 90 min incubation is not a recommendable labeling time. ABP **12** optimal labeling conditions were determined to be 0.5 µM for one hour-exposure in lysate and 4 hours incubation with 4 µM probe end concentration for *in situ* labeling for both mouse and human cell lines. Figures 5 C&D show that the fluorescent signal of the proteasome-bound ABP **12** is directly proportional to the amount of protein loaded on SDS-PAGE in both lysate and living cells exposures. The high R-square values in both graphs illustrate the applicability of ABPP for relative quantification purposes in mouse samples.

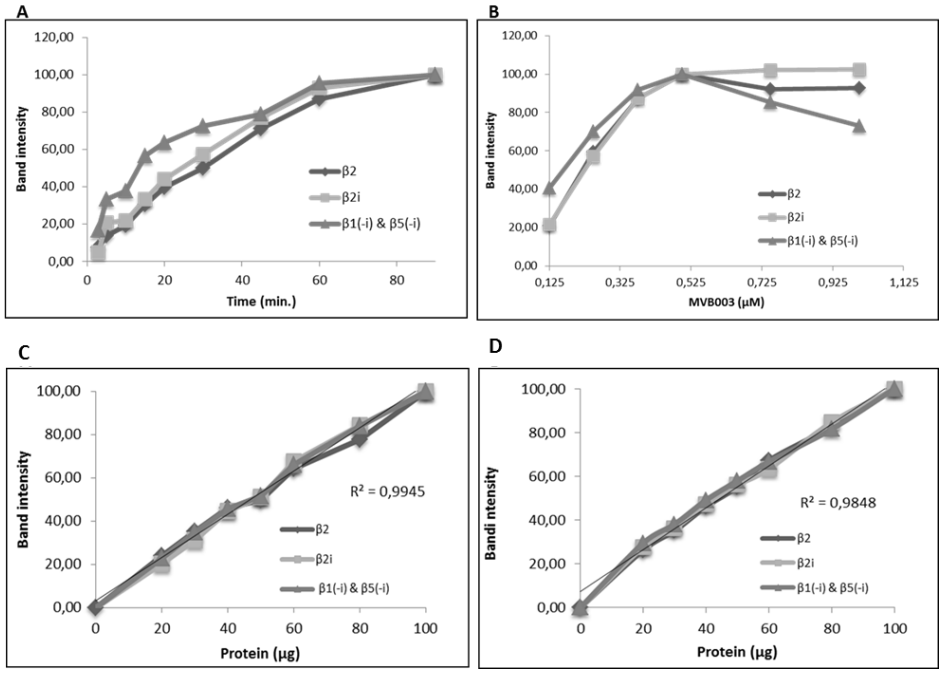

Figure 5. *A) Incubation time of ABP **12** up to 90 minutes in murine B3/25 cell line lysate. B) Lysate was incubated for 1 hour with different probe concentrations. Calibration curves for ABP **12** C) in lysate and D) in living cells.*

In order to remove probe excess when performing the labeling in lysates, samples were loaded on a size-exclusion column prior posterior incubation with ABP **13**, a Cy2-fluorescent analog of ABP **12**. Figure 6 shows that applying the sample on a size-exclusion column directly after addition of ABP **12** allows removal of the unbound ABP (lane D) and that subsequent incubation with probe **13** results in almost full labeling of proteasome subunits (lane C). The light proteasome band (probably β5/5i) visible in the Cy3-fluorescent channel (lanes C and D) indicates that ABP **12** reacts very quickly with the proteasome subunits highlighting the ABP selectivity against proteasome. Incubation of the probe after size-exclusion yields in a small loss of proteasome activity signal compared to its exposure before size-exclusion (lanes A vs. B and E vs. F in figure 6). This small loss (about 10%) was corrected afterwards with the use of coomassie stain as loading control, resulting in a comparable signal for both conditions. No size-exclusion columns were used in the unlabeled proteasome fraction determination. Instead, cells were thoroughly washed with PBS after incubation with the probe prior lysing and posterior exposure to Cy2-fluorescent counter-ABP **13**.

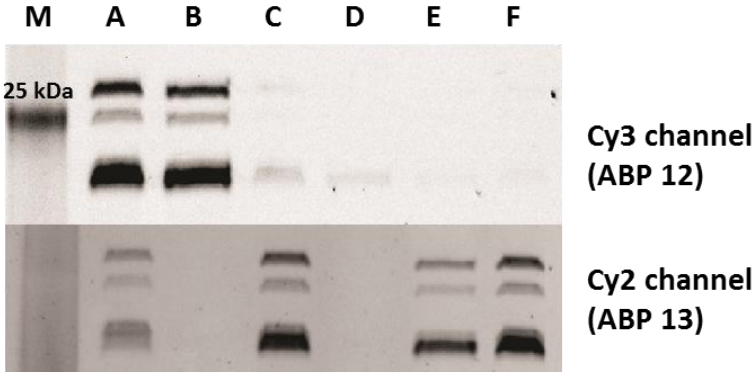

Figure 6. *Gel image showing the different signals for both ABP* ***12*** *(top) and ABP* ***13*** *(bottom) for the free fraction determination.* ***M****: Marker.* ***A****: 1h ABP* ***12****, size exclusion, 1h ABP* ***13****.* ***B****: size exclusion, 1h ABP* ***12****.* ***C****: ABP* ***12*** *short exposure before size exclusion, 1h ABP* ***13****.* ***D****: ABP* ***12*** *short exposure before size exclusion.* ***E****: 1h ABP* ***13****, size exclusion.* ***F****: size exclusion, ABP* ***13****.*

Table 1 shows the unlabeled proteasome subunits percentage obtained in lysate and living cell labeling respectively. Due to the poor separation of the β5/5i/1/1i subunits achieved on gel with both ABPs, these subunits were considered as a single moiety and were quantified together. The overall non-labeled proteasome fraction in the human cell line by probe **12** was found to be around 10% for the different subunits. These residual activity percentages were comparable between *in vivo* and *in vitro* labeling strategies, with the ones found in lysates slightly bigger than those from *in vivo* labeling. Labeling of mouse cells *in situ* yields in a similar free fraction percentage as the one obtained for human living cells (around 5%). Unexpectedly, this fraction increases dramatically (up to 35%) when labeling is performed in mouse cellular extracts (figure 6 lane A; table 1). The large difference between *in vivo* and *in vitro* labeling of mouse samples suggests a systematic error during the *in vitro* experiments performance.

Human

Lysate	Free fraction (%)	Standard deviation (%)
beta2	12	5
beta2i	14	10
beta1+5	7	2

Living cells	Free fraction (%)	Standard deviation (%)
beta2	6	0
beta2i	6	3
beta1+5	4	2

Mouse

Lysate	Free fraction (%)	Standard deviation (%)
beta2	39	8
beta2i	34	16
beta1+5	31	5

Living cells	Free fraction (%)	Standard deviation (%)
beta2	2	1
beta2i	2	0
beta1+5	3	1

***Table 1**. Free fraction percentage for the human (left) and mouse (right) proteasome subunits after 1h incubation with ABP **12** in lysate and for 4h exposure in living cells. The values are the average of 3 replicates.*

Discussion

As it can be appreciated in figure 2A, the used cyclooctynes and phosphine concentrations, or the reaction times, were insufficient for complete ABP labeling, characterized by a shift in the fluorescent gel image. Despite the copper-free cycloadditions were more efficient in terms of reagents concentrations and reaction times compared to the Staudinger-Bertozzi reaction, the ligations with the three cyclooctynes yielded in a much higher background than the one observed with the Staudinger ligation. This suggests that cyclooctyne moieties are able to react with natural biological entities and thus are not truly orthogonal. Further investigations are needed in order to decipher which proteins react with the cyclooctynes and in which manner. The phosphine reagent in the Staudinger-Bertozzi ligation is prone towards oxidation, which is probably the explanation for the high reagent concentration.

The triple ligation strategy [13] shows that it is possible to perform several biorthogonal reactions in one test tube. In this strategy though, a buffer exchange between the tetrazine and the click ligations is needed to prevent undesired side reactions. All three ligation reactions show low or almost no background labeling. Click ligation showed higher background labeling than the other two, but much smaller than the background obtained in the previously discussed study by the cyclooctynes, indicating that although copper-

catalyzed click chemistry is not the optimal reaction for its performance in living cells due to its Cu(I)-induced toxicity, it still is favorable compared to copper-free cycloaddition in terms of background labeling, at least in the case of proteasome two-step ABPP. This triple ligation strategy should be also tested under denaturing conditions where, click ligation is supposed to have a better performance since most of its background labeling is thought to be due to a side reaction between alkyne and reactive cysteine residues, which might be less reactive under denaturing conditions. If the tetrazine ligation is also successful under these conditions, the tandem ligation strategy may have broader applications, allowing researchers to decide at which moment to perform the ligations.

The low proteasome residual activity percentages and the low standard deviations obtained with ABP **12** shows the use of this probe and of ABPP for quantifications purposes, because although having a small fraction of proteasomes not labeled with the probe, this portion seems to remain constant. The little variations among the different proteasome subunits prove that ABP **12** has broad-spectrum activity towards the proteasome subunits. The large percentage differences found when exposing the probe to mouse cellular extracts compared to living cells suggest the appearance of a systematic error, which is supported by the low standard deviations (table 1). This is reinforced by the fact that the probe has the same optimal labeling conditions in both organisms and also by the high amino acid sequence similarity between the proteasome subunits, thus the values were expected to be similar as those found for human proteasome subunits, same as it is for the *in vivo* labeling. Taking a look at the free fractions found in human proteasomes, the values between *in vivo* and *in vitro* labelings do not differ much, although it seems like the *in vivo* labeling may be slightly more efficient. A plausible reason for this may be the capacity of the ABP to access the active-site threonine. Biological systems, or like in this case machineries, are tightly regulated and proteasomes are not an exception. Although it is known that the 20S core particle itself is already catalytically active with some known substrates, most of its substrates are dependent on the presence of regulatory particles like the 19S cap or the 11S. These regulatory particles trigger a rearrangement of the core particles subunits, which results in the opening of the alpha rings allowing the protein substrates to enter the catalytic core. The binding of these regulatory particles with the 20S proteasome is not very strong and the lysing and sample preparation procedures may be enough to disrupt it. Although the proteasome-directed ABPs are known to diffuse through the 20S particle to its inside to react with the active sites, the rearrangement of the 20S proteasome when regulatory particles are attached might induce holes or cavities permitting a faster diffusion of the probe. Another possible explanation would be that the probe gets degraded before it labels all proteasome subunits, although this option is less likely due to the ABPs high stability in aqueous

solutions. In both cases, pulse labeling should allow the ABP to efficiently reach and bind all different subunits decreasing in this manner the unlabeled proteasome pool.

Conclusion

The one-step ABP **1** and the two-step ABP **2** used by van der Linden and coworkers [12] are a good example of the versatility of ABPP, having in a single probe two different tags, a BODIPY for fluorescent read out, and a biotin moiety which can be used as enrichment tag or for visualization via Strep-HRP blotting. One-step ABPs are useful tools in proteasome enzymology research and may be also applied in the clinic, for example as fluorescent indicators of the proteasome activity in a specific tissue or sample but also of its cellular location using fluorescent microscopes. ABPP can be used to screen and compare proteasome activities in different tissues or organisms (see Chapter 4) but its applications can be extended to the study of the different roles proteasomes have in for example antigen presentation, or in cellular stress responses (see Chapter 5). ABPP could, in theory follow the proteasome half-life, by blocking first all proteasomes with one probe (or perhaps better yet just one subunit due to cellular toxicity) and posterior addition of a second probe which will only bind the non-occupied newly synthetized proteasomes. Being able to follow the localization and activity of different proteasomes in time until their destruction and recycling should in principle be achievable by means of proteasome ABPP.

Experimental procedures

Cell culture and probe treatment

Human cell line Amo1 (plasmacytoma) was grown in RPMI-1640 medium. The mouse cell line B3/25 (myeloma) was grown in IMDM medium. The entire medium was supplemented with 10% fetal calf serum and 0.1 mg/mL of streptomycin and penicillin. Both cell lines were grown at 37ºC with 5% CO_2 in a humid incubator. Both cell lines were purchased from ATCC.
ABP was dissolved in DMSO before use. 1000x stock solution of the desired end concentration of the ABP was added to the cell culture to have the DMSO concentration lower than 1% in the culture media. Treatments were done for different probe concentrations for 4 hours and for different amounts of time with 4 μM probe. Cells were washed couple of times with cold PBS, pelleted and stored at -80ºC until its usage.

Activity-based protein profiling

Cell pellets were lysed in 3 volumes of lysis buffer (50 mM Tris-HCl pH 7.5, 250 mM sucrose, 5 mM $MgCl_2$, 1 mM DTT, 2 mM ATP, 0.025% digitonin and 0.2% NP40), kept on ice for 1 hour and further disrupted by 30 seconds sonication. After cold centrifugation at 13.000 g for 10 min, protein concentration was measured with the Qubit Protein Assay on the soluble fraction and kept at -80ºC until use. Equal amounts of protein were incubated with the desired concentrations of ABP for 1 hour at 37ºC, resolved by 12.5% SDS-PAGE and scanned with the ChemiDoc™ MP System with the Cy3 and Cy2 settings. When specified, prior resolution on gel some samples were loaded on a 30 kDa size-exclusion column. The procedure was carried on as suggested by manufacturer. Commassie blue staining was used as loading control. All gel images were analyzed by the Image Lab software (Bio-Rad).

References

1. Li, N., H.S. Overkleeft, and B.I. Florea, *Activity-based protein profiling: an enabling technology in chemical biology research.* Curr. Op. Chem. Biol., 2012. **16**(1-2): p. 227-233.
2. de Jong, A., *et al.*, *Fluorescence-based proteasome activity profiling.* Meth. Mol. Biol., 2012. **803**: p. 183-204.
3. Heal, W.P., T.H. Dang, and E.W. Tate, *Activity-based probes: discovering new biology and new drug targets.* Chem. Soc. Rev., 2011. **40**(1): p. 246-257.
4. Willems, L.I., H.S. Overkleeft, and S.I. van Kasteren, *Current developments in activity-based protein profiling.* Bioconj. Chem., 2014. **25**(7): p. 1181-1191.
5. Patterson, D.M., L.A. Nazarova, and J.A. Prescher, *Finding the right (bioorthogonal) chemistry.* ACS Chem. Biol., 2014. **9**(3): p. 592-605.
6. Shieh, P. and C.R. Bertozzi, *Design strategies for bioorthogonal smart probes.* Org. Biomol. Chem., 2014. **12**(46): p. 9307-20.
7. Saxon, E. and C.R. Bertozzi, *Cell surface engineering by a modified Staudinger reaction.* Science, 2000. **287**(5460): p. 2007-2010.
8. Tornoe, C.W., C. Christensen, and M. Meldal, *Peptidotriazoles on solid phase: [1,2,3]-triazoles by regiospecific copper(i)-catalyzed 1,3-dipolar cycloadditions of terminal alkynes to azides.* J. Org. Chem., 2002. **67**(9): p. 3057-3064.
9. Agard, N.J., J.A. Prescher, and C.R. Bertozzi, *A strain-promoted [3 + 2] azide-alkyne cycloaddition for covalent modification of biomolecules in living systems.* JACS, 2004. **126**(46): p. 15046-15047.
10. Devaraj, N.K., R. Weissleder, and S.A. Hilderbrand, *Tetrazine-based cycloadditions: application to pretargeted live cell imaging.* Bioconj. Chem., 2008. **19**(12): p. 2297-2299.
11. Ovaa, H., *et al.*, *Chemistry in living cells: detection of active proteasomes by a two-step labeling strategy.* Ang. Chem., 2003. **42**(31): p. 3626-9.
12. van der Linden, W.A., *et al.*, *Two-step bioorthogonal activity-based proteasome profiling using copper-free click reagents: a comparative study.* Bioorg. Med. Chem., 2012. **20**(2): p. 662-666.
13. Willems, L.I., *et al.*, *Triple bioorthogonal ligation strategy for simultaneous labeling of multiple enzymatic activities.* Ang. Chem., 2012. **51**(18): p. 4431-4434.

Chapter 4: Comparative Activity-Based Proteasome Profiling in Zebrafish and Mice

Introduction

In the last years, two different proteasome inhibitors (PIs) have been approved for the treatment of two hematopoietic cancers, multiple myeloma and mantle cell lymphoma [1]. Today proteasome inhibition is being investigated as a potential treatment for different diseases including solid tumors, muscle disorders, autoimmune syndromes and also in the field of organ transplants [2, 3]. Mammalian tissue can express up to six different catalytic proteasome subunits (up to seven in the thymus), which exhibit different substrate preferences. These subunits are basically assembled in two different proteasomes types, the constitutive proteasome, containing the β1, β2 and β5 subunits, and the immunoproteasome, where the constitutive subunits are replaced by their counter subunits β1i, β2i and β5i [4]. Bortezomib, the first PI approved in the clinic, shows selectivity towards the β5/5i and β1/1i subunits, being able to block them substantially while leaving the β2/2i activity almost unchanged. The second PI approved for the treatment of multiple myeloma is Carfilzomib, a β5/5i driven inhibitor, which at its therapeutic concentration partially also blocks the other proteasome subunits. The fact that both clinically accepted PIs show a subunit preference and that full proteasome inhibition is not necessary for its therapeutic benefit, has increased the effort of developing not only new and more potent inhibitors but also subunit specific inhibitors [5, 6]. The development of activity-based probes (ABPs) that facilitate the activity measurement of individual constitutive and immune subunits was one important step forward in the proteasome research field [7-9]. Broad-spectrum ABPs allow the simultaneous measurement of all different proteasome activities. Most of these pan-reactive ABPs do not show complete separation of the different proteasome subunits on SDS-PAGE, especially when immunoproteasomes are present. Due to the similar molecular weight of the β5/5i and the β1/1i subunits, resolving these subunits by SDS PAGE is complicated. Recently, several proteasome subunit specific inhibitors and probes have been developed, expanding the possibilities of inhibition using different combinations but also in a controlled manner, being possible to decide which subunit to inhibit and to what extent [10]. These subunit specific ABPs allow separation and direct activity determination of their target subunits. This has increased the knowledge about the different activities and substrate preferences of the proteasome active subunits, such as that more bulky, hydrophobic amino acids at P1 (first amino acid position after warhead) confer selectivity

towards immunoproteasomes, allowing the development of selective immunoproteasomes inhibitors [11, 12].

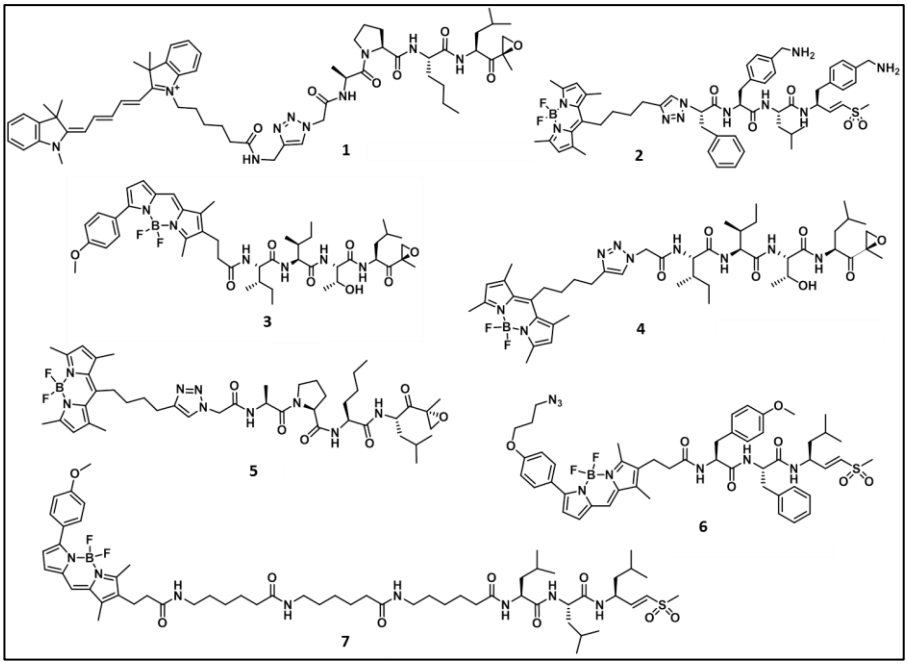

***Figure 1**. Structures of the activity-based probes used in this study. ABP **1**, Cy5-NC001, is β1/1i selective; ABP **2**, BODIPY(FL)-LU112, targets β2/2i; ABPs **3** (MVB003) and **4** (LWA300) are both an epoxomicin-based ABP with pan-reactive selectivity; probe **5** (LW124) is a β1/1i selective ABP; ABP **6**, BODIPY(TMR)-NC005, is a β5/5i targeting probe; ABP **7** (MV151) is a broad-spectrum proteasome probe.*

Most of the studies with PIs and ABPs have been mainly performed on human proteasomes and thus the newly synthetized inhibitors and probes have been chemically engineered to selectively target human proteasomes. Only a small fraction of these have been tested in other animals, mostly in mice. In this chapter, a pool of broad-spectrum and subunit selective ABPs (figure 1) has been screened in different murine organs and in zebrafish. Both organisms are broadly used in academic and clinic research, thus testing the applicability of these ABPs in these organisms will expand the usefulness of ABPP.

Results

Mice brain and testis, expressing only constitutive proteasomes, and spleen, which expresses both immuno- and constitutive proteasomes, were used in order to test the ABPs. Zebrafishes are only 1-3 cm and isolating their different organs is tidy and difficult. The easiest accessible organ suitable for extraction is the brain. Thus it was decided to perform the screen only on zebrafish brains and on full fish extracts. Figures 2 and 3 show a representative gel image for each ABP in the different murine and zebrafish tissues, and the optimal concentrations determined for each tissue are listed in table 1.

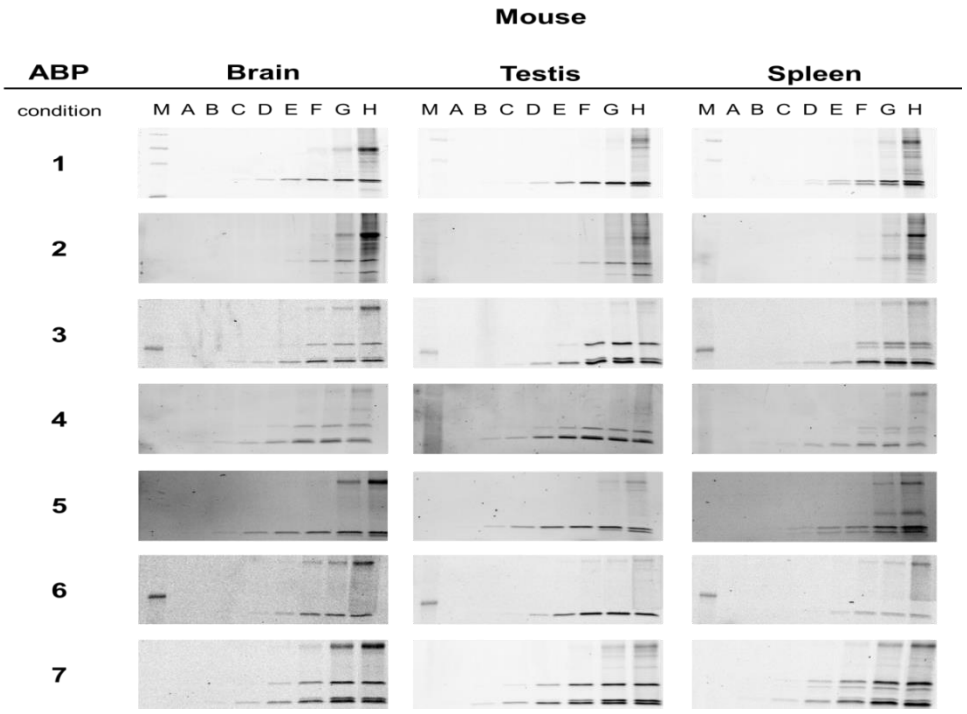

***Figure 2**. Representative SDS-PAGE gel images for each ABP in the mice tissues screened in this study. In the first lane of each gel the pre-stained protein marker was loaded (condition M). Highest concentration chosen for each probe was 10 µM (condition H). This concentration was diluted 5-fold in each lane ending with the end concentrations for each condition as follows: A: 0.13 nM; B: 0.64 nM; C: 3.2 nM; D: 16 nM; E: 80 nM; F: 400 nM; G: 2 µM and H: 10 µM.*

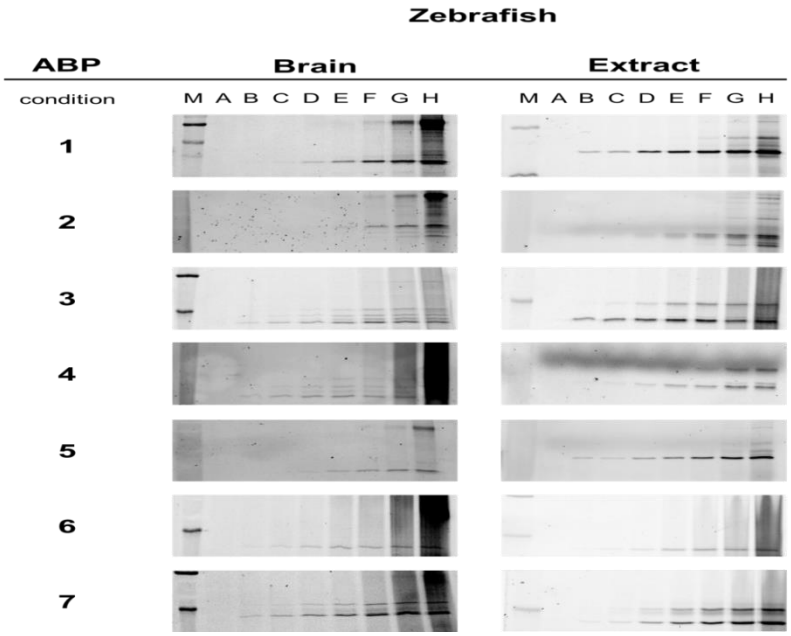

Figure 3. *Representative SDS-PAGE images for each ABP in the zebrafish. The ABPs concentrations where the following: A: 3 nM; B: 10 nM; C: 30 nM; D: 100 nM; E: 300 nM; F: 1 µM; G: 3 µM and H: 10 µM. M: protein marker.*

TISSUE	Activity-based Probe optimal concentration (µM)						
	1	2	3	4	5	6	7
Mouse Brain	0,4	0,4-2	0,4	0,4	0,1	0,4	2
Mouse Testis	0,4	0,4-2	0,4-2	0,4	0,1	0,4	2
Mouse Spleen	0,4-2	2	0,4-2	0,4-2	0,1-0,4	0,4	2
Zebrafish Brain	0,3-1	1	0,3-1	1	1	0,3-1	0,3-1
Zebrafish Extract	0,3-1	1	0,3-1	3	1	0,3-1	1-3
Human cell line extracts	0,1	0,25	0,25-0,5	0,25-0,5	0,1	0,25	0,5-1

Table 1*. Optimal labeling concentrations for each ABP in the different tissues and organisms.*

All probes retain their selectivity towards the proteasome subunits while their optimal labeling concentrations are, in general, slightly higher than the ones used in human cell lines extracts. β1/1i selective probes **1** and **5** and pan-reactive ABPs **3** and **7** show a similar pattern in all different tissues as the one observed in human cell line extracts, a high selectivity towards the proteasome and off-targets are only visible at high concentrations.

Interestingly, ABP **4**, a Cy2-fluorescent analog of probe **3**, shows lower overall signal/noise ratios compared to ABP **3**. This is especially significant in the murine spleen and in the zebrafish samples, where the β2/2i bands are hardly visible due to low band intensity (figure 2) or high background (figure 3). This high background labeling at high probe concentrations in zebrafish brain and extracts is in general obtained with most of the probes. ABPs **2** and **6** label efficiently the β2 and β5 subunits, respectively, in all screened tissues but murine spleen. For both probes the bands are very weak compared to their performance in the other tissues. In the case of ABP **2** the concentrations needed to obtain labeling are much higher than the ones used for human proteasome labeling and in some cases, like in the spleen (figure 2), at the optimal labeling concentration shows some off-target bands. Interestingly, although ABP **6** labels β5 or β5i selectively, the separation of these two subunits was poorly achieved on SDS-PAGE (figure 2, spleen), while they were proven to separate properly human β5/5i subunits. To check whether this was due to poor subunit separation or to the ABP being only able to label one of the subunits, a 2D-gel electrophoresis was performed. Three distinct stripes can be observed in the middle of the 2D-gel (figure 4), two having a bright signal and the third a much lighter one. This third stripe seems to run lower than the other two, suggesting that this might be the stripe for the labeled β5i subunit and the brighter stripes might correspond to the β5 subunits. Their position in the gel compared to the marker and their separation is similar to the one observed for human subunits (figure 4).

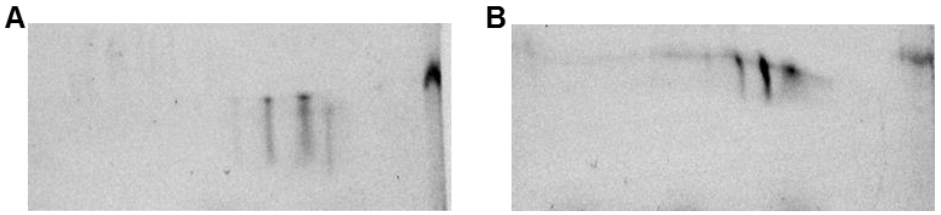

***Figure 4**. 2-D SDS-gel image of a mouse cell lysate (A) and a human cell line extract (B), which were incubated with ABP **6** at the concentration of 0.5 μM for 1 hour. Sample were loaded on a non-linear pH gradient (3-10) strip and resolved on 12.5% SDS-gel after isoelectric focusing. A pre-stained marker was added to the SDS-gel (bright band on the right side of the image). As it can be seen in both gel images, two isoforms of the β5c subunit are visible (the two left stripes). The β5i subunit can be visualized running a slightly lower on the gel than the β5c subunit bands.*

Discussion

All here tested ABPs target selectively the proteasome subunits from both organisms. Although losing a bit of potency compared to their performance in human cell lines extracts, this difference is very small and all probes maintain a low micromolar concentration for optimal labeling (table 1). For some probes, the concentrations needed in the murine spleen are slightly higher than the ones in the other murine tissues. This can possibly be explained by the fact that this organ expresses both immuno- and constitutive proteasomes, and is probable that the total amount of proteasomes is higher than in the other tissues where only one type of proteasomes is expressed. Table 2 shows the alignment percentage of the mouse and zebrafish subunits with the human ones. The largest differences with the human amino acid sequence are found in zebrafish, especially for the β1i and the β2i subunits. These differences might explain the probe potency variation when used in zebrafish, and the poor resolution found when labeling these subunits with the selective β1-directed ABP **1** or the β2-directed ABP **2.**

		β5	**β5i**	**β1**	**β1i**	**β2**	**β2i**
Mouse	identity (%)	95	93	97	90	97	89
	similarity (%)	97	98	98	98	99	93
Zebrafish	identity (%)	84	80	79	67	82	56
	similarity (%)	91	91	92	84	94	72

Table 2*. Alignment percentage of the proteasome active subunits amino acid sequence from mouse and zebrafish with the human subunits. Identity is showing the percentage of shared amino acids; similarity includes the amino acid replacement by another with similar characteristics.*

As can be seen in figure 1, ABPs **3** and **4** have the same peptide backbone and only differ in their fluorescent tag, BODIPY(TMR) and BODIPY(FL) respectively. In the case of human or mice proteasomes this does not influence their output, both sharing a similar optimal concentration, although the signal obtained with probe **4** in spleen is lower than in the other tissues. In zebrafish this difference increases up to three times. This increase seems to be due to the reporting tag of **4**. It causes a large background signal, making it hard to properly visualize the proteasome bands. This phenomenon of high background noise is especially significant for **4** but not for the other ABPs with a BODIPY(FL) fluorescent tag, probes **5** and **2**. This indicates that is not due to the reporting group but more likely a

combination of fluorophore and the inhibitor backbone. Although the three BODIPY(FL)-bearing ABPs have an acceptable signal to noise ratio in zebrafish, when labeling full fish extracts a vague and diffuse band shows around 35 kDa (figure 3). This band is probably an endogenous fluorescent protein that can interfere specially with the identification or quantification of the β2 subunits due to their close position in the gel. A straightforward strategy to avoid this fluorescent protein interfering with the band analysis could be to use an ABP with a different fluorescent tag, scanning the gel in a different fluorescent channel. Another possibility is to precipitate the proteins, for example by a chloroform/methanol precipitation, which might remove the fluorescent molecules. Subjecting the sample after ABP exposure to a size-exclusion column might separate all small proteins from the large protein complexes like proteasomes, which has been successfully proven in the Chapter 3 of this thesis, since ABPs label only active subunits of fully assembled proteasomes but not single subunits.

Another interesting feature in the zebrafish brains and full extracts is the additional band or smear that appear between the β2 and the β1/5 subunits when incubating them with high concentrations of ABPs **2** or **7** (figure 3). These could be off-targets of the probes, but since they are only visible in zebrafish and not on mice or human samples it should be a unique zebrafish protein. Another possibility is that these probes also label post-translationally modified β2 subunits. This theory is supported by the fact that ABP **2** does not show a sharp β2/2i band, as it does for mouse, but a wide and diffuse one. This is in concordance with PTMs (post-translational modifications), as depending on the type and the amount they may influence and vary the molecular weight and charge of the modified protein thus shifting its position in the gel. These diffuse or extra bands are only visible with these two ABPs but not with the other probes, which also label the β2/2i subunits, ABPs **4** and **5**. The main difference between these probes and the rest are the warheads, ABPs **2** and **7** have a vinyl sulfone warhead while probes **4** and **5** have an epoxyketone. It seems that vinyl sulfone probes are the only ones that label and separate these modified subunits. Further experiments, like on-gel digest or pull-downs need to be performed in order to validate this hypothesis and identify these extra bands.

Off-targets or high background labeling is only observed when incubating ABPs at high concentrations. The high background labeling is mainly observed in zebrafish brains and also in extracts but it is not obtained in the murine tissues, suggesting that the probe off-targets could be larger in zebrafish than in mice. Another explanation for this high background labeling could be that the signal to noise ratio is not very large, thus when adjusting the image contrast to obtain substantial signal, the background at high probe concentration gets also larger due to the ABPs probably just sticking to proteins. Washing away the excess of probe after the incubation period might be beneficial to remove the

high background due to stickiness of the ABPs and will show how much of this background is actual an off-target of the probe, which could be then easily identified by in-gel digestion coupled to mass analysis.

Conclusion

In conclusion, all here used ABPs are suitable for their application in mouse and zebrafish, although the probes show less potency in mouse and zebrafish in comparison to human proteasome labeling. The largest difference is found in zebrafishes where the optimal concentrations are in some cases three times higher than in human and where optimal labeling from the immunoproteasome subunits β1i and β2i is compromised (figure 2). The low alignment percentage of these subunits between human and zebrafish (table 2) might explain the low efficiency of the probes labeling these subunits. This leaves room for improvement in generating ABPs that can bind to many species with a comparable potency and selectivity, but also in the production of an organism-selective proteasome inhibitor or probe. If an organism-selective inhibitor could be developed, it might be a plausible treatment against infections for example, thus allowing the targeting of only non-host cells, but it could also be beneficial for the food industry plague control by using human harmless chemicals to fight the responsible organisms that cause the plague.

Experimental procedures

Animals and tissues

Mouse organs were isolated from adult mice. Zebrafish brains were isolated from adult zebrafish while full body extracts were obtained from zebrafish larvae.

Activity-based protein profiling

Organ tissues were homogenized in 3 volumes of lysis buffer (50 mM Tris-HCl pH 7.5, 250 mM sucrose, 5 mM $MgCl_2$, 1 mM DTT, 2 mM ATP, 0.025% digitonin and 0.2% NP40) with a tissue homogenizer and further disrupted by 30 seconds sonication. After cold centrifugation at 13.000 rpm for 10 min, protein concentration was measured with the Qubit Protein Assay on the soluble fraction and kept at -80 ºC until use. Zebrafish full body extract supernatants were cold centrifuged again at 30.000 *g* for 60 min to separate the membrane fraction and to pellet cell debris. The protein concentration in the soluble fraction was measured as before and stored at -80ºC. Equal amounts of protein were incubated with different concentrations of ABP for 1 h at 37ºC, resolved by 12.5% SDS-PAGE and scanned with the ChemiDoc™ MP System with the Cy2, Cy3 and Cy5 settings. Commassie

blue staining was used as loading control. All gel images were analyzed by the Image Lab software (Bio-Rad).

2D-gel electrophoresis

Before starting the protocol note that the fluorescent probes are light sensitive and every 1-3 hour it will lose half of fluorescent intensity in the final result. The samples were kept in the dark or covered with aluminium foil as much as possible.

Some 100 µg protein was taken in 90µL total volume with lysis buffer and 10 µL (10xstock) of probe was added. Sample was incubated for 1 h at 37 ^{o}C prior precipitation with TCA by adding 25 µL of 70% TCA and incubating for 0.5 h on ice (Should see the liquid becoming cloudy as the protein precipitates out). After cold centrifugation for 5 min at 14000 rpm the supernatant was removed and the pellet washed twice with 500 µL ice-cold acetone (if the pellet comes loose during washing repeat centrifugation step with acetone). Sample was dried out in a speed vac overnight. Pellet can be stored at -20 ^{o}C until use. Pellet was solved in 150 µL Urea buffer (30 mM Tris-HCl pH 7.5, 7.7 M urea, 2.2 M thiourea and 4% CHAPS) with 3uL Destreak agent (end concentration 0.5%) and 0.75uL IPG buffer (3-10) (end concentration 2%) was added freshly to the solution (may take very long to dissolve; to speed up the process the solution can be warmed up to 37 ^{o}C, vortexed, or sonicated). A portion of the solution can be stored to run on normal 12.5% SDS gel if desired. The lane from the incubation cassette was filled from the non-tilted edge with the sample. Slowly the strip was put onto the lysate (gel side down and make sure there are no bubbles under the strip). 2ml of mineral oil was loaded over the top of it to prevent the solution from evaporating. It was incubated between 24 and 96 h. After rinsing the strip with distilled water it was loaded into the focusing basket with the correct orientation and wet Whatman paper was used to separate the strip form the wires. The lane was again covered with mineral oil. The following focusing program was used: Step 1, 0.1 min 50 V; Step 2, 30 min 200 V; Step 3, 30 min 200 V; Step 4 30 min 400 V; Step 5, 30 min 400 V; Step 6, 30 min 600 V; Step 7, 30 min 600 V; Step 8, 60 min 3500 V; Step 9, 240 min 3500 V; Step 10, 10 min 200 V; Step 11, up to x hours 200 V. Afterwards the strip was incubated in 2 mL equilibration buffer (50 mM Tris-HCl pH 8.8, 6 M urea, 30% glycerol, 20% SDS and bromo phenol blue) with 10 mg/mL DTT for 1 h at room temperature prior 1 h incubation with 2mL equilibration buffer with 25 mg/ml iodoacetamide. The strip was loaded on a 12.5% SDS-PAGE gel only consisting of running gel with the help of a 1% agarose solution to prevent air bubbles between the strip and the gel. (NOTE: Load the strip quickly, and in a diagonal fashion starting with one corner of the strip and then easing the rest of the strip in to allow air bubbles to escape. The agarose solution hardens quickly, if the loading failed, remove the agarose and try again. A slot in the agarose can be made to be filled up with protein marker). The gel was ran at 300 V for 60-75 min (Encase the running container in an ice bath to prevent excess of temperature in the gel)

References

1. McBride, A. and P.Y. Ryan, *Proteasome inhibitors in the treatment of multiple myeloma.* Exp. Rev. Anticancer Ther., 2013. **13**(3): p. 339-358.
2. Tanaka, K., T. Mizushima, and Y. Saeki, *The proteasome: molecular machinery and pathophysiological roles.* Biol. Chem., 2012. **393**(4): p. 217-234.
3. Weissman, A.M., N. Shabek, and A. Ciechanover, *The predator becomes the prey: regulating the ubiquitin system by ubiquitylation and degradation.* Nat. Rev. Mol. Cell Biol., 2011. **12**(9): p. 605-620.
4. Finley, D., *Recognition and processing of ubiquitin-protein conjugates by the proteasome.* Annu. Rev. Biochem., 2009. **78**: p. 477-513.
5. Kisselev, A.F., W.A. van der Linden, and H.S. Overkleeft, *Proteasome inhibitors: an expanding army attacking a unique target.* Chem. Biol., 2012. **19**(1): p. 99-115.
6. Goldberg, A.L., *Development of proteasome inhibitors as research tools and cancer drugs.* J. Cell Biol., 2012. **199**(4): p. 583-588.
7. Li, N., *et al.*, *Relative quantification of proteasome activity by activity-based protein profiling and LC-MS/MS.* Nat. Protoc., 2013. **8**(6): p. 1155-1168.
8. Li, N., H.S. Overkleeft, and B.I. Florea, *Activity-based protein profiling: an enabling technology in chemical biology research.* Curr. Opin. Chem. Biol., 2012. **16**(1-2): p. 227-233.
9. Willems, L.I., H.S. Overkleeft, and S.I. van Kasteren, *Current developments in activity-based protein profiling.* Bioconjug. Chem., 2014. **25**(7): p. 1181-1191.
10. de Bruin, G., *et al.*, *A Set of Activity-Based Probes to Visualize Human (Immuno)proteasome Activities*. Angew. Chem. Int. Ed. Engl., 2015. doi: 10.1002
11. Paniagua Soriano, G., *et al.*, *Toward understanding induction of oxidative stress and apoptosis by proteasome inhibitors.* Antioxid. Redox Signal., 2014. **21**(17): p. 2419-43.
12. de Bruin, G., *et al.*, *Structure-based design of β1i or β5i specific inhibitors of human immunoproteasome,* J. Med. Chem*., 2014. **57**(14): p. 6197-6209*

Chapter 5: Proteasome Inhibitor-Adapted Myeloma Cells Show Proteomic Alterations That Suggest Complex Changes in Metabolic Pathways

Introduction

Proteasome inhibition is an important therapeutic concept in the treatment of multiple myeloma (MM), the most frequent hematologic malignancy [1]. Proteasome inhibitors are also increasingly used to treat lymphoma and acute leukemia, mostly in clinical trials. Next to the first in class, reversible, boronate-type proteasome inhibitor bortezomib and the irreversible, epoxyketone-type inhibitor carfilzomib that are currently in clinical use, several boronate- and epoxyketone-type proteasome inhibitors are in advanced clinical development [2, 3]. The mechanism of action of proteasome inhibition for MM treatment exploits the highly developed protein biosynthesis machinery in B-cell derived malignancies, including MM. This extraordinarily active biosynthetic route critically relies on timely disposal of misfolded and dysfunctional newly synthesized proteins through the ER-associated degradation machinery, of which the proteasome is the rate-limiting factor. Effective proteasome inhibition disturbs the equilibrium between production and disposal of non-functional or misfolded protein, which results in proteotoxic stress and excess activation of the unfolded protein response, which triggers apoptosis [4-6].

Current proteasome inhibitor-based myeloma treatments offer reliable control of the disease during early stages. However, MM treatment is not curative and a majority of MM patients will still die from relapsed refractory MM [7]. Understanding the biology of proteasome inhibitor resistance in MM, and also in other hematologic malignancies, and finding potential therapeutic strategies to overcome this resistance, are key challenges towards a more effective use of proteasome inhibition in MM and cancer treatment.

The proteasome is composed of two pairs of three proteolytically active sites (β1, β2, β5), which differ with respect to their substrate specificity. Immune cells, including myeloma, may replace these by respective active sites of the immunoproteasome (β1i, β2i, β5i) [8]. The β5 activity is the quantitatively most important, rate-limiting individual protease in the proteasome, and consequently bortezomib and also carfilzomib were designed to target the active center of the β5 subunit.

Proteasome inhibitor-resistant cells have been generated *in situ* by continuous exposure of cell lines to proteasome inhibiting drugs, and such proteasome inhibitor-adapted cells

served as models to understand and potentially overcome proteasome inhibitor resistance. Several groups have reported mutations in the PSMB5 gene leading to amino acid changes in the β5 active site or the bortezomib-binding pocket, currently considered as the most likely mechanism of proteasome inhibitor resistance [9]. However the functional relevance of these mutations to impair bortezomib binding and hence proteasome inhibition has never been directly demonstrated. In addition, it is unknown whether such mutations would also provide resistance against irreversible, epoxyketone-type next generation inhibitors.

Extensive analysis of material derived from patients with relapsed-refractory myeloma has so far failed to confirm the presence of such PSMB5 mutations [10, 11]. Instead, an alternative model for the biological basis of bortezomib resistance in MM has been put forward, based on findings from MM cells of bortezomib-resistant patients. In this model, bortezomib resistance was the result of complex changes in the activation status of the UPR, which were initiated by decreased activity of the IRE1/XBP-1 axis, one of the three main regulatory switches that control UPR activity, which in turn is closely connected to MM cell differentiation [12, 13].

Recently, selective probes for active proteasome subunits that for the first time allow to address directly the activity states of all subunits of the constitutive proteasome and the immunoproteasome have been developed [14-18]. Using these tools, the functional relevance of the most common PSMB5 mutation for proteasome inhibition by bortezomib and carfilzomib in resistant MM cells were examined as reported in this chapter. Because the here presented results suggest that PSMB5 mutations are dispensable to mediate proteasome inhibitor resistance in myeloma cells, a global proteomics analysis is carried out to compare IRE1/XBP-1-high, proteasome inhibitor-sensitive MM cells to IRE1/XBP-1 low, bortezomib- or carfilzomib-resistant subclones to map the complex changes in functional protein networks of proteasome inhibitor resistant myeloma cells to ultimately suggest new potential therapeutic targets.

Results

Bortezomib- or carfilzomib-adapted sub-cultures were established from the AMO-1 myeloma cell line by continuous drug exposure, as described [19]. Because such sub-cultures do not exhibit uniform cell morphology, as determined by light microscopy, limiting dilution experiments were performed to derive single cell-derived, bortezomib- or carfilzomib-adapted subclones (AMO-BTZ and AMO-CFZ) as a uniform and reliable basis

for further studies. Sequencing of all six proteasome active subunits revealed the presence of an A310G mutation leading to a Met45Val change in the S1 pocket of the PSMB5 active site in bortezomib-resistant bulk cultures as well as in all single cell-derived clones from these cultures (data not shown). In contrast, genetic changes in the PSMB1, PSMB2 and PSMB5 genes could be excluded in carfilzomib-adapted AMO cells, as well as in all respective single-cell derived clones. The absence of a PSMB5 mutation in AMO-CFZ cells demonstrates that point mutations in proteasome genes are not required in proteasome inhibitor resistant myeloma cells.

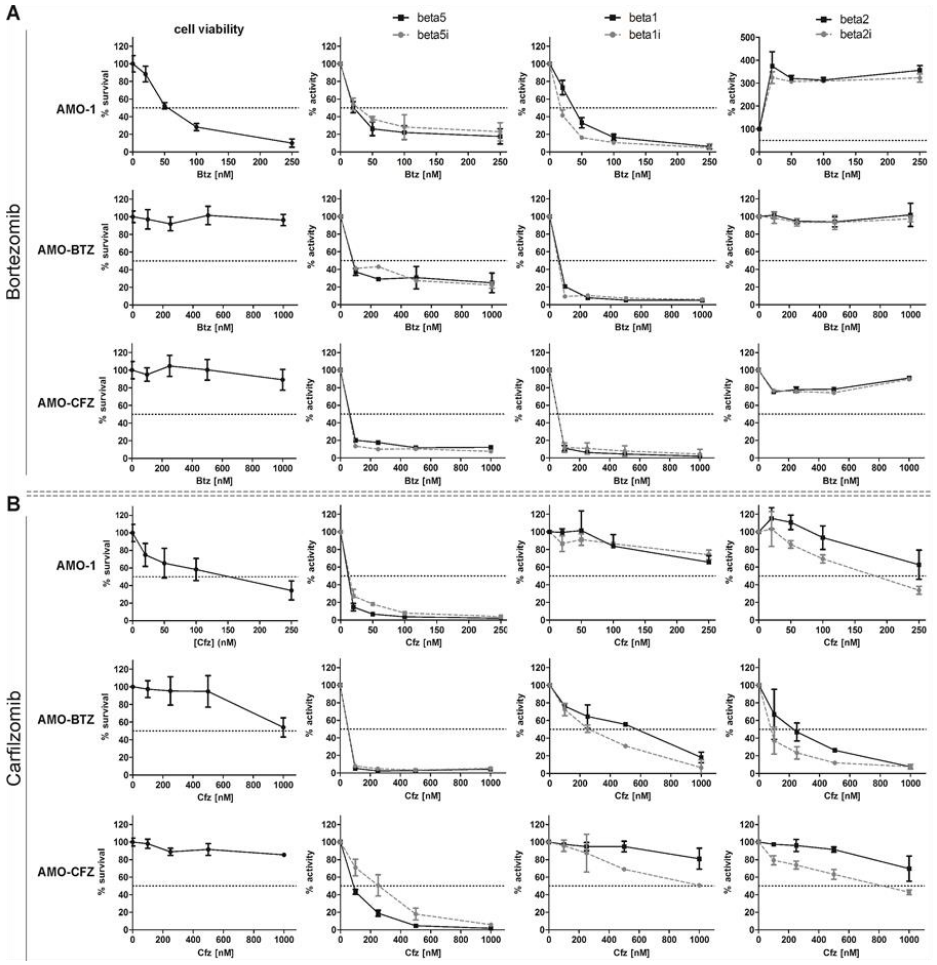

***Figure 1**. Activity-based protein profiling for all proteasome subunits in every cell line after 1 h exposure to bortezomib (A) or carfilzomib (B) and their proliferation rate after 48 h.*

Next a set of newly developed activity-based probes (described in Chapter 4 in more detail) is used to directly visualize changes in the proteasome-inhibiting on-target activity of bortezomib in the respective proteasome inhibitor-adapted MM cells (figure 1a). To this end, the proteasome inhibitor-adapted AMO-BTZ and AMO-CFZ cells were grown in the absence of proteasome inhibitors for 14 days and consecutively exposed to increasing concentrations of either bortezomib or carfilzomib for one hour, followed by removal of the drugs, mimicking the pharmacokinetic situation after intravenous (i.v.) administration of proteasome inhibitors in the clinic. Cells were subsequently analyzed with proteasome activity-specific chemical probes. The IC_{50} values for β1c and β1i inhibition was found to be comparable in AMO-1 and AMO-BTZ cells (table 1), while the IC_{50} value for β5c was approximately threefold lower in AMO-BTZ cells, compared to AMO-1 These data are consistent with a PSMB5 mutation hampering binding of bortezomib at the β5c, but not at the β1 subunits. Incubation with 250 nM bortezomib, a concentration that matches peak bortezomib plasma levels in myeloma patients minutes after i.v. bolus administration, resulted in approximately 75% inhibition of β5c/β5i in AMO-1 cells, and only moderately less effective inhibition (60-70%) in AMO-BTZ cells. These moderate quantitative differences in inhibition of β1/β5-type proteasome activity contrasted with the fundamentally different dose response for bortezomib-induced cytotoxicity between both cell lines, where the IC_{50} was 50 nM in AMO-1 cells, while evidence for toxicity was essentially lacking even at 1000 nM bortezomib in AMO-BTZ cells.

Bortezomib inhibited β5/β1 activity in AMO-CFZ cells with similar efficacy, compared to AMO-1 control cells, consistent with the absence of mutations in the proteolytically active proteasome subunits in AMO-CFZ cells. Strikingly, bortezomib did not induce cytotoxicity despite >80% inhibition of active β1c/β1i and β5c/β5i proteasome activities in AMO-CFZ cells. The activity of β2c/β2i proteasome subunits is not targeted by bortezomib, and a substantial upregulation of β2/β2i activity was seen in AMO-1 cells after bortezomib treatment consistent with earlier work, while AMO-BTZ or AMO-CFZ myeloma cells or HL-60 leukemia cells lacked such β2-activation by bortezomib.

		Proteasome subunit	AMO-1	AMO-BTZ	AMO-CFZ
BTZ	IC_{50} (nM) (50% functional proteasome inhibition)	β2	N.A.	N.A.	N.A.
		β2i	N.A.	N.A.	N.A.
		β1	40	60	50-60
		β1i	20-25	50	50-60
		β5	25	80-90	50-60
		β5i	30	80-90	50-60
	LD_{50} (nM) (50% cell viability)		50	> 1000	> 1000
CFZ	IC_{50} (nM) (50% functional proteasome inhibition)	β2	300	220	>1000
		β2i	180	90	800
		β1	> 500	600	> 1000
		β1i	>250	250	1000
		β5	10	50	90
		β5i	10	50	250
	LD_{50} (nM) (50% cell viability)		150	> 1000	> 1000

***Table 1**. IC_{50} values obtained for Bortezomib and Carfilzomib in each cell line after 1 hour exposure*.

The effect of carfilzomib on proteasome activity in adapted and non-adapted AMO cells was analyzed in the same way (figure 1b). Carfilzomib was much more selective for β5c/5i over β1c/1i and in addition had some β2c/2i-inhibiting activity, both in contrast to bortezomib. The pattern and the dose response of inhibition of β2c/2i and β1c/1i were identical between AMO-1 and AMO-BTZ cells during carfilzomib treatment, while the IC50 for β5c/5i was approximately 5 fold higher (10 nM vs. 50 nM) in AMO-1 vs. AMO-BTZ cells, suggesting that the PSMB5 A310G mutation affects β5 binding of carfilzomib in a fashion comparable to bortezomib. Carfilzomib treatment was significantly less effective in proteasome inhibition in AMO-CFZ cells, in contrast to bortezomib in the same cells. However, this was not a subunit-selective feature and had the same order of magnitude (approximately 5-10 fold lower IC50) also for β1c/1i and β2c/2i proteasome activity, suggesting that active drug export may be involved. If equally effective proteasome inhibition was achieved in AMO-1 and AMO-CFZ cells (>90% inhibition of β5c/5i, 20% inhibition of β1/1i, β2/2i), this resulted in marked (>50%) cytotoxicity in AMO-1 cells, whereas no cytotoxicity was observed in AMO-CFZ cells with the same degree of proteasome inhibition.

Together, these results indicate that adaptive resistance to proteasome inhibitors *in situ* can render myeloma cells largely independent from activity of both the constitutive proteasome and the immunoproteasome, that this is not specific for a given type of proteasome inhibitor, and that also active site mutations are not required to reach

adaptive proteasome inhibitor resistance. Complex biological adaptations outside the proteasome pathway are thus likely to be involved.

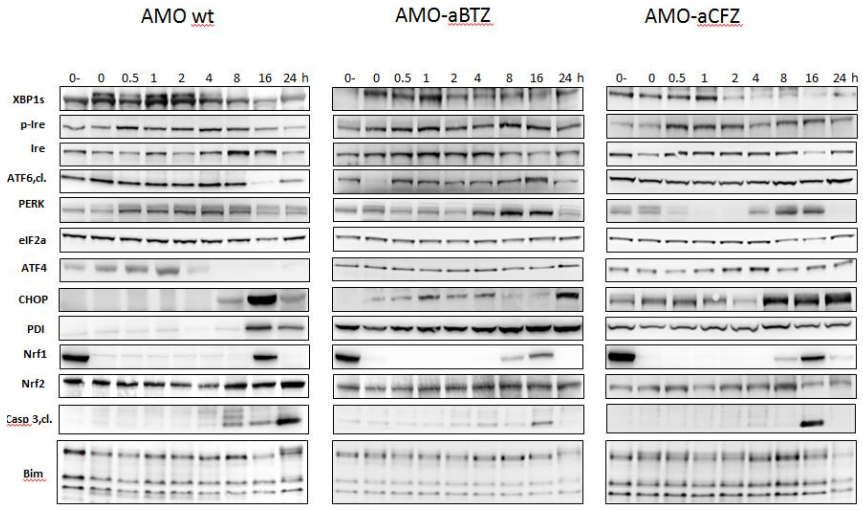

Figure 2. *Western blot analysis of UPR-induced apoptotic machinery*.

Next the effects of bortezomib on the UPR-induced apoptotic machinery in AMO-1, AMO-CFZ and AMO-BTZ cells were compared by Western blot (figure 2). The active version of the Nrf1 transcription factor is generated by partial proteolysis through the proteasome [20]. Exposure of AMO-1, AMO-BTZ and AMO-CFZ cells to bortezomib abolished production of active Nrf1 for approximately 8 hours, functionally confirming that proteasome inhibition and blockade of its protein turnover has been achieved in all three cell types, independent from the PSMB5 mutation status. Of the three major UPR-controlling transmembrane regulators IRE-1, PERK and ATF6, it was found that upon bortezomib challenge phosphorylation of IRE-1 was triggered within 1-2 hours in all cell types, leading to a consecutive increase in the spliced version of XBP1 also in all three cell types. Increased expression of PERK is initiated at later time points. Triggering of the UPR-related apoptotic machinery via ATF4 and CHOP is observed in AMO-1 and AMO-CFZ cells, but only poorly in AMO-BTZ cells, and downstream activation of caspase 3 is again less prominent in AMO-BTZ cells. Interestingly, bortezomib treatment led to a marked increase in PDI expression in AMO-1 cells, as expected, no change in PDI expression was observed in AMO-BTZ or AMO-CFZ cells, suggesting adaptive changes in the reducing and protein folding machinery of the endoplasmatic reticulum. In summary the data shows that

functionally efficient proteasome inhibition is being achieved with bortezomib in proteasome inhibitor-adapted cells, independently from the presence or absence of a mutation in the PSMB5 gene, and that comparable downstream signaling along the UPR apoptotic pathway is initiated, albeit less efficient in AMO-BTZ cells, while no cytotoxicity is achieved in proteasome inhibitor-adapted cells.

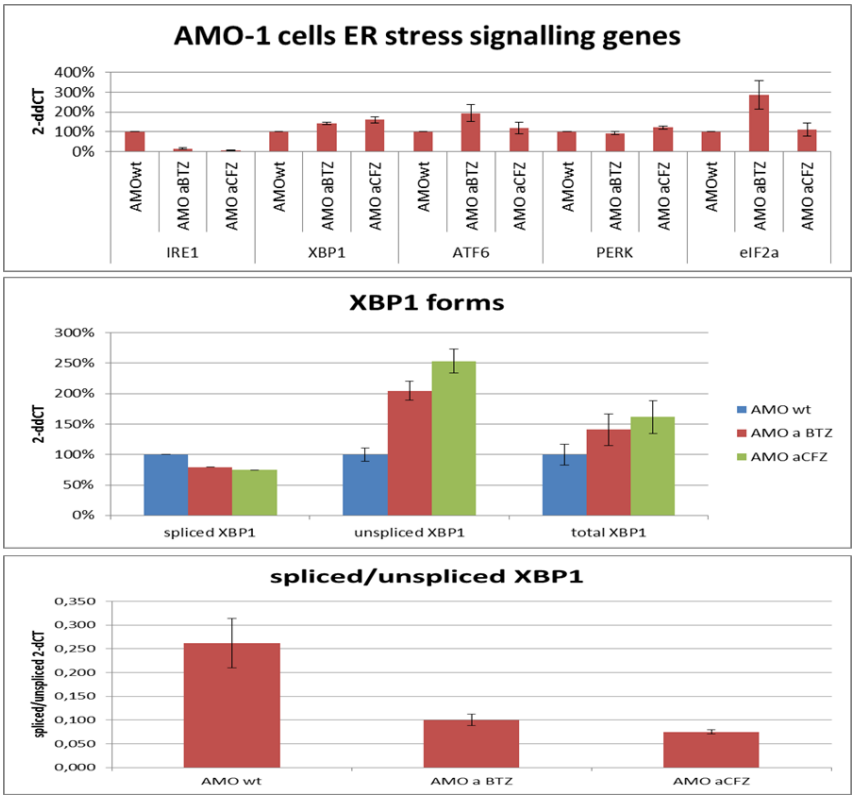

Figure 3. *UPR sensors screen. RNA quantification of the different UPR sensors and screen on the different XBP1 isoforms.*

Quantitative changes in the regulatory machinery of the UPR, namely IRE-1 and the product of its activity, sXBP1, result in bortezomib resistance in genetically engineered myeloma cells and have also been found in myeloma cells from BTZ-resistant patients. Whether such downregulation of the IRE1/XBP1 regulatory axis evolves during the adaptation of myeloma cells to proteasome inhibitor treatment was analyzed next. Only IRE-1 showed a quantitatively significant difference on mRNA levels in AMO-1 vs. AMO-BTZ and AMO-CFZ cells, in contrast to ATF6, PERK and eIF2a (figure 3). Consistent with this, significantly reduced levels of spliced XBP-1 mRNA, the functional result of IRE-1

activity, were found. On protein level, IRE1 and sXBP1 were uniformly strongly reduced in AMO-BTZ and AMO-CFZ, in contrast to eIF2a, ATF6 and PERK.

In order to unravel the biological complexity of adaptation to PIs, a proteomics approach was used to identify proteins with significant changes in expression levels in the adapted vs. non-adapted cells. In each experiment, from around 3500 different identified proteins, 2000 were quantified of which more than 600 were differentially expressed in proteasome inhibitor-adapted cell lines, com-pared to the non-adapted controls (using as cut-off a statistically significant two-fold change in expression over 3 replicates, figure 4). Interestingly, in the bortezomib-adapted leukemia cell line HL60-BTZ, only 300 proteins showed significantly changed expression levels, although a similar total number of proteins as in the myeloma cell lines was identified and quantified, suggesting a more complex adaptation pathway of myeloma cells, compared to leukemia cells, consistent with our experience that the adaptation process *in situ* takes considerably longer in myeloma cells.

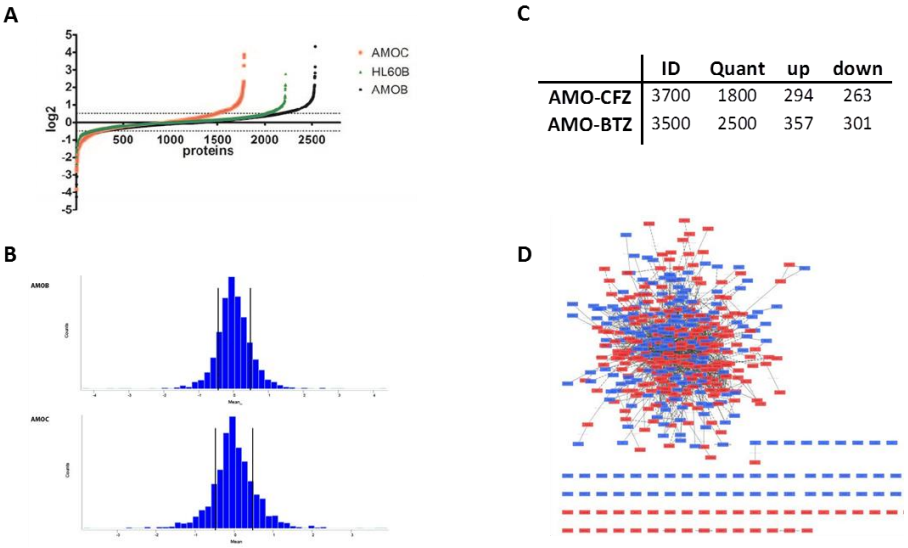

	ID	Quant	up	down
AMO-CFZ	3700	1800	294	263
AMO-BTZ	3500	2500	357	301

Figure 4*. Global proteome analysis for differentially expressed proteins. A)* Distribution of proteins according to their log2 value. B) Histogram plot of the log2 distribution for AMO-BTZ and AMO-CFZ of the differentially expressed genes; the solid vertical lines indicate the log2 cut-off. C) Table 1 showing the average values obtained in each analysis. (ID= found in either of the 3 replicates. Q=found in at least 2 out of 3 replicates. Light and heavy peptides are found in each replicate. Difference between ID and Q is due to absence of light or heavy peptide in the analysis) D) Protein-Protein interaction network where red boxes are proteins upregulated and blue boxes are downregulated.

The differentially expressed proteins were subjected to a protein-protein interaction (PPI) search to build a PPI network. This resulted in a highly complex adaptive net-work in proteasome inhibitor-resistant myeloma cells that cannot easily be reconciled with a single point mutation mediating proteasome inhibitor resistance by interfering with the on target activity of the inhibitor. Differentially expressed proteins were subjected to a Gene Ontology (GO) analysis, resulting in an average of 30 GO terms for the overexpressed proteins and 10 for the downregulated species in all three adapted clones. GO terms involving the proteasome were highly enriched in all samples, as expected, in agreement with proteasome over-expression. GO terms were then manually grouped into functionally related clusters resulting in 5-6 functionally connected groups of differentially expressed proteins (table 1). This supervised clustering showed high concordance between the different adapted clones and therefore suggested that acquired resistance to PI is characterized by a typical, complex pattern of changes in protein expression.

Change	GO term	p-value range	number of proteins	mean fold change (range)
AMO-BTZ				
upregulated	protein catabolism	10^{-8}	19	1.646 (2,30-1,41)
	redox homeostasis	$10^{-7} – 10^{-6}$	25	1.875 (6,06-1,41)
	folding and complex formation	$10^{-3} – 10^{-2}$	53	1.955 (19,70-1,41)
	transport/signaling	$10^{-3} – 10^{-2}$	116	1.730 (4,29-1,41)
	metabolic regulation	$10^{-3} – 10^{-2}$	114	1.805 (9,19-1,41)
downregulated	transcription/translation	10^{-2}	63	0.559 (0,71-0,20)
	differentiation	10^{-2}	13	0.557 (0,71-0,38)
	cytoskeleton organization	10^{-2}	22	0.478 (0,71-0,08)
	metabolic regulation	10^{-2}	45	0.589 (0,71-0,38)
	transport/signaling	10^{-2}	89	0.518 (0,71-0,05)
	apoptosis	10^{-1}	8	0.547 (0,71-0,26)
AMO-CFZ				
upregulated	protein catabolism	10^{-8}	22	1.741 (2,64-1,41)
	transport/signaling	$10^{-6} – 10^{-2}$	85	1.891 (12,13-1,41)
	metabolic regulation	$10^{-6} – 10^{-2}$	110	1.795 (4,59-1,41)
	folding and complex formation	$10^{-3} – 10^{-2}$	39	2.148 (13,93-1,41)
	redox homeostasis	$10^{-3} – 10^{-2}$	15	2.201 (4,29-1,41)
downregulated	apoptosis	10^{-3}	7	0.468 (0,71-0,16)
	metabolic regulation	$10^{-3} – 10^{-2}$	58	0.536 (0,71-0,22)
	transport/signaling	10^{-2}	72	0.509 (0,71-0,14)
	transcription/translation	10^{-2}	58	0.555 (0,71-0,19)
	differentiation	10^{-2}	10	0.479 (0,71-0,23)
	cytoskeleton organization	10^{-2}	24	0.451 (0,71-0,07)

***Table 2**. Manually annotated GO (gene ontology) terms. P-values indicate the range of the clustered GO terms. Mean fold change is representative for the proteins grouped in each term.*

The functional protein clusters found overexpressed in this analysis were proteins involved in protein catabolism, redox control and protein folding, consistent with proteotoxic stress induced by proteasome inhibition. Almost all proteasome alpha (PSMA

1,2,3,4,7) and beta (PSMB 1,2,3,4,5,7) subunits were individually detected as significantly overexpressed polypeptide species in in both adapted myeloma cells, as expected from previous studies, corroborating the sensitivity and specificity of our analysis. Interestingly, only the constitutive proteasome active subunits were found upregulated, while the β2i subunits were found down-modulated in the bortezomib-adapted cells.

The adapted clones had higher concentrations of antioxidant and ROS scavenging proteins, like NQO1, PRDX1 or SOD1, illustrating an increased importance of redox cycling in adapted cells. Adapted cells also expressed increased amounts of proteins involved in glutathione regulation, one of the most potent cellular antioxidants. Variations were found in the individual proteins up-regulated in a given functional pathway between bortezomib-adapted and carfilzomib-adapted clones (e.g., GPX1, one of the major enzymes responsible for glutathione peroxidation and thus removal of oxygen peroxide, was only overexpressed in AMO-BTZ, but not in AMO-CFZ, while glutathione transferase 1 (MGST1), which acts by conjugating reduced glutathione to a wide number of exogenous and endogenous hydrophobic electrophiles, was only found upregulated in AMO-CFZ, of which a variant (MGST3) was found upregulated in AMO-BTZ). However, the upregulation of proteins involved in redox pathways overall showed a very consistent pattern between AMO-CFZ and AMO-BTZ cells. Of the 16 proteins significantly upregulated in this cluster in AMO-CFZ cells, 12 were likewise found upregulated in AMO-BTZ cells, suggesting a central role of the redox equilibrium in proteasome inhibitor-adapted myeloma cells.

The protein folding/chaperoning capacity of the adapted cells was also markedly increased, compared to non-resistant control cells. The heat shock proteins HSP70, HSP90 and HSP105 were consistently among the top 15 quantitatively most strongly upregulated proteins (2.3 fold to 13 fold increase) in the group of proteins involved in folding/chaperoning in both adapted cell clones.

A pattern of uniform downregulation was observed for protein clusters involved in transcription/translation, differentiation, apoptosis and structural/cytoskeletal functions. Transcription and translation regulation proteins comprised about one fourth of the total downregulated protein species. In this group, transcription factors (e.g. GTF2I), histone subunits (e.g. HIST1H1B) or DNA/RNA processing enzymes (e.g. TOP2A or DCPS) were found, as well as the Ki67 antigen that is involved in RNA biosynthesis and is commonly used as a marker for a proliferative cell fraction. The apoptosis protein cluster comprised the lowest number of proteins. Both adapted cells markedly downregulated individual key proteins involved in apoptosis: AMO-CFZ had decreased expression of BAX, while the AMO-BTZ had a lower expression of the CASP10 and DIABLO proteins. BCLAF2, a transcriptional repressor, which promotes cell death, was the only protein shared in this

group by both adapted clones. Downmodulation of cytoskeleton proteins were indicated by CORO1A or CAPG, both modulators of the cytosolic or nuclear structure. The last biological cluster found downregulated in this model was the group of proteins involved in cell differentiation, which included for example VAV1, involved in the activation of Rho/Rac GTPases, or IKZF3, a transcription factor implicated in lymphocyte differentiation.

The quantitatively largest group of proteins with significantly altered expression levels in adapted vs. control cells was the one involved in metabolic regulation. This big cluster comprised close to 50 % of all polypeptide species with significant quantitative changes identified, suggesting that metabolic homeostasis is a major challenge for myeloma cells adapted to proteasome inhibitor treatment. This group of upregulated proteins consisted mainly of proteins involved in the respiratory chain (e.g. CYC1 or UQCR1), the generation of metabolites (e.g. BLVRA or APOA1BP), glycolysis (e.g. PFKP or PKM) and amino acid (e.g. GOT1 or EEFSEC) or nucleic acids metabolism (e.g. UMPS or BOP1). On the other hand, the metabolic regulation category also comprised a significant fraction of proteins (30%) that were significantly downregulated. These were in particular proteins involved in lipid and cofactor metabolism (e.g. ACST2 or ACLY) as well as proteins involved in glycolysis events (e.g. B4GALT3 or NAGK). Interestingly, of the top 25 quantitatively downregulated proteins in the metabolism protein cluster, 12 proteins were mitochondrial proteins and mostly involved in the biosynthesis of fatty acids (ACSF2, ACSF3) in carfilzomib-adapted cells, and likewise 5 respective mitochondrial proteins were found among the top 25 downregulated in bortezomib-adapted cells.

Likewise, in the transport and signaling protein cluster upregulated and down regulated proteins were found, however, there was quantitatively a rough balance between upregulated and down-regulated species. The upregulated protein/ion transport and signaling group was characterized by upregulation of ion transporters (e.g. ATP1A1 or ATP2B4), which allow cations to cross the plasma membrane, and which transfer small charged molecules through the mitochondrial outer membrane (STIM1 or VDAC2). Amino acid pumps like SLC1A4 or SLC7A5 were also found in this cluster as well as protein transporters, for example SEC23A which promotes the transport of proteins from the ER to the Golgi complex. Proteins species with decreased protein expression were pumps involved in ion transport into the ER (e.g. STIM1 or ATP13A1) and also proteins involved in ER signaling (e.g. ERP29 or SRPR), consistent with changes in the ER homeostasis. Other signaling molecules with lower expression in the adapted cells included some G-proteins (GNAI3 or GNG7) involved in cell division and other signaling pathways or proteins implicated in cell adhesion (e.g. CD44, one of the top hits in the quantitative ranking of downregulated proteins).

A manual search was performed for individual proteins which showed quantitatively prominent changes in protein expression levels, at the same time have key functions in their pathways that can rationally be explained as compensation mechanism for a lack of proteasome function, and that are definitively or at least potentially druggable. The quantitatively most significantly upregulated protein was the multidrug resistance protein 1 (ABCB1, 12 fold upregulated in AMO-ACFZ), suggesting that carfilzomib, a predicted substrate of MDR proteins, is quantitatively exported from the extracellular space, limiting the intracellular efficacy of proteasome inhibition. ABCB can be targeted with calcium channel blockers such as verapamil. Of note, ABCB was not upregulated in AMO-BTZ cells. The second most prominent quantitative hit in AMO-CFZ cells was the N-myc downstream-regulated gene NDRG1 (>9 fold upregulated in AMO-CFZ, 4.4 fold up-regulated in AMO-BTZ), a protein that is known as the molecular cause of Charcot–Marie–Tooth type 4D disease. NDRG1 is a hydrolase related to cell stress and cancer conditions, and is strongly upregulated under hypoxic conditions. NADPH dehydrogenase is the quantitatively most important reducing enzyme in eukaryotic cells. It was overexpressed 4-6 fold in AMO-BTZ and AMO-CFZ, respectively, and in addition the enzymes that generate NADPH (malate dehydrogenase and enzymes of the pentose phosphate pathway) were also overexpressed, high-lighting the crucial functional role of maintaining reducing conditions under the selective pressure of proteasome inhibitor treatment. The anti-diabetes drug metformin has been shown to suppress the activity of NADPH dehydrogenase. The transcription factor IKZF3 is known as an essential transcription factor in myeloma, which is targeted by treatment with lenalidomide. IKZF3 was the top downregulated protein in the cluster of differentiation-related proteins in AMO-BTZ cells it and was also found significantly reduced in AMO-BTZ cells.

Discussion

It has been postulated that point mutations in the proteasome β5 pocket are sufficient to confer proteasome inhibitor resistance. This feature though, was only observed in PI adapted cell lines but not in relapsed patients, suggesting that a different adaptation mechanism apart from mutations in the β5 subunit might be triggering the resistance against proteasome inhibitor induced cytotoxicity. In the adapted cell line AMO-BTZ a single point mutation was found in the β5 subunit pocket, and indeed this was causing a lower binding affinity for both inhibitors tested in this study, needing higher inhibitor concentrations to reach a comparable inhibition rate as the one obtained in the wild type AMO-1 cells. In AMO-CFZ cells no mutations were found in any of the active proteasome β-subunits. The proteasome inhibition rates for bortezomib and carfilzomib in these cells

were comparable with those observed in AMO-1 cells. At high inhibitor concentrations the β5/5i subunit activity was almost fully inhibited in all three cell lines, showing that proteasome inhibitors are still efficiently blocking proteasome activity even in resistant cells and that a comparable downstream signaling among the UPR pathway is initiated. However no cytotoxicity is induced in the adapted cell lines even at high inhibitor concentrations (1000 nM) while the wild type AMO-1 cells on the other hand experience high proteotoxic stress already at 250 nM which induces apoptosis in these cells. When analyzing the mRNA levels of the UPR sensors and downstream effectors in all three cell lines, it was found that the mRNA levels of the IRE1/XBP1 branch had substantially changed which is in concordance with previous observations in patients. This data shows that proteasome inhibitor resistance is independent of the type of proteasome inhibitor used and that site mutations are not required for adaptation.

The comparison of protein levels between AMO-1 cells and the adapted subclones shows high concordance between the found biological clusters in both resistant cell lines. Most of the proteins grouped in each cluster are shared between both resistant clones and the ones that are not have a comparable biological function suggesting that resistance is characterized by a typical pattern of changes in protein expression. Among the upregulated clusters, the proteasome machinery, the redox apparatus and the protein folding capacity are in concordance with PI induced proteotoxicity, thus an overexpression of these cellular mechanisms is in agreement with a lower sensitivity towards proteasome inhibition due to the cellular capacity to couple proteolytic stress. Taking this together with the fact that the protein synthesis machinery is downmodulated might explain why proteasome inhibition is not a suitable treatment for adapted cells. Adapted cells seem to have a lower basal ER-stress due to their lower production of proteins and an increased folding and degradation army. The fact that a cluster comprising apoptosis signaling was found to be downregulated in adapted cells does support this hypothesis. Having a downmodulated cluster covering differentiation proteins gives an additional indication towards this theory since plasma cells are fully differentiated B-cells, whose main function is to produce immunoglobulins for secretion. This high protein production is increased in neoplastic plasma cells and is what makes this cancer suitable for proteasome inhibition treatment. Therefore de-differentiation might be beneficial for adaption towards PI. This is in agreement with the loss of IRE1/XBP1 expression, which overexpression is fundamental for full differentiation into functional antibody producing plasma cells. This phenomenon was observed in patients with relapsed or refractory myeloma, where a subpopulation of progenitor cells was found to have lower expression levels of IRE1 and XBP1 [13] and was conferring resistance towards proteasome inhibitors.

Finding that the ion and protein transport into the ER and between this organelle and the Golgi apparatus is hampered in the resistant subclones does support the hypothesis of a rearrangement in the cellular secretion machinery since secreted proteins are mainly synthetized and folded inside the ER and translocated to the Golgi for their transport to the extracellular matrix. While this specific transport signaling is downmodulated in resistant cells, some ion pumps and amino acid transporters are overexpressed. Having enhanced the ion import/export machinery may be beneficial for redox homeostasis being able to quickly exchange protons or ions between organelles or with the extracellular matrix when dealing with redox stress. Overexpressing pumps to export potentially dangerous compounds may influence the intracellular drug efficiency and thus be favorable for adaptation.

About 50% of the proteins found in this study were involved in metabolic regulation indicating that metabolic homeostasis is a major challenge for adapted cells. Even having in this cluster proteins up- and downregulated, their biological functions are different. In the downmodulated group mainly proteins involved in the lipid and cofactor metabolism were found while the overexpressed proteins could be grouped into metabolites, amino and nucleic acids metabolism, glycolysis and into the respiratory chain machinery. This is indicating that tight regulation of the cellular metabolism is necessary for adaptation against proteasome inhibition.

From all the different protein clusters found in this study the most potentially druggable target groups might be the ion transporters and the redox machinery. It gives the impression that the antioxidant capacity of the cells plays a central role in resistant cells thus obstructing these mechanisms by blocking ions/proton channels or inhibition of reducing enzymes, or even by inducing reactive oxygen species, might be a valuable option as alternative or supplementary treatment.

Conclusion

It has been proven that proteasome inhibitor acquired resistance is independent of point mutations in the active proteasome subunits and of the type of proteasome inhibitor used and that efficient proteasome blockade is achieved in adapted cells in a comparable manner as in wild type cells without experiencing proteotoxic stress. This indicates that the adaptation mechanism might be a complex cellular rearrangement rather than a simple mutation that disrupts an efficient proteasome inhibition. Having comparable results in the complex protein expression changes and also in the pathways affected by

these adjustments in this proteomic study for both resistant cell lines, does support this hypothesis. This is also in accordance with the recent literature reports with patient material were no point mutations have been found and an imbalance in the ER homeostasis has been observed.

The here presented data shows that a complex regulation of cellular homeostasis has taken place to couple proteasome inhibition. From all the different pathways found affected by this rearrangement, the antioxidant machinery and the ion transporters seem to be the best targets for supplementary treatments. It might be wise combining proteasome inhibitors with ion channel blockers alone or together with oxidative agents or inhibitors of reducing enzymes. This combination of drugs might be a useful tool to fight proteasome inhibitor acquired resistance.

Experimental procedures

Activity-based protein profiling (ABPP) and survival

Adapted cells were grown for two weeks without the presence of inhibitor before performing the experiments. Cells were seeded to an end concentration of $0.5x10^6$ cells/mL and treated with the indicated inhibitor concentration. After 1 h of pulse treatment, medium was refreshed and 25000 cells were seeded in a new dish and grown for extra 48 h to measure the cell proliferation rate. Rest of the cells were harvested immediately and subjected to ABPP. Three different activity-based probes (ABPs) were used to independently quantify each active subunit of the proteasome. Each experiment was performed in triplicate. Fluorescent bands were measured with the ChemiDoc™ MP System and quantified using Image Lab software (BioRad). Untreated cells were used as control and its band intensity was defined as 100, the rest of the samples were normalized to the control. Proliferation assay was performed using the CellTiter-Glo Luminescent Cell Viability Assay kit (Promega) and performed as indicated by manufacturer. Each experiment was performed in triplicate.

Global Proteomics

Whole cell lysate was first digested with trypsin and then dimethyl labeled light (wildtype cells) or heavy (resistant cells). After labeling the samples were pooled together, subjected to SCX fractionation (strong cation exchange) and analyzed by LC/MS. Identification and quantification was done by MaxQuant software. A cut off of log2=0.5 was used to identify differentially expressed proteins. Each analysis was performed at least in triplicate. Only proteins being identified and quantified in at least 2 out of 3 replicates were used for further analysis. The differentially expressed

proteins were subset to a protein-protein interaction analysis by the Cytoscape software. The Cytoscape app BINGO was used to perform a gene ontology (GO) analysis looking for biological processes being overrepresented in the network. The search gave around 20-30 biological processes being either up- or downregulated in the resistant cell lines. From these 20-30 terms, a manual curation was done in order to cluster these GO terms in more general groups. P-values indicate the range of the clustered GO terms. Proteins not classified by the software were manually assigned to the different clusters.

References

1. McBride, A. and P.Y. Ryan, *Proteasome inhibitors in the treatment of multiple myeloma.* Expert Rev. Anticancer Ther., 2013. **13**(3): p. 339-358.
2. Goldberg, A.L., *Development of proteasome inhibitors as research tools and cancer drugs.* J. Cell. Biol., 2012. **199**(4): p. 583-588.
3. Kisselev, A.F., W.A. van der Linden, and H.S. Overkleeft, *Proteasome inhibitors: an expanding army attacking a unique target.* Chem. Biol., 2012. **19**(1): p. 99-115.
4. Ron, D. and P. Walter, *Signal integration in the endoplasmic reticulum unfolded protein response.* Nat Rev. Mol. Cell. Biol., 2007. **8**(7): p. 519-529.
5. Tabas, I. and D. Ron, *Integrating the mechanisms of apoptosis induced by endoplasmic reticulum stress.* Nat. Cell Biol., 2011. **13**(3): p. 184-190.
6. Walter, P. and D. Ron, *The unfolded protein response: from stress pathway to homeostatic regulation.* Science, 2011. **334**(6059): p. 1081-1086.
7. Kale, A.J. and B.S. Moore, *Molecular mechanisms of acquired proteasome inhibitor resistance.* J. Med. Chem., 2012. **55**(23): p. 10317-10327.
8. Tanaka, K., T. Mizushima, and Y. Saeki, *The proteasome: molecular machinery and pathophysiological roles.* Biol. Chem., 2012. **393**(4): p. 217-234.
9. Ri, M., *et al.*, *Bortezomib-resistant myeloma cell lines: a role for mutated PSMB5 in preventing the accumulation of unfolded proteins and fatal ER stress.* Leukemia, 2010. **24**(8): p. 1506-1512.
10. Niewerth, D., *et al.*, *Molecular basis of resistance to proteasome inhibitors in hematological malignancies.* Drug Resist. Updat., 2015. **18**: p. 18-35.
11. Politou, M., *et al.*, *No evidence of mutations of the PSMB5 (beta-5 subunit of proteasome) in a case of myeloma with clinical resistance to Bortezomib.* Leuk. Res., 2006. **30**(2): p. 240-241.
12. Gu, J.L., *et al.*, *Differentiation induction enhances bortezomib efficacy and overcomes drug resistance in multiple myeloma.* Biochem. Biophys. Res. Commun., 2012. **420**(3): p. 644-650.
13. Leung-Hagesteijn, C., *et al.*, *Xbp1s-negative tumor B cells and pre-plasmablasts mediate therapeutic proteasome inhibitor resistance in multiple myeloma.* Cancer Cell, 2013. **24**(3): p. 289-304.
14. Li, N., *et al.*, *Relative quantification of proteasome activity by activity-based protein profiling and LC-MS/MS.* Nat. Protoc., 2013. **8**(6): p. 1155-1168.
15. Li, N., H.S. Overkleeft, and B.I. Florea, *Activity-based protein profiling: an enabling technology in chemical biology research.* Curr. Opin. Chem. Biol., 2012. **16**(1-2): p. 227-233.
16. Verdoes, M., *et al.*, *A panel of subunit-selective activity-based proteasome probes.* Org. Biomol. Chem., 2010. **8**(12): p. 2719-2727.
17. Willems, L.I., H.S. Overkleeft, and S.I. van Kasteren, *Current developments in activity-based protein profiling.* Bioconjug. Chem., 2014. **25**(7): p. 1181-1191.
18. de Bruin, G., *et al.*, *A Set of Activity-Based Probes to Visualize Human (Immuno)proteasome Activities.* Angew. Chem. Int. Ed. Engl., 2015. doi: 10.1002.
19. Kraus, M., *et al.*, *Activity patterns of proteasome subunits reflect bortezomib sensitivity of hematologic malignancies and are variable in primary human leukemia cells.* Leukemia, 2007. **21**(1): p. 84-92.
20. Li, X., *et al.*, *Specific SKN-1/Nrf stress responses to perturbations in translation elongation and proteasome activity.* PLoS Genet., 2011. **7**(6): p. e1002119.

Chapter 6: Summary and Future Prospects

The work described in this thesis focuses on the characterization of proteasome directed activity-based probes (ABPs) as well as on the adaptation mechanisms that make multiple myeloma derived cell lines resistant against proteasome inhibitors (PIs). **Chapter 1** comprises a general introduction to the ubiquitin proteasome system (UPS) and to the techniques and tools used in this thesis to its study. The UPS is the main pathway for cellular protein degradation in eukaryotic cells. In the UPS pathway ubiquitin marks proteins destined for destruction by the proteasome, the actual protein degradation machinery. Partial inhibition of the proteasome has been approved as a treatment for two types of blood cancers (multiple myeloma and mantle cell lymphoma) but in most cases patients relapse and become insensitive against proteasome inhibition regimes.

Chapter 2 presents a literature review and entails an in-depth analysis on the UPS, its inhibition and its relation with cellular redox homeostasis. PIs are used in the clinic for treatment of hematopoietic malignancies. They induce endoplasmic reticulum (ER) and oxidative stress, disruption of signaling pathways, mitochondrial dysfunction and eventually cell death caused by apoptosis. PIs designated as clinical candidates include natural product derivatives and compounds developed by rational design and feature a wide diversity of structural elements. Research in recent years has brought a deepened insight into the molecular mechanisms of PI induced apoptosis. However there are some paradoxes and controversies in the literature. In chapter 2 the advances and uncertainties, in particular on the time course events that makes cells commit to apoptosis are discussed. Also some mechanisms of evolved PI resistance are presented, and speculations on the difference in sensitivity between cell or tumor types are brought forward.

Increased understanding of the systems biology at mRNA and protein level and the kinetics behind the interaction between proteasome inhibitors and cells is imperative. Design and synthesis of subunit specific inhibitors for each of the seven known proteasome activities and for the enzymes associated to proteasomes will aid in unraveling biology of the UPS in relation to ER stress, ROS production and apoptosis and will generate leads for therapeutic intervention.

The first part of **Chapter 3** describes different bio-orthogonal strategies to label the proteasome subunits by means of two-step activity-based protein profiling (ABPP). Because the reporter groups can alter the properties of ABPs, introducing bio-orthogonal

handles instead of readout tags allows performing first the proper binding of the ABP to the enzyme and a posterior addition of the reporter group in a second reaction. Bio-orthogonal handles are small chemical moieties which are inert in complex biological environments. The bio-orthogonal reactions can be performed both *in situ* and *in vitro*. In fact, some of the bio-orthogonal ligations can be performed simultaneously. Alkynes and cyclooctynes respective ligations show background labeling, which in the case of cyclooctynes is very large, suggesting that cyclooctyne ligations are not truly bio-orthogonal. These extra bands should be analyzed in more detail, for example by in-gel digestion coupled to LC-MS analysis or by a pull-down experiment. Finding the biological groups that react with these molecules could be beneficial for developing new bio-orthogonal handles or for inhibitors and probes development. Although the pool of tools in bio-orthogonal chemistry has increased considerably in the last decade, there is still room for improvement as many chemical reactions might also be suitable thus expanding the tools for researchers. Ideally, finding new reactions which are orthogonal between them and also with biological samples would be the best. This would increase the tools for a simultaneous labeling of different proteins or other constructs.

The second part of **Chapter 3** is a technical study about the capacity of an ABP to label the whole pool of active proteasomes from human and murine cell lines both *in vitro* and *in situ*. The optimal conditions for the labeling are determined, incubation with 0.5 μM for 1 h *in vitro* and 4 μM for 4 h *in situ*. Interestingly these conditions were the same for both cell lines studied, namely AMO-1 and B3/25. The unlabeled fraction after labeling with the probe was found to be very small (1-10%) in all the cases except for mice cell lysates where the percentage increased up to 30%. This large difference between the unlabeled proteome *in vitro* and *in situ* suggests that it might be caused by a systematic error while performing the experiments. The experiments in murine cells need to be repeated in order to validate the here obtained results. Performing this screen with different ABPs and on different species may give an indication on the specificity and potency of not only the probes but also the inhibitors, and could help in the development of new and more potent and, perhaps also, organism selective probes and inhibitors.

Chapter 4 describes a screening of 7 different proteasome-directed ABPs in mouse and zebrafish tissue extracts. The ABPs used in this study vary from subunits specific probes to broad-spectrum ones. Their application in human samples has been validated previously and here it is shown that these are also suitable for their use in mouse and zebrafish, two species broadly used in research due to their similarity to human biology. Although all ABPs retain their subunit specificity with a low lose in potency (all working in the low micromolar range, 0.1-3 μM) in both organisms, some observations can be made. Probe **6**, a β5-selective probe, does not give a proper separation of the mouse β5 and β5i subunits

when running on SDS-PAGE as it does with the human counterparts. Only when performing a 2D gel electrophoresis the separation and visualization of the two subunits is achieved. Possibly replacement of the reported tag by a different fluorophore might allow its separation on a regular SDS-PAGE. In the case of zebrafish extracts, the use of BODIPY(FL)-bond ABPs is not recommended when labeling the β2 or β2i subunits due to an endogenous green fluorescent protein which runs slightly higher than these subunits in the gel. The presence of extra bands next to the β2 subunit when labeling zebrafish brains or full fish extracts with probes **2** and **7** was not expected, since these bands are not visible in human or mouse samples. Further research needs to be done on this, since it could be that the probes are allowing the separation of different post-translationally modified β2 subunits or they could also be off-targets. Probably an in-gel digestion procedure coupled to a mass spectrometry analysis will be an appropriate solution to identify those unexpected bands.

The large changes in probe potency in the different organisms tested indicates that there might be a window where the probes or inhibitors might be selective towards one organism but not another. The development of organism selective proteasome ABPs and inhibitors might be beneficial not only for fundamental but also for clinic research. This would allow for example the specific proteasome inhibition of the pathogen but not of the host in infections. The development of these types of inhibitors might be also useful in the food and agriculture industry, where plagues could be avoided by compounds that only target the organism causing the plague but not the plant itself and neither individuals who might consume these afterwards.

Chapter 5 reports on the characterization of two PI resistant cell lines by means of ABPP and quantitative proteomic techniques. This study shows that adaptation towards proteasome inhibition is not only independent from the type of inhibitor but also from point mutations in the β5 active site binding pocket, which have been previously reported in cell lines studies but not in patients with relapse or refractory myeloma. The significant changes in the proteome of two resistant subclones of a multiple myeloma cell line were characterized and compared to their progenitor cell line. When combining the identified proteins into clusters according to their biological function, both cell lines showed the same biological pathways being altered compared to the wild type cells. This, together with to the fact that around 50% of the proteins found in the analysis were shared between both adapted subclones, is indicating that a complex biological network rearrangement is driving the adaptation towards proteasome inhibition induced cytotoxicity. The data point towards some potential druggable targets including antioxidant enzymes and ion pumps, which blockade might induce apoptosis in the adapted cell lines. In figure 1 a model of the obtained results that characterize the

resistant adaptation mechanisms is presented. All these different biological process could be a suitable target for alternative treatment against PI resistant cells.

In order to validate these targets and in general the global adaptation mechanisms found in our data, this type of analysis should be repeated with different disease-stage cell lines and if possible it would be ideal if this is done with patient material. In fact, the global procedure of the analysis can be extrapolated and used in the study of any drug resistance development in other diseases or even just in the differentiation characterization between two cell types. This technique if applied in the clinic could drive towards patient-based therapies, by finding the specific and optimal altered signaling pathway to target.

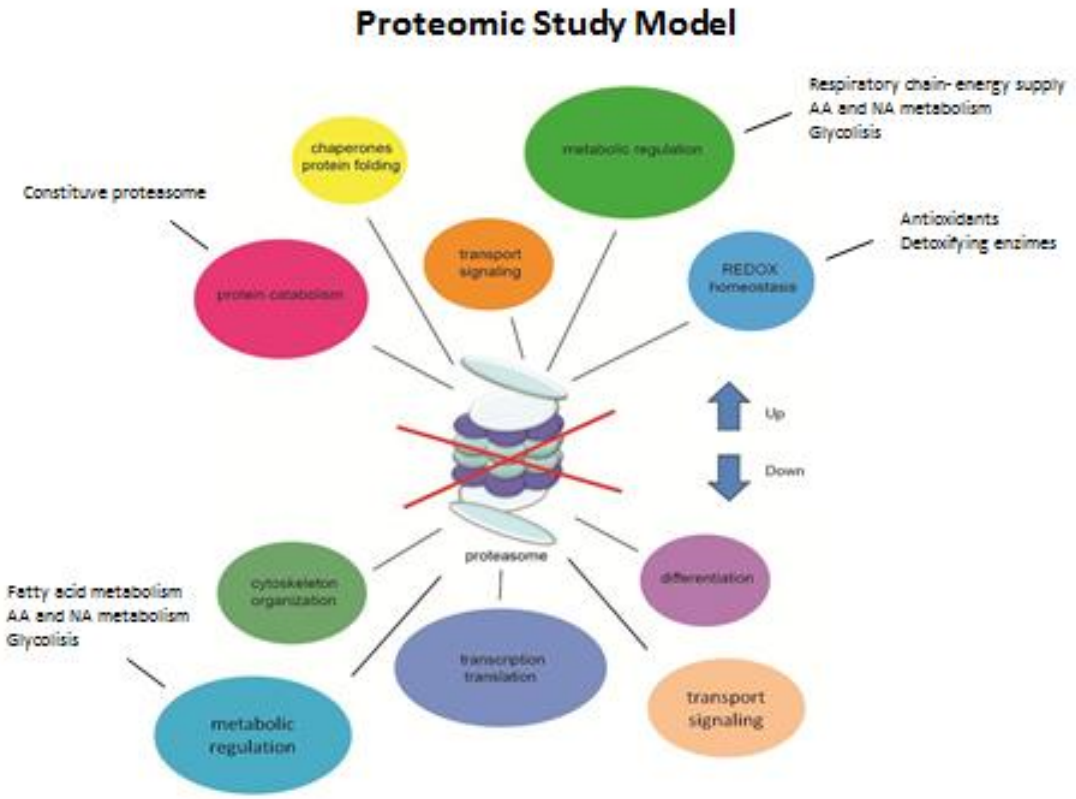

***Figure 1**. Model showing the different biological processes inducing proteasome inhibitor resistance in our cell lines adaptation model. The size of the different biological bubbles is related to the proteins found in each cluster.*

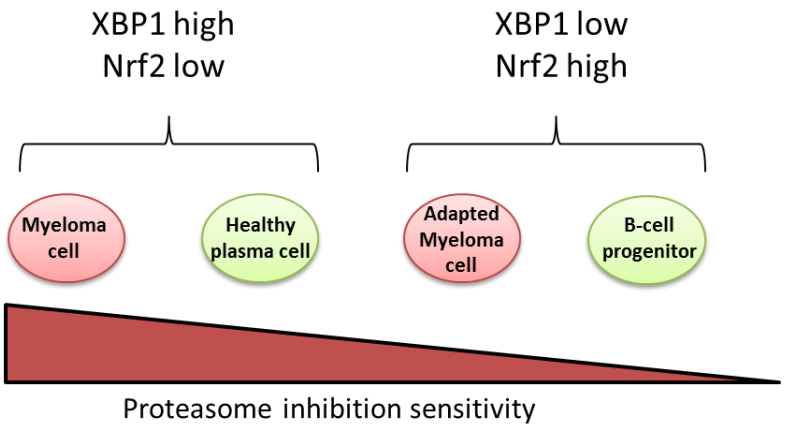

Figure 2. *Proposed model for proteasome inhibition adaptation.*

Fully functional plasma cells are characterized by a high XBP1 and a low Nrf2 expression, while their progenitors are characterized by the opposite, a low XBP1 and a high Nrf2 expression. The high need of plasma cells for protein quality control makes them potentially sensitive for proteasome inhibition (figure 2). The malignant plasma cells have an increased protein synthesis rate, making them more sensitive against PI induced apoptosis. It can be hypothesized that the adaptation results in a loss of XBP1 (actually a factor revealed by the presented data) and an increase of the transcription factor Nrf2. These changes trigger cellular de-differentiation and thus making the cells insensitive against proteasome inhibition. The transcription factor Nrf2 is essential for antioxidant response in all cell types, by inducing the expression of antioxidants like NQO1, one of the top proteins found overexpressed in the adapted clones. It is also known for the induction of constitutive proteasome subunits, another feature found in our analysis. This data is suggesting that Nrf2 transcriptional activation or overexpression might trigger the response mechanisms, at least in some extend, but this still needs to be validated. To check whether Nrf2 is essential for PI adaptation, it could be attempted to develop PI resistance in a knocked down cell line. Alternatively, the use of Nrf2 inhibitors or activators should also indicate if this transcription factor is needed for the adaptation process.

Resumen

El trabajo descrito en esta tesis se centra en la caracterización de sondas, conocidas como activity-based probes (ABPs), dirigidas hacia el proteasoma y también en los mecanismos de adaptación de líneas celulares derivadas de mieloma múltiple resistentes a la inhibición del proteasoma. El capítulo 1 es una introducción general al sistema ubiquitino proteosómico (UPS) y a las técnicas utilizadas para su estudio. El UPS es la principal ruta intracelular de degradación de proteínas en células eucarióticas. En esta ruta, la ubiquitina marca las proteínas para ser destruidas por el proteasoma, el aparato degradatorio del sistema. La inhibición parcial del proteasoma ha sido aprobada como tratamiento contra dos tipos de cáncer sanguíneos (mieloma múltiple y linfoma de células de manto) pero en la mayoría de los casos los pacientes recaen y se vuelven insensibles a regímenes de inhibición del proteosoma.

El capítulo 2 presenta una revisión literaria que profundiza en el estudio del UPS, su inhibición y la relación que mantiene con la homeostasis redox celular. Los inhibidores del proteasoma (PIs) son usados en medicina para el tratamiento de enfermedades hematopoyéticas. Éstos inducen estrés de retículo endoplásmico así como estrés redox, disrupción de rutas de señalización, disfunción mitocondrial y finalmente muerte celular o apoptosis. Los PIs designados como candidatos clínicos incluyen derivados de productos naturales así como compuestos desarrollados por diseño racional, lo cual constituye una gran variedad de elementos estructurales. En los últimos años se ha aumentado el conocimiento de los mecanismos moleculares en la apoptosis inducida por PIs, pero aún existen paradojas y controversia en la literatura científica. En este capítulo los avances e incertidumbres en la inducción de apoptosis, con especial interés en su desarrollo en el tiempo, serán discutidos. Se presentaran algunos posibles mecanismos en el desarrollo de resistencia contra PIs y se especulará sobre la diferencia de sensibilidad contra este tratamiento entre células o tipos de cáncer.

La primera parte del capítulo 3 describe diferentes estrategias bio-ortogonales para marcar el proteasoma haciendo uso de two-step activity-based protein profiling (ABPP). El grupo indicador puede alterar las características de la sonda por lo que su sustitución por un compuesto bio-ortogonal permite realizar la unión de la sonda con la enzima primero y posteriormente la incorporación del grupo indicador en una segunda reacción. Compuestos bio-ortogonales son pequeñas entidades químicas inertes en medios biológicos complejos. Las reacciones bio-ortogonales pueden ser llevadas a cabo tanto *in situ* como *in vitro*, de hecho algunas de ellas pueden ser ejecutadas simultáneamente. La

segunda parte del capítulo 3 engloba un estudio técnico sobre la capacidad de las sondas (ABP) de marcar completamente todos los proteosomas activos en líneas celulares humanas y de ratones tanto *in vitro* como *in situ*. Las condiciones óptimas de incubación de las sondas obtenidas son 0.5 µM durante 1 hora *in vitro* y 4 µM durante 4 horas *in situ.* Cabe destacar que estas condiciones de incubación son las mismas en ambas líneas celulares estudiadas, AMO-1 y B3/25. La fracción de porteasomas activos sin ser marcada por la sondas encontrada es bastante pequeña (1-10%) en todos los casos excepto en lisados de ratones donde esta fracción aumenta hasta el 30%.

En el capítulo 4 un cribado de 7 sondas diferentes del proteasoma es llevado a cabo en muestras de ratones y peces cebra. Las sondas utilizadas en este estudio varían desde exclusivas para una sola subunidad del proteasoma hasta pan-reactivas con todas las subunidades. La aplicación de estas sondas en tejidos humanos había sido validada previamente y aquí se demuestra su validez para estudios en ratones o peces cebra, dos especies ampliamente utilizadas en investigación debido a su gran similitud con la biología humana. Todas las sondas mantienen su selectividad hacia las diferentes subunidades del proteasoma en ambos organismos aunque con una pequeña pérdida de potencia, manteniéndose en un bajo rango micro molar (0.1-3 µM).

El capítulo 5 es un estudio sobre la caracterización de dos líneas celulares resistentes a inhibidores del proteasoma utilizando ABPP y análisis proteómicos. El estudio demuestra que la adaptación a la inhibición del proteasoma es independiente del tipo de inhibidor utilizado y de mutaciones puntuales en la subunidad β5, mutaciones que han sido anteriormente encontradas en líneas celulares pero no en muestras de pacientes con mieloma refractario. Los cambios significantes en el proteoma de dos subclones de mieloma resistentes a regímenes de inhibición del porteasoma comparados con su línea celular progenitora son caracterizados en este estudio. Al agrupar las proteínas identificadas en grupos dependiendo de su función biológica, se demuestra que las rutas biológicas alteradas son las mismas en ambas líneas celulares resistentes. Esto, sumado al hecho de que alrededor del 50% de las proteínas encontradas en el análisis son comunes en ambos subclones, es indicativo de que un complejo cambio en el funcionamiento interno de las células es necesario para la adaptación contra la toxicidad inducida por la inhibición del proteasoma.

Curriculum Vitae

Guillem Paniagua Soriano was born on 14th September 1984 in Valencia, Spain. In 2003, he graduated from the Deutsche Schule Valencia. During this period he got interested in chemistry and other science related subjects. Thereafter he followed the Chemistry licentiature at the Faculty of Chemistry of the University of Valencia. In 2010 he moved to Leiden University to perform a 9 months research project supported by an Erasmus grant. During this period he worked on the quantification of Bortezomib effect on 26S proteasomes in the Bio-organic Synthesis group under supervision of Dr. B. Florea.

From October 2011 to December 2015, he worked as a PhD student in the group of Bio-organic Synthesis, Leiden Institute of Chemistry under supervision of Prof. Dr. Hermen Overkleeft and Dr. Bobby Florea. In 2012 he assisted the Proteomics Bioinformatics workshop in Cambridge, UK, organized by Wellcome Trust together with the EMBL-EBI. In 2012 and 2014 he presented posters at the 4th and 5th EMBO Chemical Biology meetings in Heidelberg, Germany.

List of Publications

Relative quantification of proteasome activity by activity-based protein profiling and LC-MS/MS
Li N, Kuo Cl, **Paniagua G**, van den Elst H, Verdoes M, Willems LI, van der Linden WA, Ruben M, van Genderen E, Gubbens J, van Wezel GP, Overkleeft HS and Florea BI
Nat. Protoc., 2013 Jun; **8**(6): p. 1155-1166

Toward understanding induction of oxidative stress and apoptosis by proteasome inhibitors
Paniagua Soriano G, de Bruin G, Overkleeft HS and Florea BI
Antioxid. Redox Signal., 2014 Dec 10; **21**(17): p. 2419-2443

Systematic analyses of substrate preferences of 20S proteasomes using peptidic epoxyketone inhibitors
Huber EM, de Bruin G, Heinemeyer W, **Paniagua Soriano G**, Overkleeft HS and Groll M
JACS, 2015 Jun 24; **137**(24): p. 7835-7842

Proteasome inhibitor-adapted myeloma cells are largely independent from proteasome activity and show complex proteomic changes in particular in redox and energy metabolism
Paniagua Soriano G, Besse L, Li N, Kraus M, Besse A, Meeuwenoord N, Bader J, den Dulk H, Overkleeft HS, Florea BI and Driessen C
Submitted